Comparison of Environmental Conditions Surrounding the 2005 and 2006 Atlantic Hurricane Seasons

A thesis submitted in partial fulfillment of the requirements for the degree of Master of Science at George Mason University

By

Laura Clemente
Bachelor of Science
The Pennsylvania State University, 2007

Director: Dr. Zafer Boybeyi, Professor
Department of Geography and Geoinformation Science

Summer Semester 2009
George Mason University
Fairfax, VA

DEDICATION

This work is dedicated to my amazing family.
Mom, Dad, Jason, Kim, Kevin, Mike, Taylor, Kelsey, Austin, Uncle Chris, Uncle Pete, Aunt Diane, Uncle Tom, Aunt Linda, Grandma and Grandpa Clemente, and Grandma and Grandma Beebe – this is for you.

In loving memory of Dorothy Beebe – Grandma.

ACKNOWLEDGEMENTS

I first want to thank my adviser Dr. Zafer Boybeyi who guided me and was continually willing to share his vast knowledge of the subject material with me. He is a gifted teacher and I look forward to the opportunity to continue this research with him in the near future. Dr. Guido Cervone – committee member, mentor, and friend. Thank you for the many conversations on all topics, for introducing me to R, for your continual patience, the opportunities to teach, and much more. Many thanks as well to Dr. Michael Summers for being a part of my committee, always being accessible, for his thorough and helpful comments and interest in this project.

I am grateful to Dr. John Zack, Dr. Glenn Van Knowe, and those at Meso, Inc. Their passion for meteorology was contagious – they ignited my interest in the field and have continued to impart their wisdom to me every time our paths cross. I am also thankful for the strong foundation I received at Penn State in the College of Earth and Mineral Sciences. Special thanks to Dr. Robert Crane and Dr. David Babb who imparted knowledge, wisdom, and advice to me through all four years at Penn State. Dr. Jason Beringer of Monash University in Australia who taught my first graduate level class on Earth Systems. If it were not for these individuals, I probably would not be in this field or be pursuing a higher degree.

This thesis would not have been possible without the loving and consistent encouragement from my family. It is because of their unwavering support that I am where I am and who I am today. I cannot begin to count the number of papers I wrote and Mom critiqued or the number of evenings spent with Dad working on math assignments as a child. They always encouraged me to do my best. It is a tremendous blessing to have such wonderful parents. Jason! Thank you for the days you encouraged me to keep working and for the days you told me to go have fun. Whether it has been questions about school or life, you have always been there for me!

To my classmates, officemates, and friends here at GMU – Terry Idol, Priyanka Roy, Terri Fede, Federico Solano, Jacek Radzikowski ("Helloooo"), József Bakosi, John Lindeman, and Gary Butcher, and Eric Stofferan – thank you for all the conversations,

study sessions and fun. Jaime Backus (Jambassador!) and Elizabeth Ouellette – thank you for your friendship and for keeping me sane! "Jump into a handstand!" I also want to thank friends both near and far that supported me during this process – Mike and Kelly Tischler, Liz Lyons, Cory Colhouer, Megan Graham, Robin Rodgers, Janejira Kalsmith, Laura Jane, Devon Grace, Meghan Anderson, Karin Moore, Jenn Tambasco, Jenn Saddlemire, Frieda Miller, Ashley Sweeney, Leigh Patterson, Sara Engelder, Michael Bredderman, Rob Smythe, and Megan Matheny. Special thanks to my new roommates Autumn, Gideon, and Rachel Steinberg for their thoughtful and prayerful support these last three months.

I again want to thank my family: my parents, my brother and his wife, my cousins, my Aunts, my Uncles, and Grandparents. Your support was invaluable.

"But we have this treasure in jars of clay to show that this all-surpassing power is from God and not from us." 2 Corinthians 4:7

This research was supported by the National Science Foundation (NSF), grant # ATM-0543330.

TABLE OF CONTENTS

LIST OF TABLES

LIST OF FIGURES

LIST OF ABBREVIATIONS

ACE	Accumulated Cyclone Energy
AEW	African Easterly Wave
AIRS	Atmospheric Infrared Sounder
AOML	Atlantic Oceanographic and Meteorological Laboratory
AVHRR	Advanced Very High Resolution Radiometer
CPC	Climate Prediction Center
FNMOC	Fleet Numerical Meteorology and Oceanography Center
GHRSST-PP	Global High Resolution Sea Surface Temperature – Pilot Project
GODAE	Global Ocean Data Assimilation Experiment
HRD	Hurricane Research Division
HURDAT	Atlantic Basin Hurricane Database
MDR	Main Development Region
NAMMA	NASA-African Monsoon Multidisciplinary Analysis (AMMA)
NASA	National Aeronautics and Space Administration
NHC	National Hurricane Center
NOAA	National Oceanic and Atmospheric Administration
OMI	Ozone Mapping Instrument
POE	Probability of Exceedence
SAL	Saharan Air Layer
SALEX	Saharan Air Layer Experiment
SST	Sea Surface Temperature
TCs	Tropical Cyclones
TS	Tropical Storm
WAC	Western Atlantic and Caribbean

ABSTRACT

COMPARISON OF ENVIRONMENTAL CONDITIONS SURROUNDING THE 2005 AND 2006 ATLANTIC HURRICANE SEASONS

Laura Clemente, M.S.

George Mason University, 2009

Thesis Director: Dr. Zafer Boybeyi

The 2005 North Atlantic Hurricane season resulted in 28 named tropical cyclones (TCs), placing this season in the record books as the strongest and most costly Atlantic Hurricane season on record. The 2006 North Atlantic Hurricane season was expected to be almost as strong as the 2005 season, but instead resulted in an average season with 10 named TCs. Numerous factors are involved in the genesis and lifecycle of a TC. This research explores the tropical system as a whole, with the goal of understanding each of the factors that play a role in TC genesis. The objective of this study is to determine if there was a particular variable that played a significant role. This study will pave the way for future research on Hurricane seasons and the potential effects of Saharan dust on the genesis and lifecycle of TCs in the North Atlantic region. To achieve this objective, observations and analysis fields are used to examine environmental factors important to

TC behavior, such as sea surface temperature (SST), mid-tropospheric moisture, atmospheric stability, and vertical wind shear. Saharan dust is studied as it has been a topic in recent literature and the role it plays in the tropical system is yet uncertain.

The results indicate that warmer waters across the Main Development Region (MDR) along with favorable winds coming off the west of Africa mainly produced active hurricane season in 2005 as compare to 2006. Other environmental factors, such as lower wind shear (changing winds with height), existence of a moist mid-tropospheric layer and moist instability, were also partially the cause of the active 2005 hurricane season. More importantly, the results also indicated that Saharan Air Layer (SAL) interaction with TCs may be another environmental factor that influences TC activity. Therefore, SAL interaction with TCs may be yet another important piece of the puzzle in advancing our understanding of TC activity and intensity change in the Atlantic basin that demands further comprehensive research.

Chapter 1: Introduction

Accurate forecasting of tropical cyclones (TCs) is a high priority topic of research due to their large potential economic impact and public safety issues. Hurricanes rank among the most destructive and costly of natural phenomena.

For example, Hurricane Galveston (one of the oldest hurricanes on record) hit Galveston, Texas on September 8, 1900. Galveston, home to just under 40,000 people, was a thriving seaport situated 2.65 m above sea level. The hurricane brought storm surge heights of 4.8 m high, wind speeds estimated at 58 m/s, and an observed barometric pressure of 966.7 hPa resulting in the destruction of 3,600 buildings and $20 million in damages (based upon 1900 dollar value). In 1992, hurricane Andrew hit Florida, Louisiana, and Mississippi where it finally weakened to a tropical depression. Andrew had a minimum central pressure of 922 hPa and one minute sustained winds of 175 mph at its maximum intensity. The storm resulted in approximately $27 billion in damages (in 1992 dollars). It is still the second most costly Atlantic hurricane on record. Even more alarming, Pielke and Landsea (1998) reported that potential total loss estimates for a category-4 hurricane striking Miami, Florida are estimated at $60 billion. Katrina, a recent example and the most costly hurricane to have impacted the United States, caused about $82 billion in damage (in 2005 dollars). Katrina made landfall at three different

locations in its lifetime striking the Bahamas and southern Florida before hitting Louisiana. Hurricane Katrina showcased good forecasting but brought to light the many weaknesses in emergency response to natural hazards in that region. It has been estimated that the return period for another storm of the same strength as Katrina or greater than Katrina is every 21 years in the Gulf region and every 14 years when the entire U.S. coast is considered (Elsner et al., 2006).

The cost of warning citizens in the event of landfall is also expensive. For every mile of coastline warned it costs roughly $600,000 (Jarrell and DeMaria, 1998; McAdie and Lawrence, 2000). Couple this with the fact that the average length of coastline warned is approximately 460 miles (McAdie and Lawrence, 2000). With improved forecasts, potentially smaller lengths of coastline will need to be warned, thus defraying the cost of warnings. Even a decrease of 50 miles in coastline warned would, based the above estimates would, result in a savings of $30 million.

These historical and potential enormous damages highlight the importance of and need for a better understanding of TC behavior – such as TC activity, track, and intensity forecasting. Despite large reductions in hurricane track forecast errors over the past three decades (*cf.* Figure 1), forecast errors have not reached estimated predictability limits (McAdie and Lawrence, 2000). In contrast to the improvements in track forecasts, there has been little improvement in forecasts of storm intensity and surprisingly little effort to forecast and verify storm structure, including the overall size (Liu *et al*., 1997; Camp and Montgomery, 2001). Globally, about 15% of all hurricanes experience a period of rapid intensification. Since many damaging hurricanes undergo rapid intensification prior to

landfall, considerable improvement is still needed in understanding and predicting TC intensity change and inner core structure.

While the TC forecasting has received significant attention on the scale of weather prediction (~3-5 days forecasting) and climate timescales, it has yet to be comprehensively studied on both scales when coupled together. On the climate scale, TC behavior is influenced by climate factors, such as changes in large-scale circulation anomalies associated with the El Niño-Southern Oscillation (ENSO), the North Atlantic Oscillation (NAO), by shifts in tropical storm origins or regional changes in land use. On the scale of weather prediction, TC behavior is characterized by strong multi-scale interactions: the hurricane vortex is hundreds of kilometers in horizontal size (synoptic-scale), the eye is tens of kilometers (mesoscale), and the embedded convective clouds are in the order of kilometers (cloud-scale), with a vertical scale of up to 20 km.

The local environmental flow in which the hurricane vortex is embedded is the main factor that determines its short-term track. At longer timescales, an accurate forecast of the flow at a considerable distance from the cyclone is needed. The internal structure of the TC as well as the interaction between the structure and the hurricane's environment are the primary determinates of hurricane intensity. TC activity is also strongly controlled by environmental conditions (such as sea surface temperature, mid tropospheric moisture, wind shear, etc.). Clearly, these space-time scales should be represented as accurately as possible when TC behavior is studied.

This thesis studies and contrasts the TC activity of the 2005 and 2006 North Atlantic Hurricane seasons to better understand the impact of environmental conditions with an

emphasize on Saharan dust storms influencing TC activity. Chapter 2 provides background and motivation. Chapter 3 discusses the data and sources used in this study. Chapter 4 describes the methodology used in this study. Chapter 5 discusses the results. Finally, Chapter 6 provides conclusion and future work. References are given in Chapter 7.

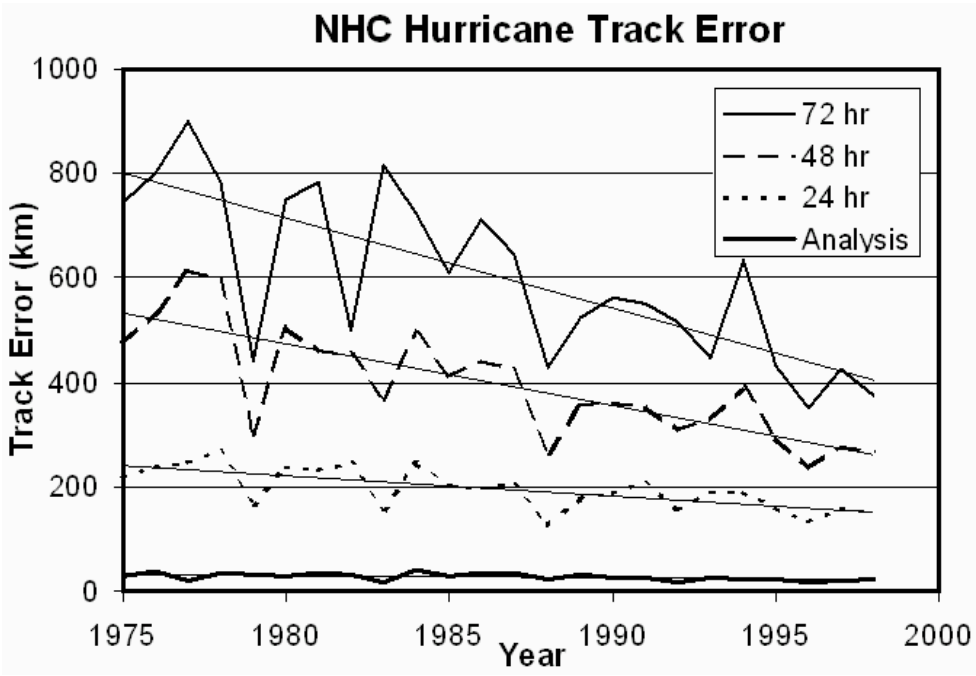

Figure 1: NHC Hurricane Track Error: Shown are the analysis and 24, 48, and 72 hour National Hurricane Center forecast track errors from 1975 to 1998 (based on data from McAdie and Lawrence, 2000). The linear regression trend lines show that in this 23 year period the 48 and 72 hour forecast track error improved by 50%, while the 24 hour forecast track error improved by 37%. In spite of these improvements, 72 hour forecast track error is still about 400 km, the 48 hour forecast track error is about 275 km, while the 24 hour track error is about 175 km.

Chapter 2: Background and Motivation

Over the past several years, greater attention has been paid to tropical storms occurring in the Atlantic basin. Particularly, a very active 2005 hurricane season, has been intensively studied by TC researchers. Several particularly devastating hurricanes have hit the United States causing both material and irreplaceable damage. Researchers at the Hurricane Research Division (HRD) create a forecast each year regarding the expected severity of the upcoming hurricane season. Since 2005 was such an active season, the public is now paying more attention to these forecasts. There have been a number of criticisms as hurricane potential has been over forecasted for both the 2006 and 2007 seasons.

From this, a question can be raised as to why the 2006 and 2005 seasons were so drastically different. Despite early forecasts for an above average 2006 hurricane season, as expected from the trend of the previous ten years, the 2006 season ended with an average number of storms occurring (This question was originally raised in an article by Lau and Kim, 2007 and has since been commented on in several other articles.). Researchers have been looking into other possible influences upon the severity of tropical storm seasons.

The 2005 hurricane season produced a record of 28 tropical cyclones. The goal of this study is to examine the environmental conditions to better understand why the 2005 season was so much more active than seasons prior to and following 2005. This is to be accomplished by comparing various meteorological factors known to influence tropical storm development (i.e., TC activity) as well as one factor whose effect upon the genesis and lifecycle of tropical storms is still in question. Known important factors to be compared between the 2005 and 2006 seasons are sea surface temperatures, wind shear, mid-latitude moisture availability, and atmospheric stability.

The presence/absence of dust (absorbing aerosols) is also included in this study, as recent literature has been discussing a relationship between tropical storm development and the presence of dust. This is due to the fact that the Saharan Air Layer (SAL) is an elevated layer of dry, dusty air that forms over the Sahara Desert and moves over the tropical North Atlantic during the hurricane season. Although the SAL has been investigated for several decades (Prospero and Carlson, 1972; Braun and Shie, 2008) its interaction with North Atlantic tropical cyclones (TCs) is an important and emerging area of research. Recent investigations have suggested that the SAL can inhibit both the formation and intensification of African easterly waves (AEWs) and TCs via three mechanisms: entrainment of mid-level dry air, enhanced vertical wind shear, and increased static stability through solar absorption by the SAL's suspended mineral dust (Dunion and Velden, 2004; Evan et al., 2006). Moreover, some recent studies have suggested that the SAL's suspended mineral dust may also have an influence on the microphysical

properties of clouds (Zipser et al., 2008). Other studies have indicated that the SAL can amplify the initial development of TCs (Karyampudi and Carlson, 1988).

Clearly, the interaction between the SAL and TCs is a very complex problem that may be influenced by vertical wind shear, prevailing moisture, stability in the lower atmosphere, and mineral dust effects (i.e., aerosol direct and indirect effects). In order to evaluate the effects of each of these various factors (i.e., the thermodynamic and kinematic impacts of the SAL) on TC activity, we use satellite remote sensing data and NCEP analyses as an integral part of this work. This approach is necessary, but may not be sufficient, for an adequate understanding of the complex interactions between the SAL and TCs.

The highly active 2005 season resulted in a huge loss of human life and billions of dollars spent because of storm damage and for coastal warnings. For the 2006 hurricane seasons, greater numbers of storms were initially forecast than actually occurred (Lau & Kim, 2007, Chiodi & Harrison, 2008, NHC). Similarly, more storms were forecasted for the 2007 season than were observed, but that year is not the focus of this study. Seasonal factors were expected to produce an above-normal 2006 season that was stronger than climatological but not as intense as the previous 2005 season. Instead, ten TCs occurred, a number closer to the 1950-2007 mean of 9.4 TCs for a "near-normal" season. Figure 2 displays data from the official Atlantic basin hurricane database (HURDAT) for the period of record from 1900 to 2007. Additionally, Table 2.1 shows averages of each of the parameters available from the HURDAT database. The two straight lines in Figure 2.1 indicate the average number of named storms and average number of major

hurricanes (i.e., hurricane category 3, 4, and 5) for the period of record shown in the figure, 1900-2007.

In referring to Figure 2, please note the large jump in the total number of storms in 2005 as compared to 2006. Then compare that jump with the rest of the data. Nowhere in the entire HURDAT database is there such a vast difference between seasons. At first glance, it appears something similar occurred in 1930, but a closer look at the dataset reveals that the number of storms recorded in 1930, 1931, 1932, and 1933 were 2, 9, 11, and 21 respectively. This begs the question – why was the 2005 season was so much more active than seasons prior to and following 2005? To seek an answer to this question a comparison of various meteorological (environmental) factors known to impact tropical storm development will need to be analyzed. Known necessary factors – sea surface temperatures, wind shear, mid-latitude moisture, and atmospheric stability – will be compared between the 2005 and 2006 hurricane seasons. An additional factor, the presence/absence of dust (absorbing aerosols), will also be included in the analysis as recent literature has been discussing the role dust may play in the development of tropical storms.

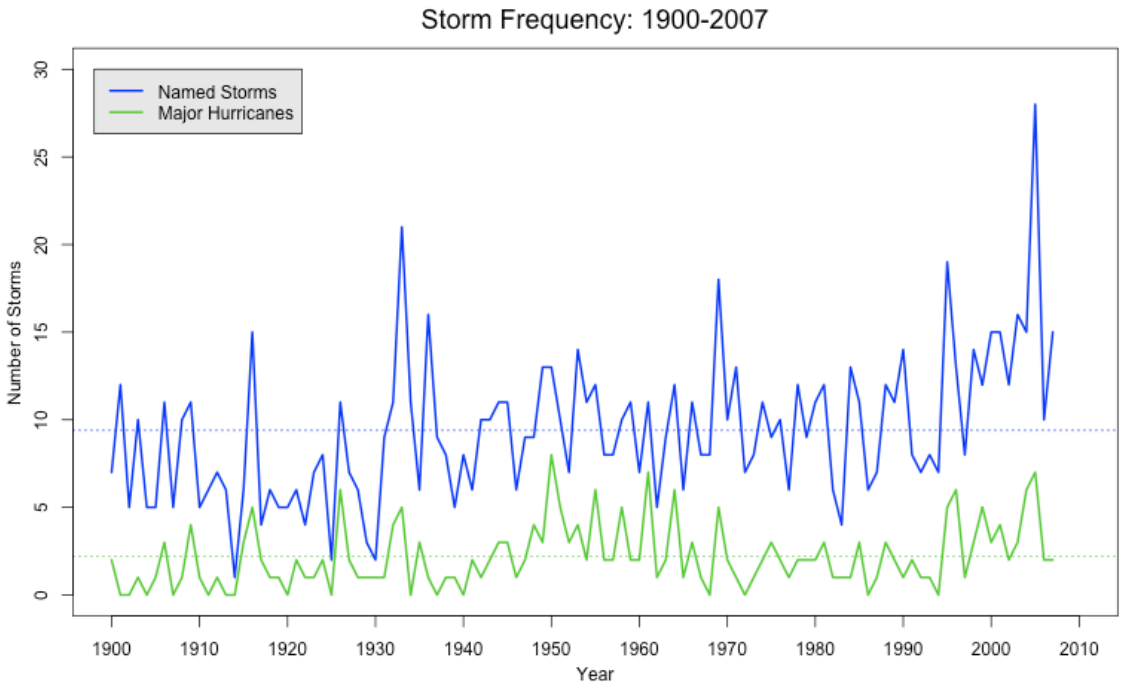

Figure 2: Storm Frequency: 1900-2007: Shows the number of revised named storms and revised major hurricanes (Category 3, 4, and 5) occurring from 1900 to 2007. Note the record number of storms occurring in 2005 and large difference in the number of named storms between 2005 and 2006 being greater than between any other two years. The two lines of the same color and pattern as the named storms and major hurricanes show the average over the period of record, 1900-2007, for each of the two categories. (Data Source: HURDAT)

Table 1: Average Calculated from HURDAT Record: Shows the averages calculated from the HURDAT record for each of the categories for which a record is available. This shows that the original and revised HURDAT records are closer to each other in TC number and intensity as the period of record moves closer to the present. It also shows the average value for each respective period of record. The Accumulated Cyclone Energy (ACE) index indicates the approximate energy used by a TC in its lifetime. This measure is calculated for each individual storm and also for each season. The index takes the number of storms in a season, the duration of the storms, and the strength into account. (Data Source: HURDAT)

Averages Calculated from HURDAT Record								
Period of Record	**Original Named Storms**	**Revised Named Storms**	**Original Hurricanes**	**Revised Hurricanes**	**Original Major Hurricanes**	**Revised Major Hurricanes**	**Original ACE**	**Revised ACE**
1851-2007	8.8	8.8	5.2	5.3	2.0	1.9	94.6	86.4
1900-2007	9.2	9.4	5.2	5.3	2.2	2.2	90.1	89.6
1970-2007	11.2	11.2	6.0	6.0	2.3	2.3	94.2	94.3

Chapter 3: Data and Sources

Data sources used in this study include the Atlantic Oceanographic and Meteorological Laboratory (AOML), the Ozone Mapping Instrument (OMI), GHRSST-PP, and the National Center for Environmental Prediction (NCEP). Each of the data sets are accessible to the public free of charge. These datasets include information pertaining to the track and intensity of TCs in the Atlantic basin, the aerosol index, SSTs, vertical wind shear, mid-latitude moisture, and atmospheric stability.

3.1 Hurricane Tracks

HURDAT re-analysis data contains the official National Hurricane Center (NHC) record of tropical cyclones for storms occurring over the Atlantic, the Gulf of Mexico, the Caribbean Sea, and eastern Pacific. The data format specifically used for this study comes from the original 80 column data for the Atlantic basin. At present, the data record extends from 1851 to the end of the 2007 hurricane season. HURDAT contains information at 00Z, 06Z, 12Z, and 18Z regarding the stage of the tropical cyclone, its location, maximum one-minute sustained surface wind speed, and central surface pressure.

This dataset has been re-analyzed to eliminate biases, systematic error and random errors present in the record between 1851 and 1910 (for more details on the re-analysis readers can refer to the "Hurricane Research Division: Re-Analysis Project"). In addition to these corrections, historical information is also used to reconstruct a better record. In 2000, the original re-analysis effort used historical information to correct the record between 1851 and 1885. Following this, the re-analysis for the period from 1886 to 1910 was finished in 2003. Changes were made in 2005 to the period from 1911 to 1914 after which 1914 held the record as the quietest season on record with one named storm. Corrections for land falling tropical storms in the period from 1851 to 2005 were added in 2006. Though the re-analysis effort has continued, the official record from 1921 onward has remained unchanged with the exception of Hurricane Andrew in 1992. Ten years after Hurricane Andrew (1992) devastated Florida the re-analysis project determined a more accurate intensity for the storm resulting in a change to the ACE index value for 1992 in the HURDAT dataset. The HURDAT record provides a post-season analysis of the track and intensity of tropical storms occurring in the Atlantic and eastern Pacific – this information is essential for studying the 2005 and 2006 hurricane seasons.

3.2 Sea Surface Temperature

The data for the Sea Surface Temperature (SST) analysis comes from the Fleet Numerical Meteorology and Oceanography Center (FNMOC). This data is a part of the L4 data from the Global High Resolution Sea Surface Temperature – Pilot Project (GHRSST-PP) but is stored and distributed from the Global Ocean Data Assimilation Experiment (GODAE). SST data is provided at varying spatial resolutions, nine

kilometers in the mid-latitudes and twelve kilometers at the equator, as the grid used for the data is in a global Mercator projection. The dimensions of this grid are 3241 by 2441. This data set from FNMOC is a composite of data from the Advanced Very High Resolution Radiometer Global Area Coverage (AVHRR GAC) and in situ measurements obtained from fixed and drifting ships and buoys. Specifically, the dataset provides the skin temperature for the present analysis.

3.3 Aerosol Index

Aerosol index data comes from the Ozone Mapping Instrument (OMI) on the Aura spacecraft. From this instrument, aerosol information is obtained once per day at an approximate resolution of 13 by 24 kilometers at nadir, extending to 28 by 150 kilometers at the extent of the instruments field of view (Torres et al., 2007). The aerosol index is determined by measuring the difference between a pure atmosphere and the wavelength dependence of backscattered ultraviolet radiation from an atmosphere containing aerosols. Thus, the pure atmosphere value can be calculated where only pure rayleigh scattering is taken into account. This calculation is known as the Lambert Equivalent Reflectivity (LER) (Torres et al., 2007). The measured backscattered ultraviolet radiation takes Rayleigh scattering, Mie scattering, and absorption into account. These values are directly determined from radiances measured at 354 nanometers and 388 nanometers. The aerosol index calculation simplifies to:

$$\text{Ultra Violet Aerosol Index (UVAI)} = -100 * \log_{10}\left[\frac{I_{354}^{obs}}{I_{354}^{calc}\left(R_{354}^{*}\right)}\right].$$

where I_{354}^{obs} refers to the measured radiance at 354 nm, I_{354}^{calc} refers to the calculated radiance at 354 nm, and R^*_{354} to the Lambert Equivalent Reflectivity at 354 nm (Torres et al., 2007). This method for determining the UVAI resulted from observations from TOMS, the pre-cursor to OMI, and empirical data. Aerosol index values are positive for absorbing aerosols such as dust and smoke and negative for non-absorbing aerosols such as sulfate. Differences between absorbing aerosols and non-absorbing aerosols have a clear delineation because the amount of UV absorption by smoke and desert dust can be observed. For obtaining information on dust events, OMI is the best for this study since it provides data with good temporal and spatial coverage as well as a characterization of absorbing aerosols. Additionally, the ability of the UVAI to register absorbing aerosols in the presence of clouds is another benefit of this instrument.

The Aqua/Moderate Resolution Imaging Spectroradiometer (MODIS) and Terra/Multiangle Imaging Spectroradiometer (MISR) are two other instruments, in addition to the OMI, that observe aerosols in the atmosphere. A study by Ahn et al. (2008) compared these three sensors. Though the OMI data was chosen primarily for its consistent temporal and good spatial resolution, several pieces of pertinent information should be noted from this study. First and foremost, at low AI values (values less than 1.0) it is difficult to determine if actual aerosols are present or if the reading is from background noise (Ahn et al., 2008). For this reason, comparisons of AI values will be done with all values and a second comparison neglecting any AI values less than 1.0 is also done. When comparisons were made between MODIS, MISR, and OMI, it was found that OMI had a tendency to observe slightly larger AI values than MODIS and

MISR. However, these slightly higher AI values maintained the same temporal and spatial variations as AI values in MODIS and MISR (Ahn et al., 2008).

3.4 NCEP Analysis Fields

Data from the National Centers for Environmental Protection (NCEP) can be obtained for free online. There is a plethora of information available in these analysis fields. For this study, temperature, dew point temperature, atmospheric pressure, wind speed, and wind direction at several pressure levels are utilized. The analyses came from the AVN model, which was the aviation run of the Medium Range Forecast (MRF) model. Presently, the AVN is called the Global Forecast System (GFS) and is still a product of NCEP. The NCEP analysis data utilizes 12 different data sources to cover 9 different regions. After the May 31, 2005 updates to the model, all forecasts are now run with 64 layers. Forecasts from the GFS are performed every six hours at 00, 06, 12, and 18 UTC. The resolution of the analysis also improved with the 2005 updates. The GFS now extends to 384 hours for the 70 km grid resolution run and to 180 hours for the 35 km resolution grid. Analysis fields from this model from the NCEP data were used for all odd days at 00 UTC during the hurricane season – June 1st to November 30th. This dataset contains 34 levels from 0.015 km to 19.995 km. Analyses created from this dataset are limited to 12 km in the vertical as that height is sufficient for studying the impact of these environmental factors. For the 2005 season, there are no analysis fields for June, 12 for July, 11 for August, 15 for September, 16 for October, and none for November. For the 2006 season, there are 14 analysis fields for June, 9 for July, 16 for August, 15 for September, 16 for October, and none for November. This leaves 52 days of data in 2005

and 55 days of data for use in 2006. Of these dates, there are 46 days worth of data in common between both years that are used for the Probability of Exceedance calculations.

Chapter 4: Methodology

Before progressing to the outcome of the SST, aerosol index, moisture, moist stability, and wind shear analyses, an explanation of the methodology used for the analyses is needed. Two primary methods were employed for the analyses: First, the Probability of Exceedance (POE) contours showing the probability that a value will exceed a given threshold; second, time history plots of parameters at eight specific points. The POE measures were used to study the SST and AI present from the first of June to the 31st of November while the time series were used to examine moisture, moist stability, and vertical wind shear from July through October.

The Probability of Exceedance (POE) measure determines the likelihood of an event exceeding a given threshold. The POE is calculated by summing the number of times the parameter of interest is present over the same geographic location and dividing that number by the total number of observations for the same region. In other words, Probability Distribution (PD) contours for the exceedance of different thresholds for SST and AI are determined. The POE calculation is conducted by tagging field observation cells with a binary indicator, depending on whether the value is above or below the specified threshold. If the number is above the threshold the field is tagged with a "1" and if the number is below the threshold the field is tagged with a "0." These binary

numbers are summed over all observations to calculate the exceedance numbers. Dividing the exceedance numbers by the total number of observations provides the POE for the specified threshold.

Differences images are made from these POE contours. The value at a specific geographic coordinate is subtracted from the same exact geographic location over the same timeframe in order to find the difference. For example, the POE values in June 2006 are subtracted from the values present in June 2005 (i.e., June 2005-June 2006). The same resolution, dates, and time periods for the SST (and AI) data are used for both years. Missing dates are present in both datasets, as described in Chapter 3, and these missing periods are thus excluded from the analyses. These figures provide a clear way to display the observed SST and AI differences for the 2005 and 2006 seasons.

These calculations were performed in the regional subset over the North Atlantic denoted by the red box in Figure 3 for different AI and SST threshold values. POE values provide a value between zero and one, zero indicating no probability that the specific parameter was met and one meaning that the specific parameter was met in each observation available. Difference images (2005-2006) are calculated for the following threshold: AI = 0.0, 1.0, 1.5, and 2.0; SST=25°C, 26.5°C, 28°C, and 30°C. There are areas where shading is present in the difference images at locations where no shading is present in the previous POE figures. There is a reason for this. Recall that the first contour for the POE indicates a value equal to or greater than 10% (i.e., 0.1). Exceedance probabilities do exist below this first 10%. It is because of the areas in which aerosols are present less than 9% of the time that difference images may have shading where there is no shading in

POE figures. For example, Figure 4 shows this lowest 9% POE for the 2006 season. When the differences are calculated, these lower values cannot be ignored because they could increase or decrease the frequency of occurrence of values above the specified threshold between seasons.

For the SST and AI analyses, Fortran code was written to read the data files and calculate the POE for the area of interest (i.e., 0-50°N, 100-0°W). The output of the program consisted of the latitude, longitude, and parameter of interest (i.e., SST, POE and AI POE). R, a computer language used for computing statistics and creating graphics, was then used to create the POE images from the data and to calculate and display the difference images.

Time history plots are generated using daily NCEP analysis fields for the hurricane season of 2005 and 2006. These time series are used to look at moisture, moist stability, and vertical wind shear at eight different points in the North Atlantic. Figure 4 shows the location of these points. At each of these points, the Skew-T data that was used included the height (km), sea level pressure (hPa), temperature (°C), dew point temperature (°C), wind speed (kts), and wind direction. The dew point depression, moist stability index, and vertical wind shear were calculated in R from the data. The time series began on the 9th of July and 5th of July for the 2005 and 2006 seasons and both end on the 31st of October. For the dew point depression, wind barbs, speed shear, and directional shear, missing dates are left blank. There are a total of 52 days for 2005, and 55 days for 2006 within the period from 1 July to 31 October. June was left out because data for this month was unavailable for 2005. This period also represents the span of time in which

the highest numbers of storms form. Skew-T diagrams were created from the data at points two and three for 2005 and 2006 in order to observe wind speed and direction as well as the availability of moisture in the vertical. Plots were also made of the 500 hPa winds in order to study the movement of the easterly jet during both seasons.

The dew point depression was calculated from the temperature and the dew point depression was used as a measure of moisture in the atmosphere. The dew point depression can be related to relative humidity by the saturated mixing ratio and the actual mixing ratio at a specific temperature and pressure. A moist stability index (MSI) was calculated as follows:

$$MSI = (T_{700} - 3*T_{500} - T_{400}) - (T_{700} + T_{500} + T_{400}).$$

Negative values from this index indicate stable conditions while positive values signify an unstable environment. Vertical wind shear was calculated between three different levels: 850-250 hPa, 700-400 hPa, and 850-500 hPa. Each level was calculated as follows:

$$VWS = \sqrt{(u_a - u_b)^2 + (v_a - v_b)^2}$$

where *a* is represents the upper level and *b* represents the lower level. Each of these levels was chosen for a different reason. Vertical wind shear between 850-250 hPa spans the troposphere from just above the marine boundary layer. The 700-400 hPa provides vertical wind shear information in the mid-troposphere. The 850-500 hPa contains the lower part of the troposphere above the marine boundary layer and is the region in which the Saharan air layer (SAL) typically exists. The speed and directional shear are also

plotted as a time series in order to have a comprehensive picture of shear in the environment.

Any TCs that passed within 2° of these points were also noted in order to observe the surrounding environmental conditions present while a storm was in the vicinity of that particular point. Within the period of the time series, storms passed in the vicinity of Points 2, 4, 7, and 8 in 2005 and Points 1, 2, 3, 6, 7, and 8 in 2006.

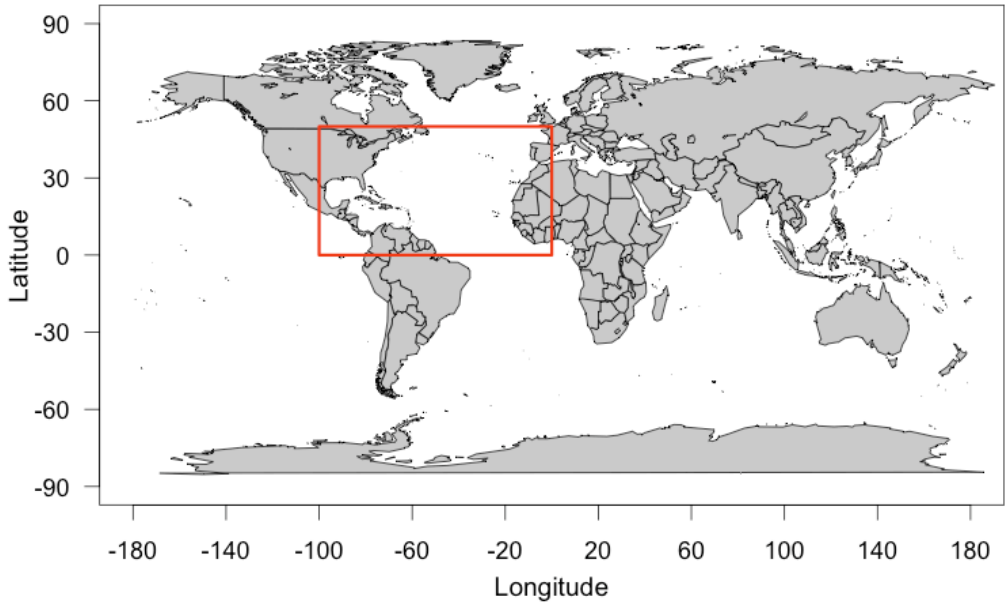

Figure 3: Region of Study: The geographic region over the Northern Atlantic for which the Probability of Exceedance (POE) contours are calculated and displayed.

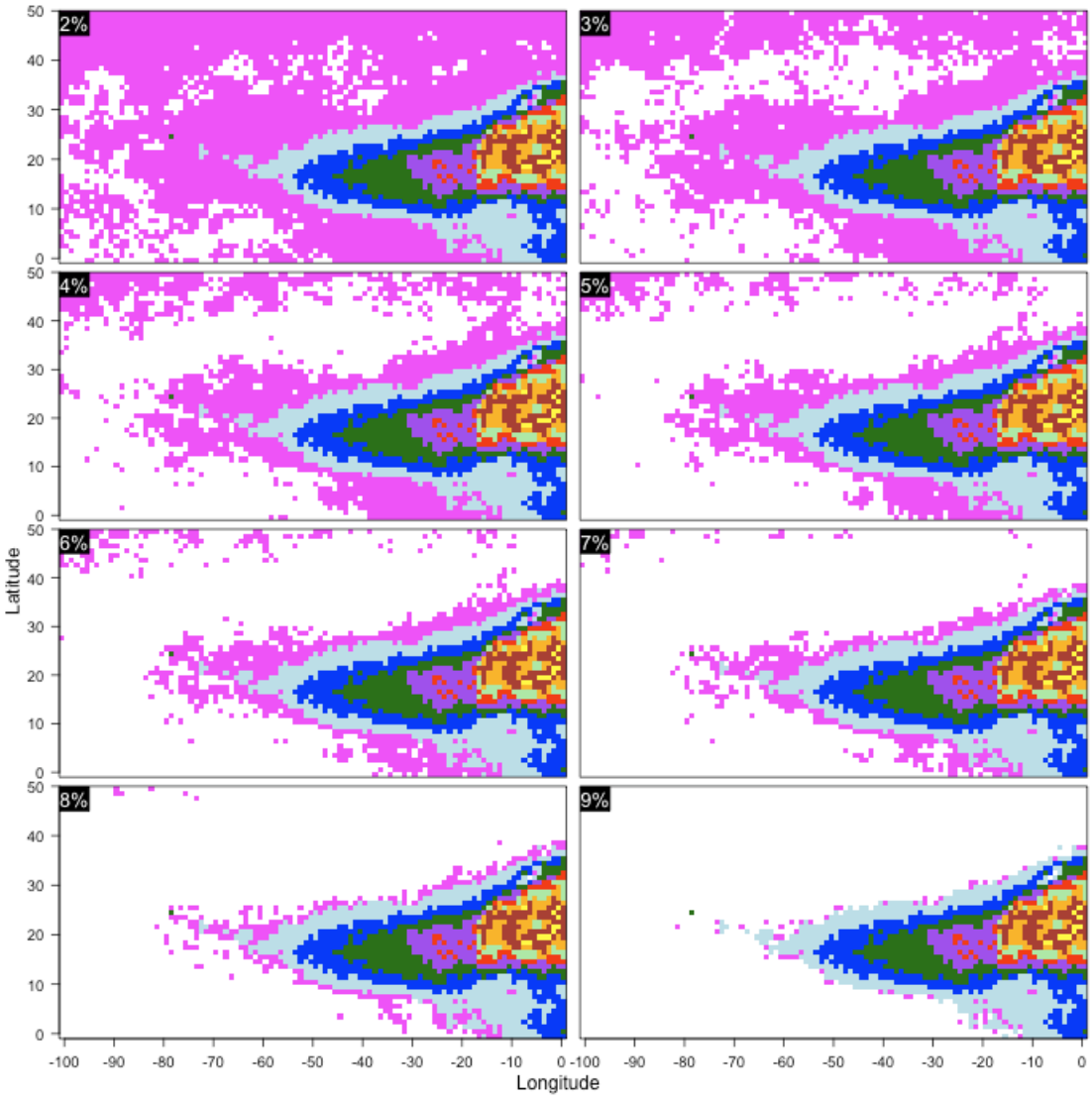

Figure 4: Exceedance Values for Given Thresholds: The first 9% of the POE values for the 2006 season AI threshold value of 1.0. This lowest 9% is excluded from the SST and AI POE images.

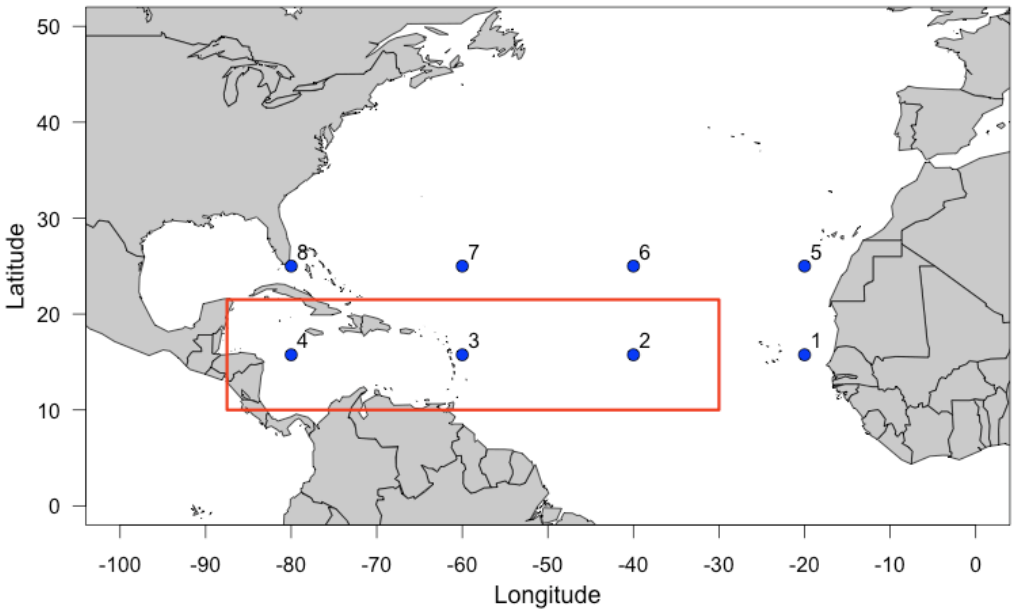

Figure 5: Time Series Points: The geographic location of eight points within and north of the main development region (indicated by a red box). Vertical profile data is taken from the NCEP analysis data for the time series analyses.

Chapter 5: Discussion of Results

5.1 TC Activity over Atlantic Basin

Each season the tropical cyclone activity varies depending upon environmental factors. Figure 6 shows TC initiation points for the period from 1900 to 2007. Panel A shows all storms while panel B shows only hurricanes. Major hurricanes are classified as TCs reaching Category 3, 4, or 5 as defined by the Saffir-Simpson scale. The cumulative strength for a season is calculated using the Accumulated Cyclone Energy (ACE) index which takes into account the total number of storms in a season as well as the strength and duration of each storm. The strength of the Atlantic hurricane season is largely determined by the number of TCs forming between Africa and the Caribbean Sea during the peak months of the season (August through October). This area is called the Main Development Region (MDR) and indicated by a yellow box in Figure 6. This region roughly extends from 10°N – 20°N and 30°W – 87.5°W in which the majority of TCs form (Goldenberg et al., 2001). Figure 7 shows the storm tracks and corresponding strength for all storms in the 2005 and 2006 season.

TCs form over warm waters from pre-existing disturbances. The process by which a tropical cyclone forms and subsequently strengthens into a hurricane depends on favorable environmental conditions. Above normal hurricane seasons (such as 2005)

result from an inter-related set of key atmospheric and oceanic environmental conditions favoring hurricane formation, particularly in the MDR. These key environmental conditions include: 1) a pre-existing disturbance with thunderstorms; 2) warm (at least 26.5°C) ocean surfaces to a depth of about 50 m; 3) relatively moist air near the middle of the troposphere (~ 5 km); 4) light upper level winds that do not change much in direction and speed through the depth of the atmosphere (i.e., low wind shear), or low values (less than about 15 m/s) of vertical wind shear between the surface and the upper troposphere; and 5) an unstable atmosphere in which air cools fast enough with height such that it is potentially unstable to moist convection.

These five environmental conditions are apparently necessary but insufficient conditions to develop and sustain TCs. In the Atlantic basin, even when all these conditions appear favorable sometimes TCs do not occur. There is much speculation on what the "missing link" (or links) might be. Studies have shown that subsidence, which suppresses cloud formation by drying the atmosphere, impedes ascending air. Therefore, Saharan dust storms that accompany the African monsoon and propagate far into the Atlantic may be the missing link or one of the missing links to better understanding environmental influences on TCs.

With the occurrence of 28 named storms, the 2005 Hurricane season was the most active season in the known history of the Atlantic basin. As well as having the largest number of storms on record – 12 tropical storms and 15 hurricanes – numerous other records were broken. The 2006 Atlantic hurricane season was forecasted to continue the trend, commencing in 1995, of above-normal hurricane seasons. Forecasts called for an above-

normal season but not one of the magnitude experienced in the 2005 season. What resulted were five tropical storms, five hurricanes, and an ACE index that was 90% of the median. Comparatively, the ACE index was 285% greater than the median in 2005. The median for the ACE index from 1950 to 2000 is 8.75×10^4 kt^2. Figure 7 shows the tracks of the 2005 and 2006 Atlantic Hurricane seasons. Storm tracks are indicated by a black line and intensity measurements taken every six hours are indicated by a colored circular dot or symbol. Category 1, 2, 3, 4, and 5 storms are indicated by light blue, blue, red, purple, and black colors, respectively. Tropical storm and tropical depression strength are signified by yellow and green. Subtropical and extratropical storm stages are indicated by an orange dot and black 'x', respectively.

According to the Climate Prediction Center's (CPC) annual report there were several factors that played a role in 2005 being such an active season. Characteristics of the 2005 season that were similar to other very active Atlantic hurricane seasons included low wind shear, low sea level pressure, a favorable African easterly jet, weak easterly trade winds, strong upper-level easterlies, and record high SSTs. The Annual Summary for the Atlantic Hurricane Season of 2005 (Beven et al., 2008) recognized record warm SST in the Caribbean Sea and tropical Atlantic with anomalies greater than 1°C as one of the primary factors resulting in such an active season. But this indicates that a considerable amount of research is still needed to fully explain the activity in this record breaking season. Additionally, several storms went through periods of rapid intensification during this season. For example, Wilma's sea level pressure dropped 88 hPa in 12 hours making it the fastest deepening rate on record for Atlantic TCs. According to Franklin and

Brown (2008), the weaker than expected 2006 season suffered from competing environmental conditions – 2006 had the second warmest SSTs on record since 1871, which created favorable conditions, while El Nino, developing late in the summer and suppressed TC activity. SST anomalies were not as great in 2006 as they were in 2005, yet SST anomalies across the tropical Atlantic and into the Caribbean, ranging between 0.5°C and 0.75°C above normal, were still high (Bell et al., 2006; Bell et al., 2007). The CPCs report noted the influence of El Nino in suppressing TC activity across the Caribbean through increased upper-level convergence and sinking air. This is considered to be a factor in the lack of TC development over the Gulf of Mexico and western tropical Atlantic because, even when wind shear values were less than 8 m/s during September and October in the Gulf, only one TC formed in that region (Bell et al., 2006; Bell et al., 2007). Vertical wind shear during the most active period of the season was anomalously weak in the MDR relative to the 1971-2000 seasons. Slightly increased wind shear, related to El Nino, was present in the western Caribbean according to the CPC report. The CPC noted an increase in vertical wind shear across the central MDR in August from a mid-oceanic trough, and this is considered to have reduced activity in the central MDR for 2006. However in 2005, only two, maybe three, TCs formed in this same area of the MDR where increased shear values were observed by the CPCs report, none of which occurred during the month of August. The increased convergence aloft and sinking air can explain the lack of storm development in the Gulf of Mexico and Caribbean Sea, but the question still remains as to why a smaller number of storms developed in the tropical Atlantic in 2005 as opposed to 2006. In 2005, eight storms

formed in the Gulf while only one storm formed in the same region in 2006. Franklin and Brown (2008), in their review of the 2006 season, also noted the presence of large-scale steering patterns caused by a midlevel trough along the eastern US which prevented storm tracks from impacting the Bahamas, Cuba, and US in September.

As indicated in Figure 7, TC activities of the 2005 and 2006 hurricane seasons show significant contrast. In this study, we will primarily concentrate on the analyses of the above mentioned key environmental conditions, along with a somewhat unconventional condition (i.e., Saharan dust) that has been suggested as a potentially influential factor in TC formation, for the 2005 and 2006 hurricane seasons to better understand the impact of environmental conditions on TC activity.

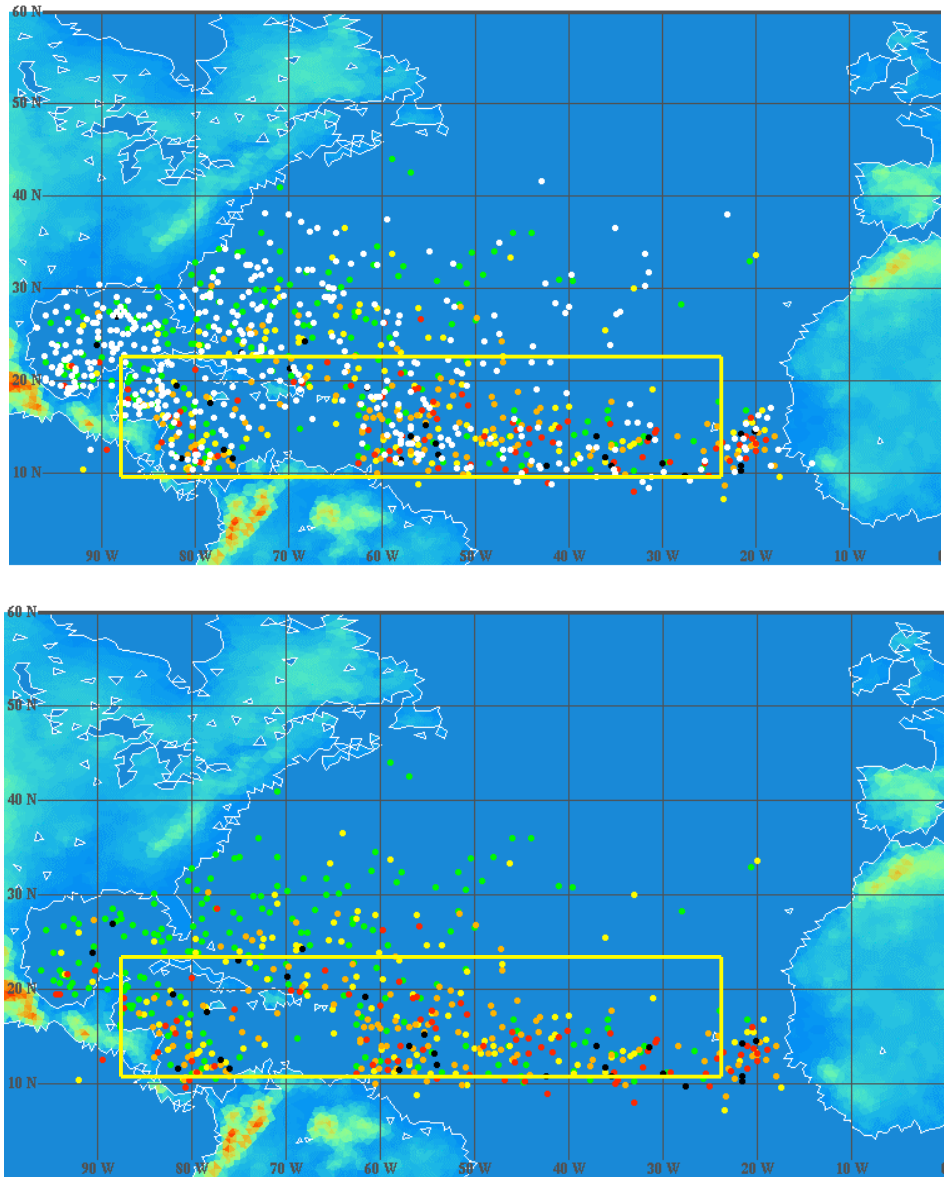

Figure 6: Initial Points for Tropical Cyclones in Atlantic Basin: TC initiation points for the period of record from 1900 to 2007. The top figure shows initiation points for all storms and the bottom figure displays points for hurricanes only. Black, red, orange, green, and yellow dots indicate Category 1, 2, 3, 4, and 5 strength storms, respectively, while white dots shows locations of tropical storms. The yellow box indicates the Main Development Region (MDR) for TCs.

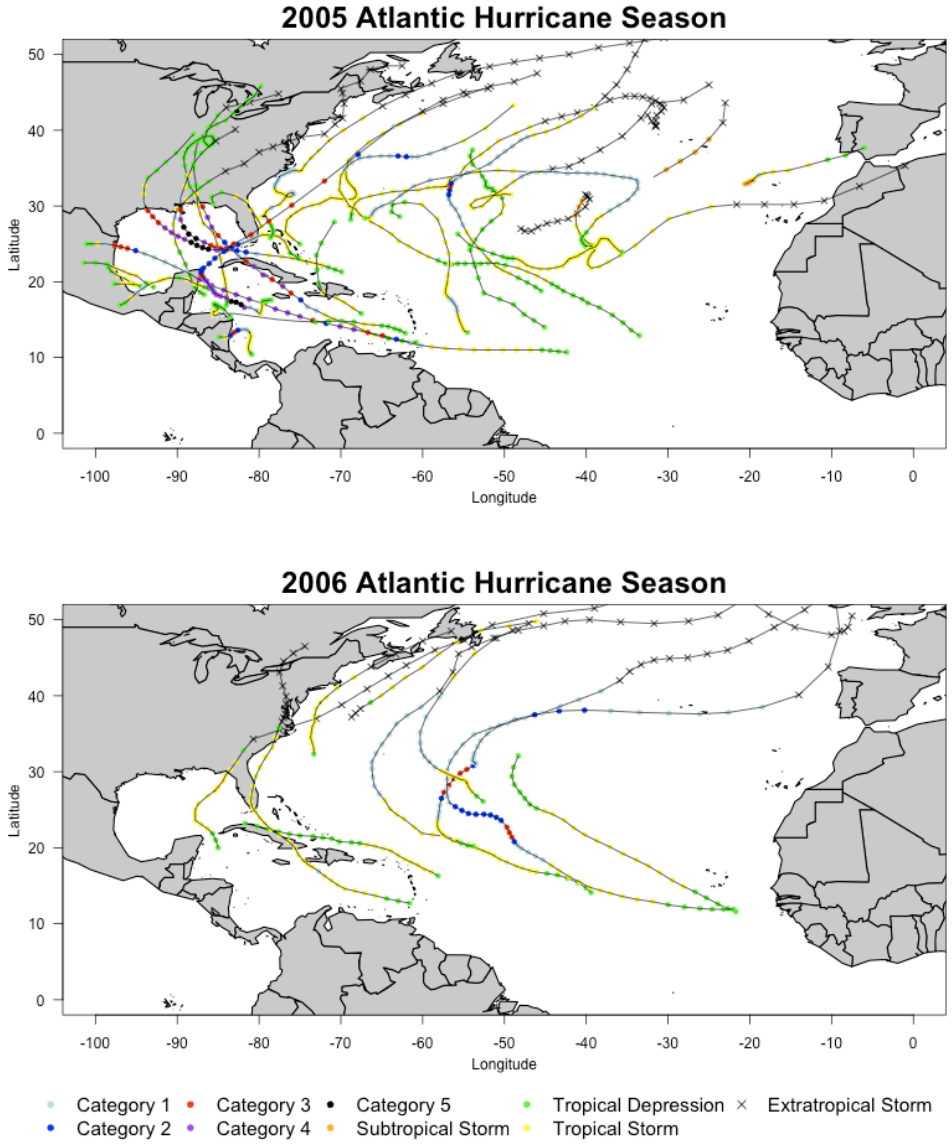

Figure 7: Atlantic Hurricane Season for 2005 and 2006: Shows TC tracks and corresponding strengths for all storms. The 2005 season experienced 28 named TCs while the 2006 season had 10 TCs. The black line indicates the path of the TC while the color code indicates the strength the storm was observed at by the NHC. Category 1, 2, 3, 4, and 5 storms, respectively, are indicated by light blue, blue, red, purple, and black, respectively. Tropical storm and tropical depression strength are signified by yellow and green. Subtropical and extratropical storm stages are indicated by an orange dot and black 'x'. (Data source: HURDAT)

5.2 Sea Surface Temperature Comparisons

The most well known and perhaps most important factor that influences TC origin, development, and activity is sea surface temperature (SST). As water vapor (water in the gaseous state) rises via evaporation from the ocean surfaces, it cools. This cooling causes the water vapor to condense into liquid (i.e., clouds). In the process of condensation, latent heat is released providing the storm with energy. This heat warms the atmosphere making the air lighter, which then still continues to rise into the atmosphere. As the air rises, more air converges near the surface to take its place. Hence, the warm water is one of the most important environmental factors as it is water that powers the TCs. It is important to note that normally, a SST value of 26.5°C reaching to a depth of 50m is considered the minimum to maintain TCs. Warm waters fuel these tropical systems and are needed to maintain the warm core. This value (26.5°C) is well above the global average surface temperature of the oceans.

The SST comparisons utilize data from the aforementioned GHRSST dataset from the first of June to the end of November (i.e., the hurricane season as defined by the NHC). The results from the SST analyses for the entire hurricane season are shown in Figure 8 where 2005 results are shown in the top four panels and 2006 results are shown in the bottom four panels. Panels A, B, C, and D show analyses for the SST threshold values of 25°C, 26.5°C, 28°C, and 30°C, respectively. The POE contours are calculated as described in the method section (Chapter 4). Each color indicates a 10% (i.e., 0.1) increase in the probability the observed value exceeds the given threshold value. For example, panel A of Figure 8 uses 25°C as the threshold value for SST. The first color

interval indicates a greater than or equal to 10% chance that SST values reached or exceeded 25°C. Each ensuing contour indicates a 10% increase, above the initial interval color, in the probability that SST in that region will be greater than 25°C. The same color scheme is used in panels B, C, and D where the threshold values are 26.5°C, 28°C and 30°C, respectively.

In order to quantify the SST differences between 2005 and 2006, Figure 9 shows difference images for each threshold for the SST probabilities and four different colors are used to denote the comparison. The difference was computed by subtracting the value at a particular point in 2006 from the value in 2005 at the exact same location. All areas in which there is no probability of SST reaching the lowest one percent of exceedance are excluded from the difference images (and therefore indicated in white color). Additionally, regions in which there is no difference in probability between one year and the other are also indicated in white color. There are however, regions where shading is present in the difference images in an area where no contours are present in the POE images – the reason for this is explained in the methods section. In the color scheme used, blue indicates negative POE difference values between -1.0 and -0.5 while purple denotes negative values greater than -0.5 and less than 0. Yellow indicates positive values greater than 0 up to 0.5 while red indicates positive values ranging from greater than 0.5 up to 1.0. Negative values (i.e., blue and purple) show a higher probability that the SSTs will exceed the given threshold in 2006, while positive values (i.e., yellow and red) show a higher probability SSTs will exceed the given threshold in

2005. For example, red is present in a region where SST were greater in 2005 than in 2006 for more than half of the observations available.

Analyses shown in Figures 8 and 9 clearly indicate that SST values during the 2005 hurricane season were significantly higher than in the 2006 season. In 2005, SST values were generally greater than 1°C above the climatological mean. SST values in the Main Development Region (MDR) were between 0.5°C and 0.75°C above the climatological mean for 2006. Based upon Emanuel's Power Dissipation Index (PDI), higher SSTs would favor stronger hurricanes (Emmanuel, 2005). Therefore, the unusually high TC activity and large ACE index in 2005 can be mainly attributed to these significantly high SST values. For example, Figures 8C and 8D show that SST values were consistently above 28°C over the MDR and Gulf of Mexico during the entire hurricane season (i.e., June to November), while the SST values were almost always above 30°C across the Gulf of Mexico during the 2005 hurricane season. In the difference image, Figure 9 panel C, warmer temperatures occur slightly more often in 2006 as compared to 2005 even though the probabilities are quite similar in both seasons. There are two possible explanations for this: 1) there is a difference in the frequency of occurrence of temperatures between seasons, and 2) storms continually passing over this region in 2005 mixed warm surface water down to lower depths and colder, deeper ocean waters up to the surface resulting in cooler surface temperatures in the Gulf.

Further monthly SST analyses (Figures 10 -21) indicated that, particularly during summer months (June, July, and August), SST values were unusually high in 2005 over both the MDR and Gulf of Mexico. In June (Figure 11) the majority of the central to western

Atlantic had higher SSTs occurring two times more often in 2005. Two TCs formed in June of 2005 and one formed in June of 2006. In July of 2006, Figure 12 shows SSTs warming but not yet reaching the warmth already present by July of 2005. Figure 13 panel C, shows a significantly higher occurrence of SSTs greater than 28°C in 2005. Five storms occurred in July of 2005 while two storms formed in July of 2006. By August, Figure 14 shows that the 2006 SSTs had reached the minimum 26.5°C threshold across the MDR with warm temperatures extending further east and north in panel B than 2005 SSTs. The differences in Figure 15 panel C, show warmer SSTs present north of the eastern portion of the MDR in 2006. However, the central portion of the MDR had SST greater than 28°C occurring more often in 2005. This means that the minimum threshold SST needed for TC development was met over a larger region in 2006 but that SST in 2005, though not extending as far eastward, reached higher SST values in the mid-Atlantic. SSTs exceeding 30°C present in the Gulf of Mexico are approximately equal in likelihood of occurrence between seasons as indicated by the white in the image. Five TCs formed in August of 2005 while three formed in August of 2006.

September is the most active month in 2006 as all four TCs that form reach hurricane strength. Despite warmer SSTs in the Gulf of Mexico in 2006, storms during this month form in the mid-Atlantic or along the southern edge of the MDR and not in the Gulf of Mexico. Considering the late summer development of El Nino resulting in the presence of enhanced convergence aloft and descending air in the Gulf of Mexico, as noted by the CPCs report, El Nino may explain the lack of storms forming in the Gulf despite such warm SSTs being present. In 2005, five storms also form in the central to western

Atlantic region. No TCs form in the Gulf in 2005 in September. By October, Figures 18 and 19, SST in both 2005 and 2006 are beginning to cool. In the central Atlantic, 2005 SST remain warmer while 2006 SSTs are warmer in the Gulf. This trend of cooling SSTs and comparable SST values continues into November.

We expected to find higher SST values in the 2005 season than the 2006 season. These results confirmed that information provided by the Climate Prediction Center (CPC) and published 2005 Atlantic season summary. Overall, SSTs in 2005 are warmer than the SSTs in 2006 and the primary contributor to a very strong 2005 season. Analyses of both years show that SST conditions needed to support development have been met by the presence of SSTs greater than or equal to 26.5°C. However, the comparison also shows that temperatures in 2005 were, in general, much higher, particularly in the Western Atlantic and MDR, than those occurring in 2006.

Three studies point towards the hypothesis that SSTs may be influenced by the presence of Saharan dust. Lau and Kim (2007a) suggest Saharan dust may be the reason why SSTs were cooler in 2006. However, there are other aspects associated with Saharan dust that may have a significant impact upon tropical storm development as opposed to directly influencing SST values. Again, the understanding of the impact of the SAL is mixed – some research points towards it enhancing convection that is needed for a TC to develop while other research efforts argue that Saharan dust inhibits TC genesis and development, and others find mixed results associated with cloud microphysics. At present, a larger number of papers point towards the inhibiting impact of Saharan dust on TCs. For example, one study found that the SAL, by enhancing baroclinic instability, aided the

formation of two storms in the Atlantic (Karyampudi and Pierce, 2002). Dunion and Velden (2004) describe Saharan dust as an environmental factor that inhibits TCs by enhancing stability, adding dry air to the system, and increasing vertical wind shear. Evan et al. (2006) established what they considered a direct link between the suppression of TCs and Saharan dust after comparing 25 years worth of aerosol and storm location data. The 2006 field program, NAMMA, which extensively studied African Easterly Waves (AEWs) and the structure and evolution of the SAL, found mixed results. Convection associated with the SAL could aid TC formation but persistent low humidity combined with high shear appears to hinder the storm development over time (Zipser et al., 2009). The next chapter will look to Saharan dust and what potential role it may or may not have played in these two seasons, as well as note any possible general observations that may aid in understanding the difference between seasons.

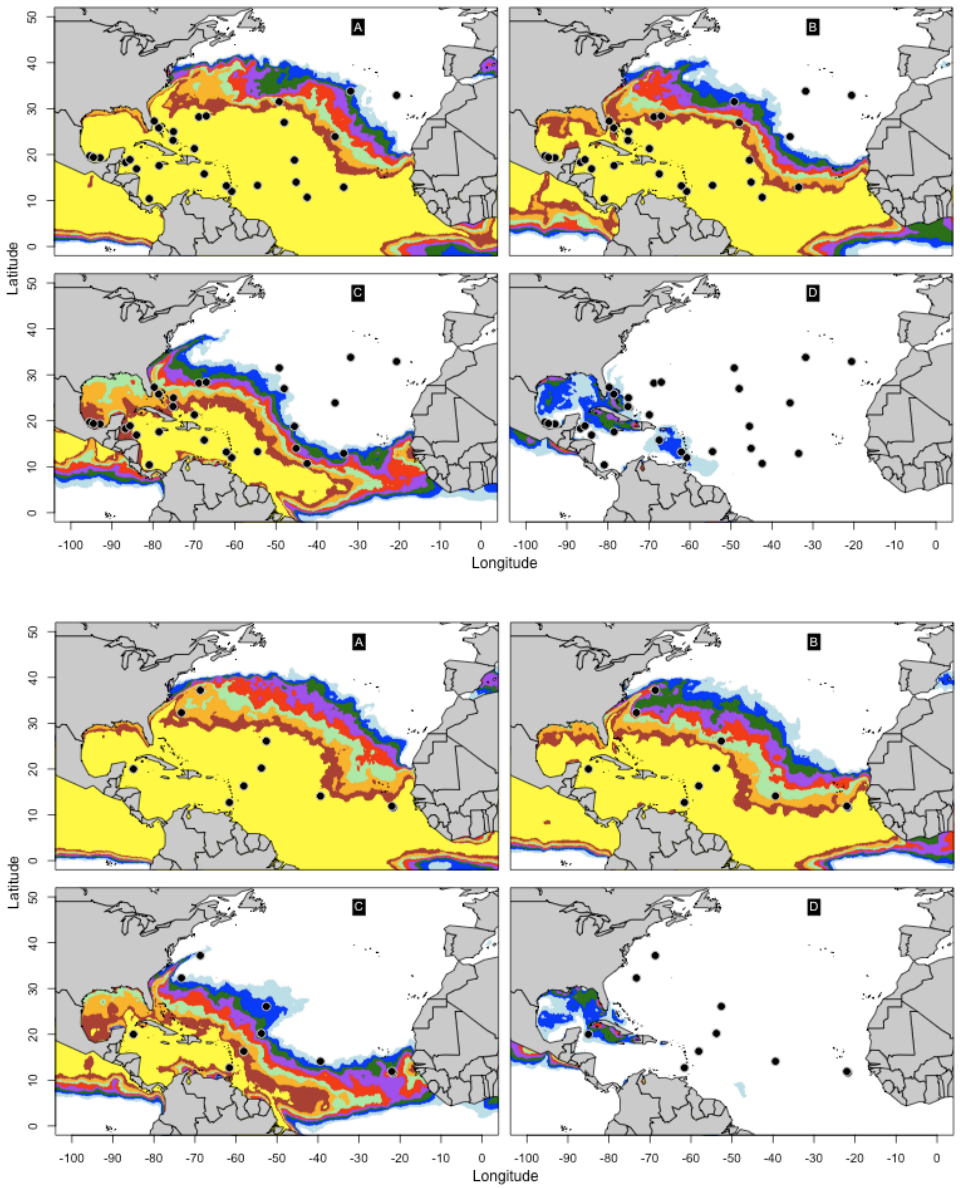

Figure 8: 2005 SST Probability of Exceedance (POE): The SST analyses for the 2005 (top four panels) and 2006 (bottom four panels) hurricane seasons. Each figure displays initial location of TCs (black dots) and the calculated POE values (color contours) for 25°C (panel A), 26.5°C (panel B), 28°C (panel C), and 30°C (panel D) SST threshold values. Color contours show the POE probabilities: light blue is greater than and equal to 10%, blue 20%, dark green 30%, purple 40%, red 50%, light green 60%, orange 70%, brown 80%, and yellow 90%.

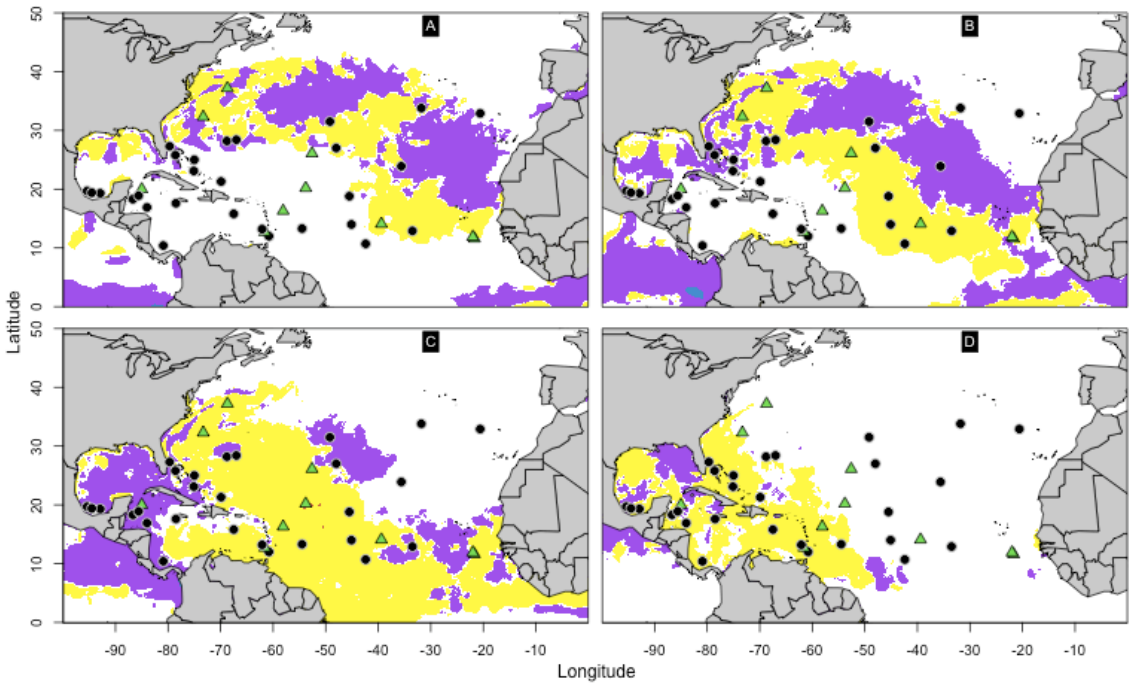

Figure 9: Seasonal SST POE Differences (2005-2006): Each of the four panels, A, B, C, and D displays the POE difference between the 2005 and 2006 for the SST threshold values of 25°C, 26.5°C, 28°C, and 30°C, respectively. Four different colors are used to denote the comparison. Blue indicates negative values between -1.0 and -0.5, while purple values denote negative values greater than -0.5 and less than 0. Yellow indicates positive values greater than 0 up to 0.5 while red indicate positive values than 0.5 up to 1.0. Negative values (blue and purple) show that 2006 SST values are greater than 2005 SST values, while positive values (red and yellow) show that 2005 SST values are higher than 2006 SST values. Black dots indicate the initial locations of TCs in 2005, while triangles indicate the initial locations of TCs in 2006.

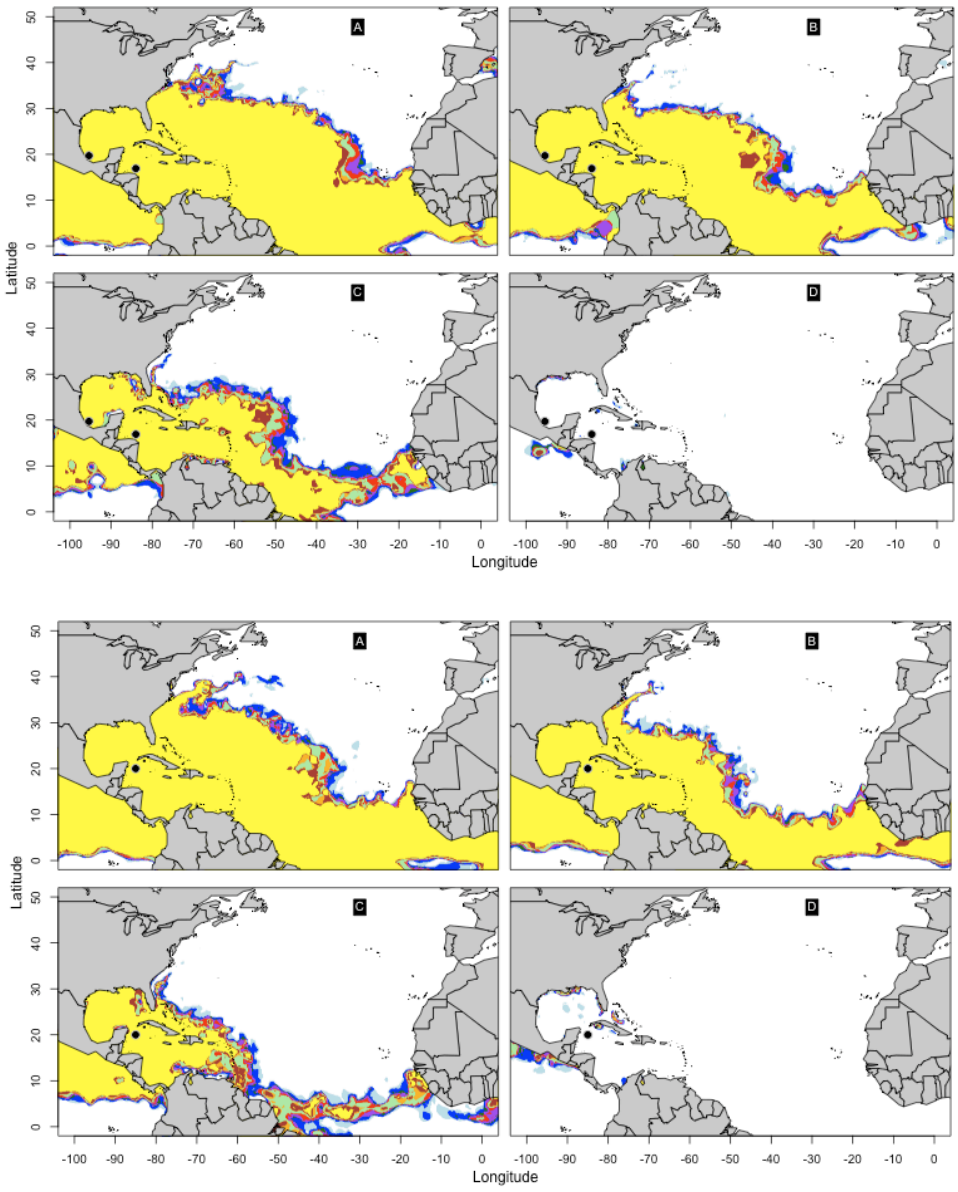

Figure 10: June SST POE: Same as Figure 8 except that this displays the SST analyses for June of 2005 (top four panels) and June of 2006 (bottom four panels).

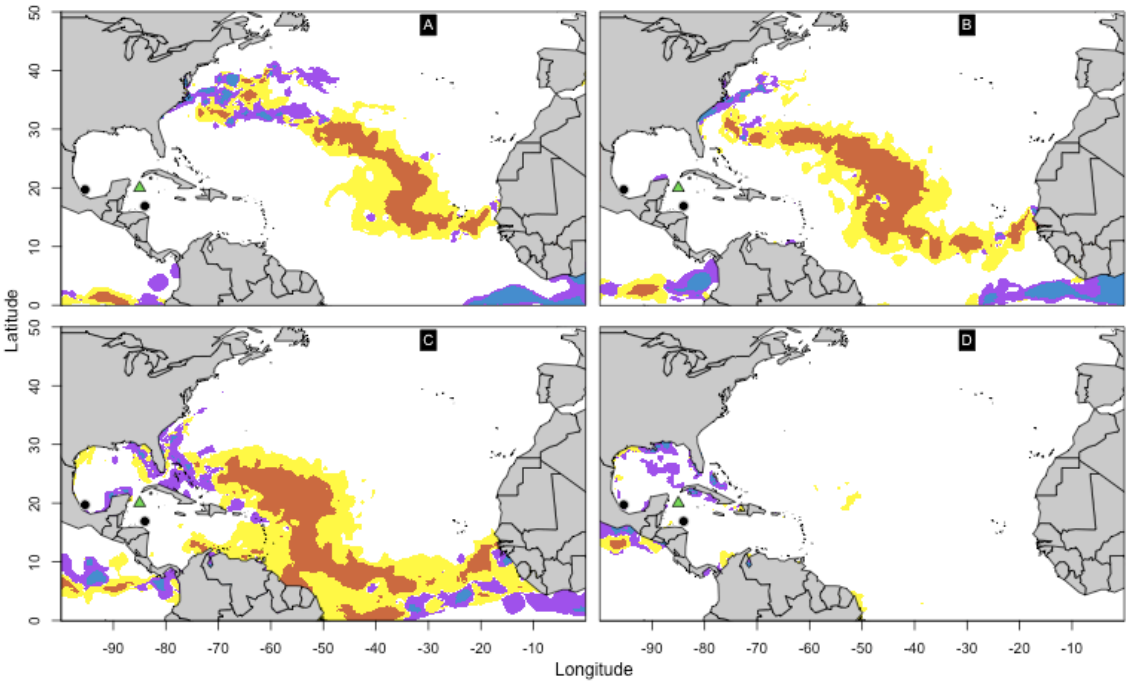

Figure 11: June SST POE Differences: Same as Figure 9 except that this displays the difference between the June of 2005 and June of 2006 SST analyses.

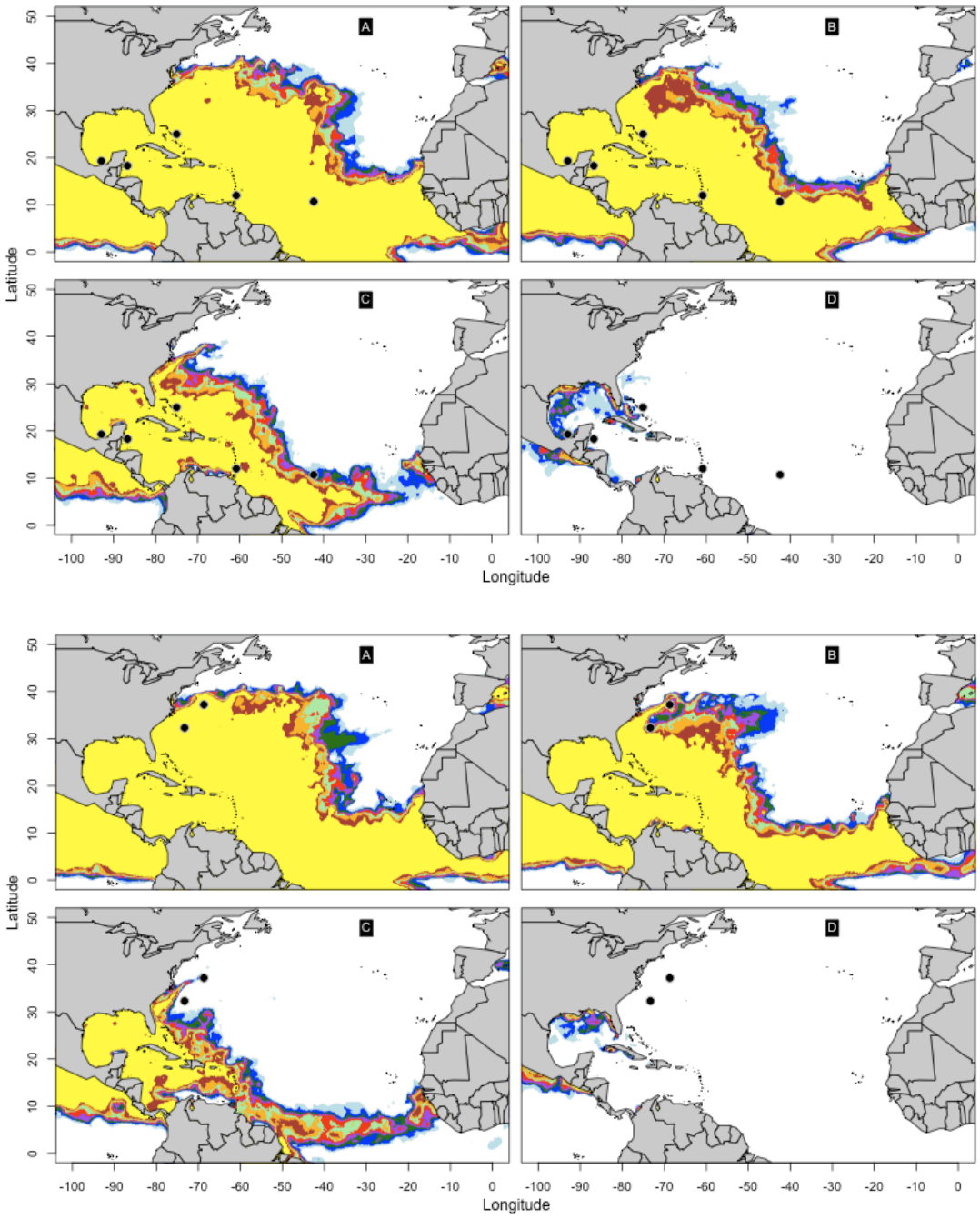

Figure 12: July SST POE: Same as Figure 8 except that this displays the SST analyses for July of 2005 (top four panels) and July of 2006 (bottom four panels).

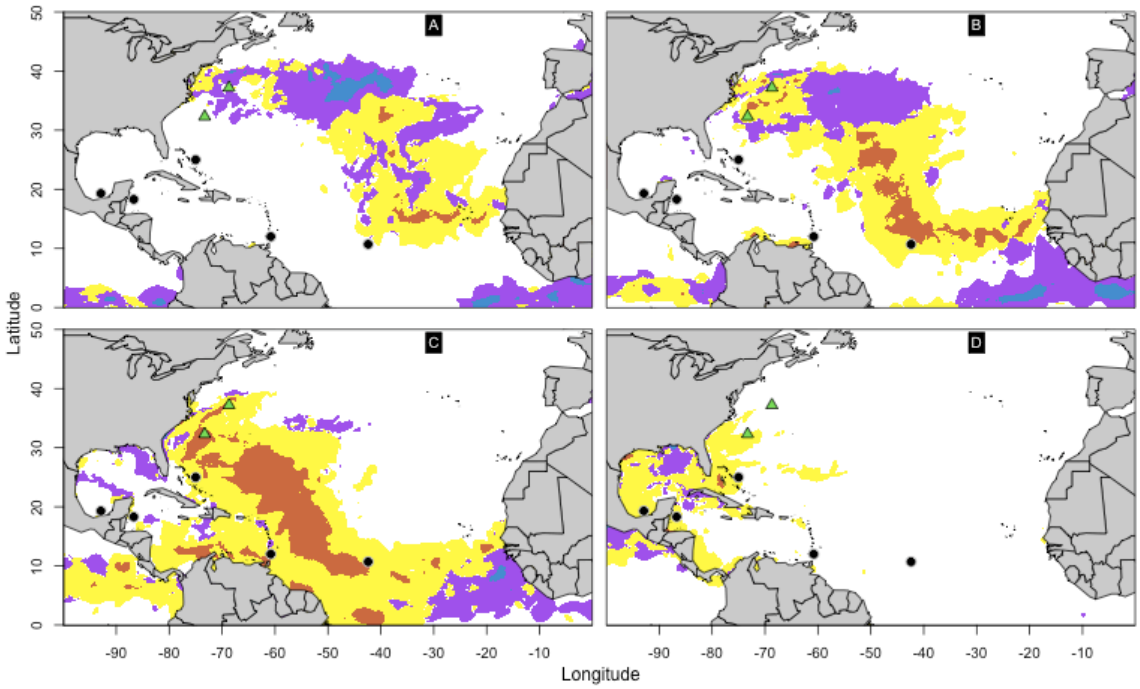

Figure 13: July SST POE Differences: Same as Figure 9 except that this displays the difference between the July of 2005 and July of 2006 SST analyses.

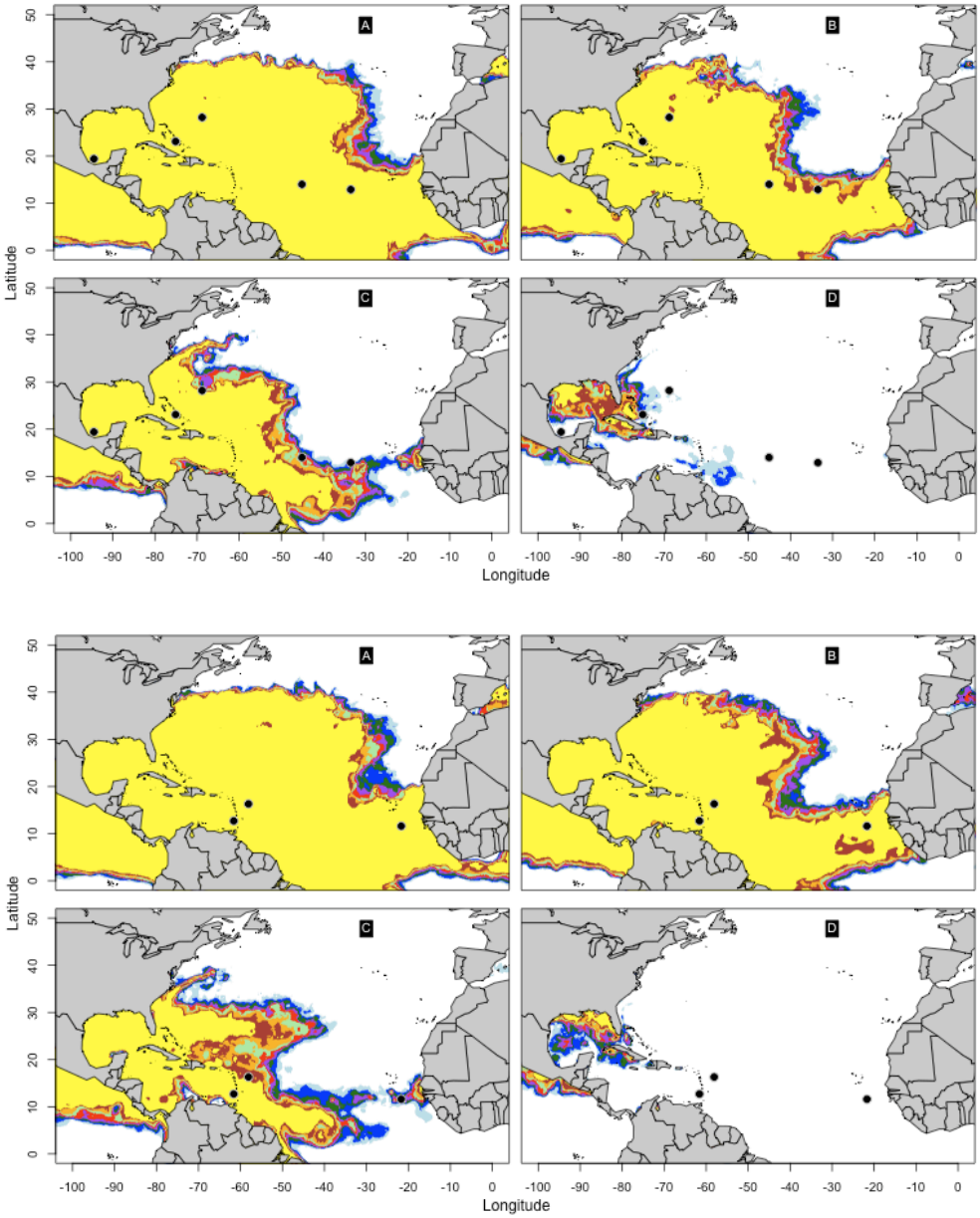

Figure 14: August SST POE: Same as Figure 8 except that this displays the SST analyses for August of 2005 (top four panels) and August of 2006 (bottom four panels).

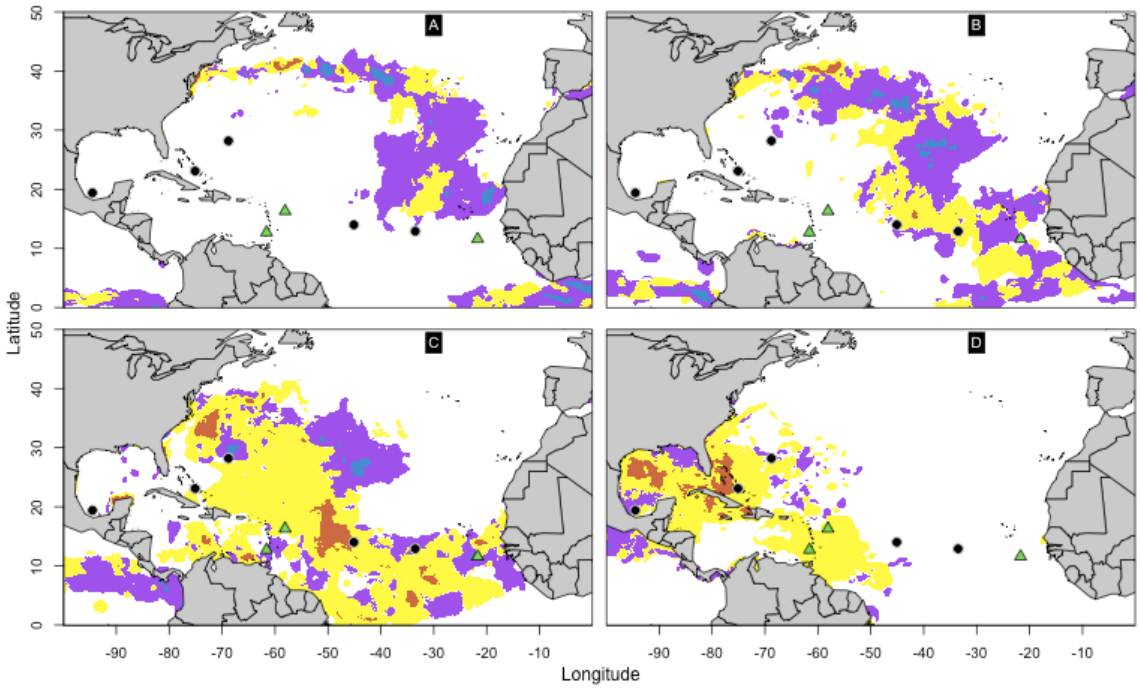

Figure 15: August SST POE Differences: Same as Figure 9 except that this displays the difference between the August of 2005 and August of 2006 SST analyses.

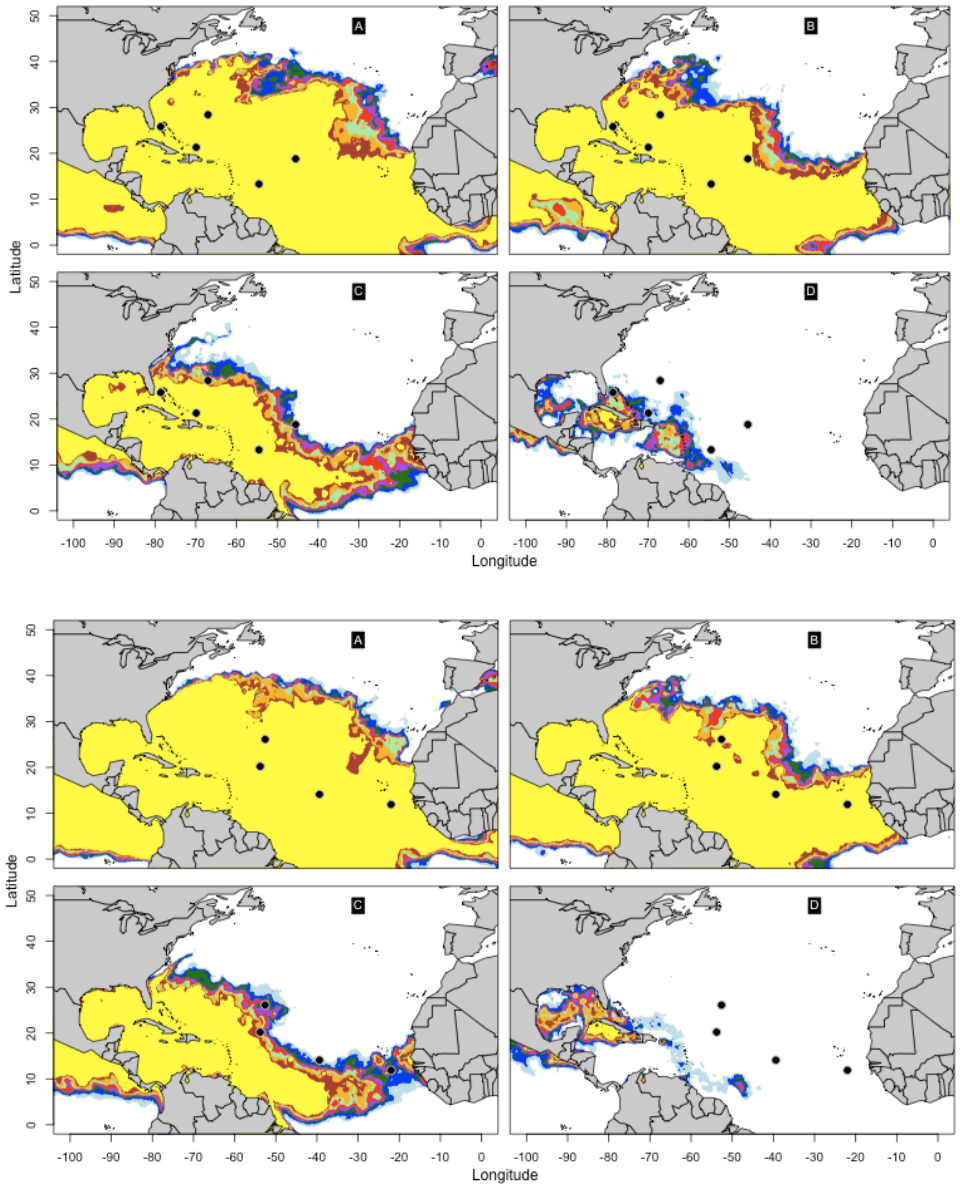

Figure 16: September SST POE: Same as Figure 8 except that this displays the SST analyses for September of 2005 (top four panels) and September of 2006 (bottom four panels).

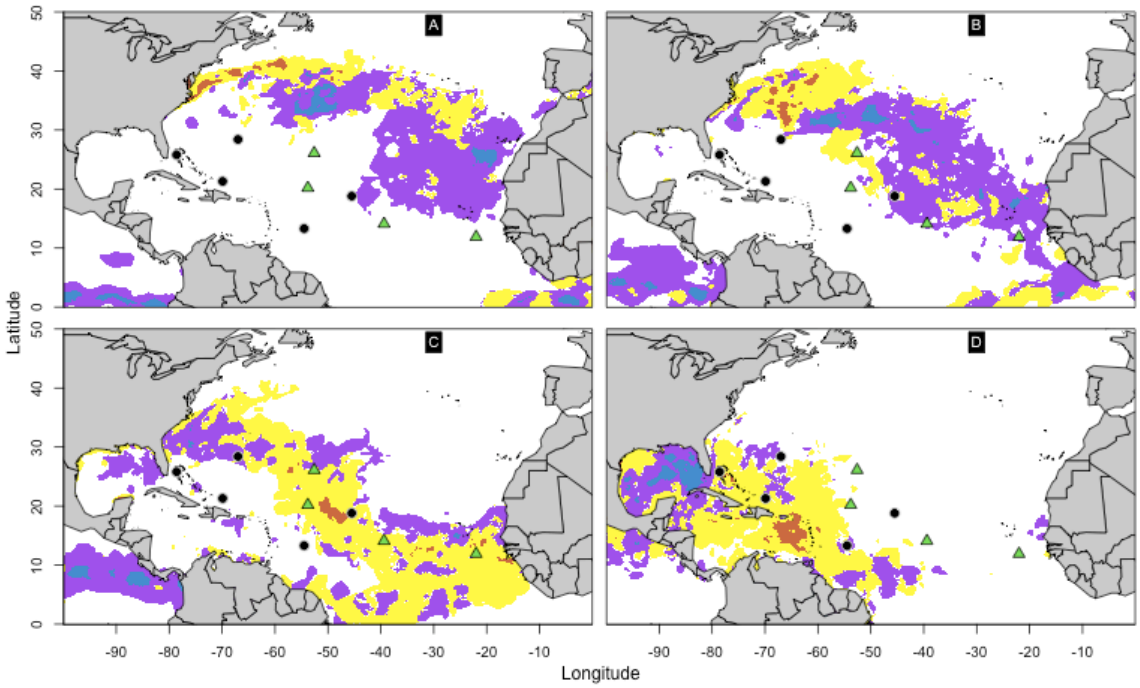

Figure 17: September SST POE Differences: Same as Figure 9 except that this displays the difference between the September of 2005 and September of 2006 SST analyses.

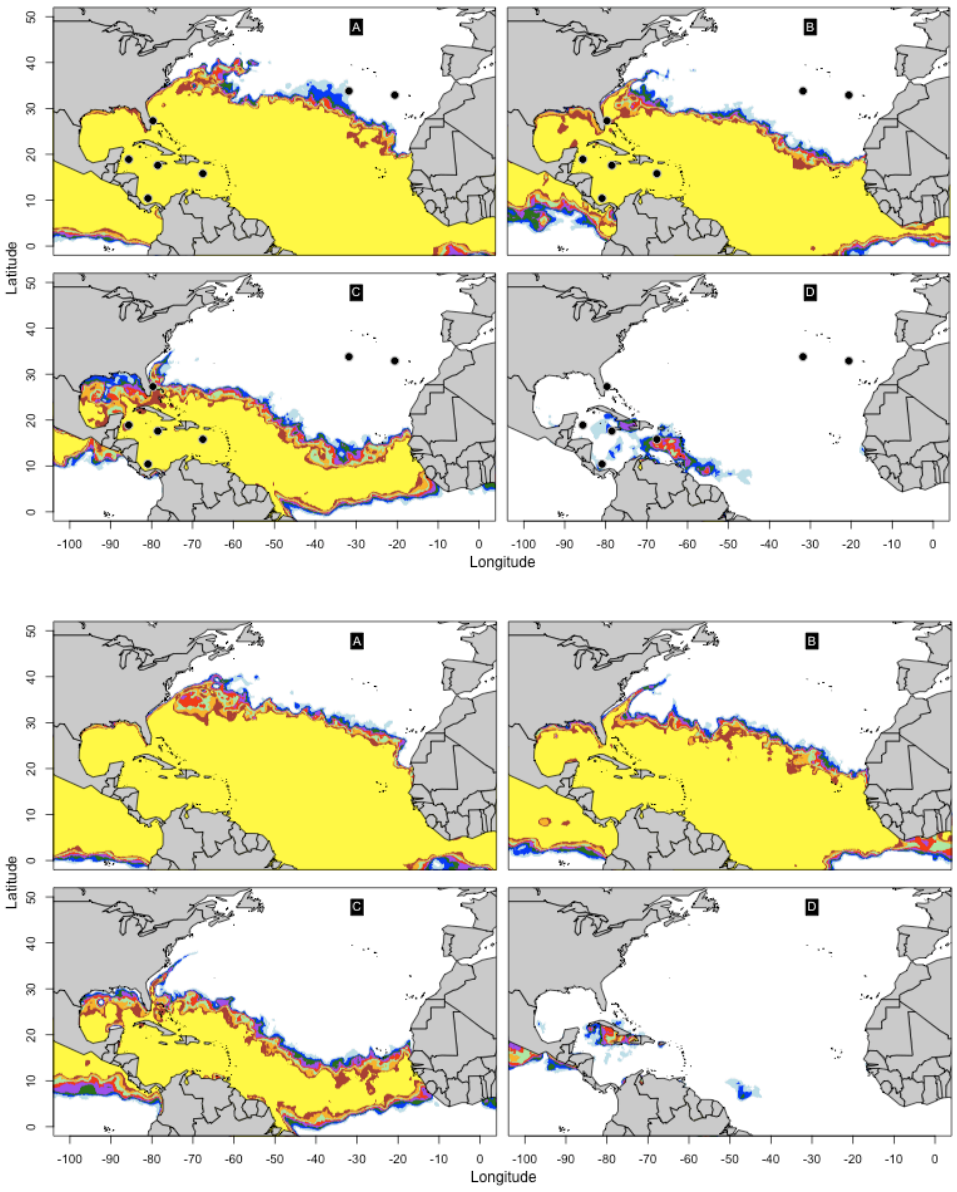

Figure 18: October SST POE: Same as Figure 8 except that this displays the SST analyses for October of 2005 (top four panels) and October of 2006 (bottom four panels).

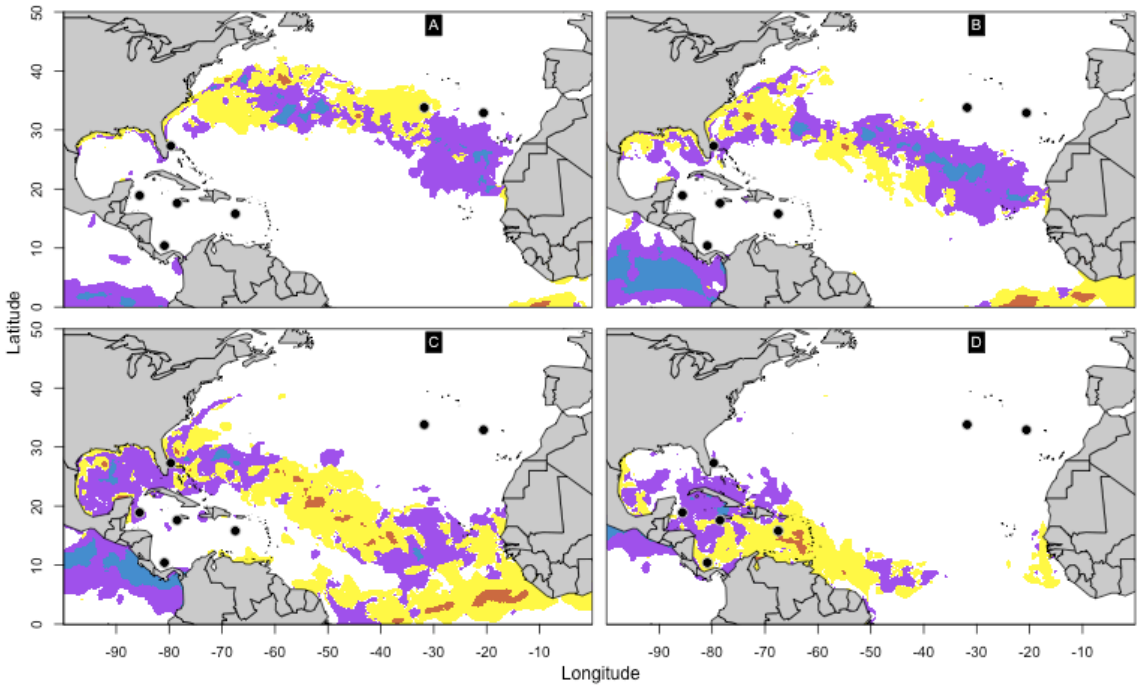

Figure 19: October SST POE Differences: Same as Figure 9 except that this displays the difference between the October of 2005 and October of 2006 SST analyses.

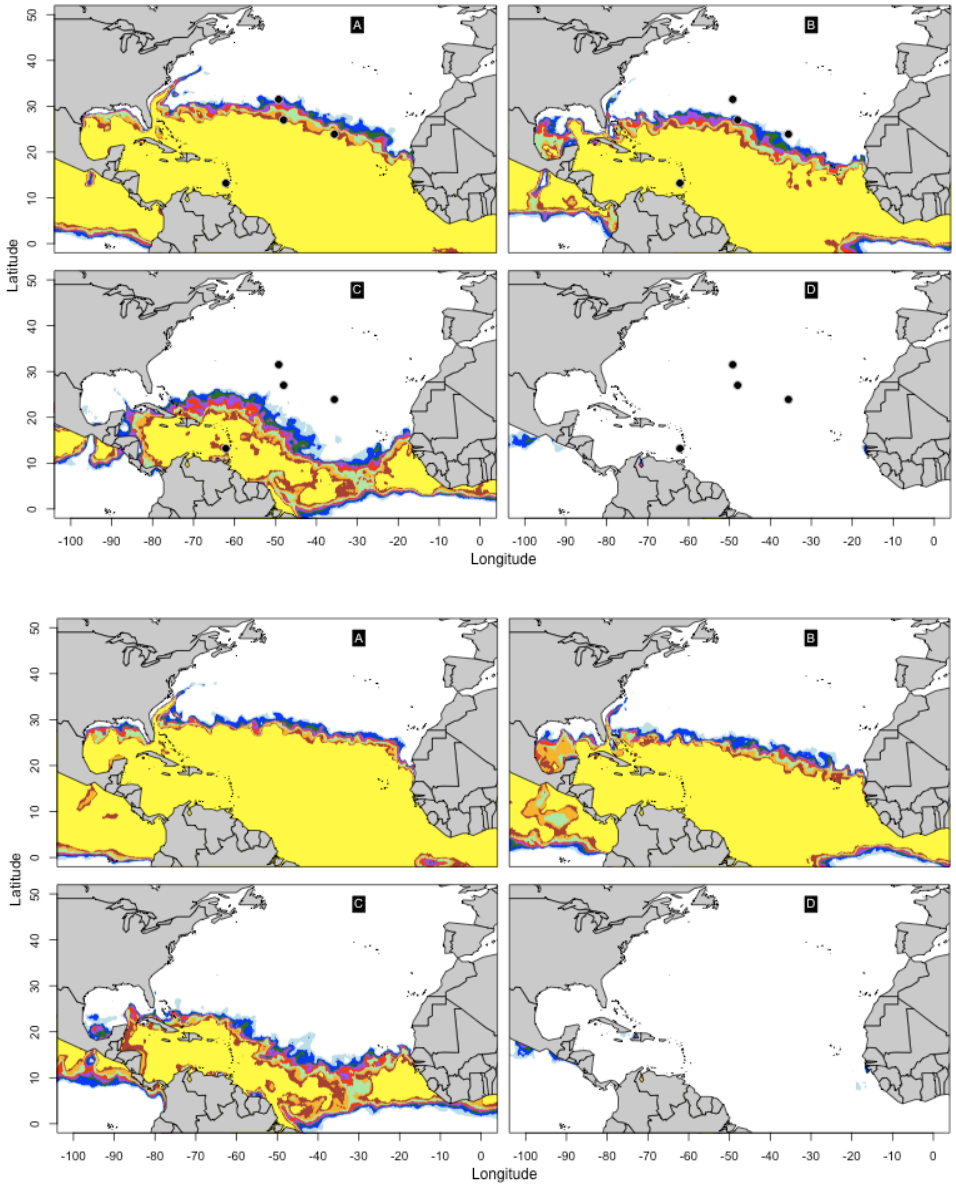

Figure 20: November SST POE: Same as Figure 8 except that this displays the SST analyses for November of 2005 (top four panels) and November of 2006 (bottom four panels).

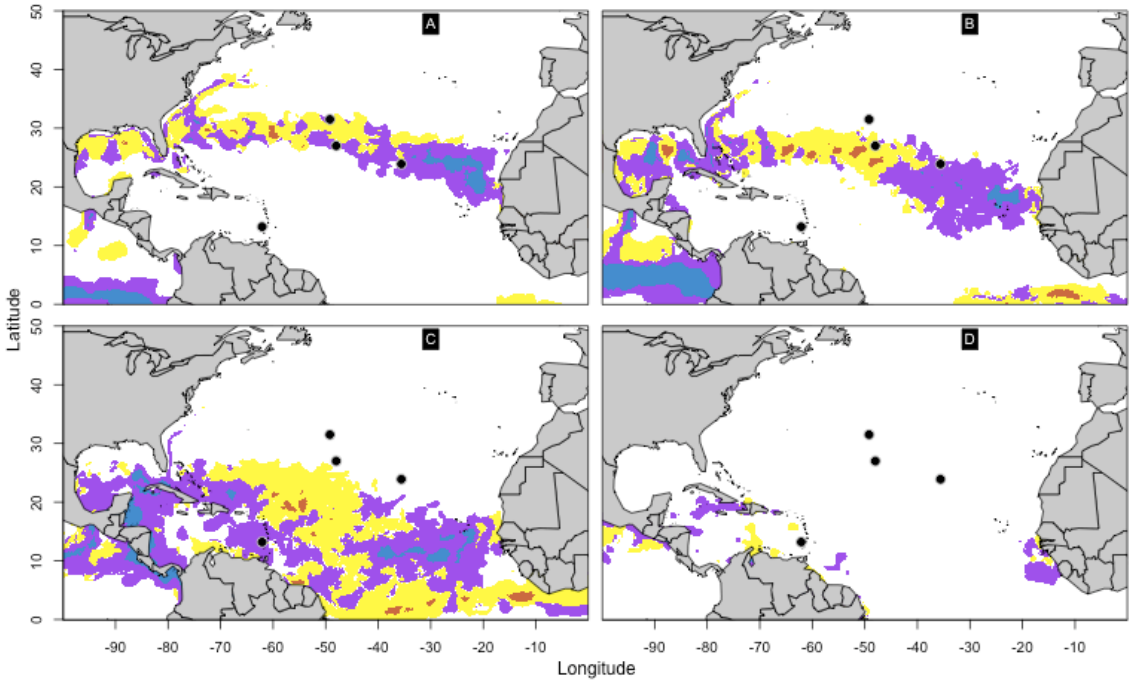

Figure 21: November SST POE Differences: Same as Figure 9 except that this displays the difference between November of 2005 and November of 2006 SST analyses.

5.3 Aerosol Index Comparisons

Although the most important factor that influences TC activity is sea surface temperature (SST) the interaction of the Saharan Air Layer (SAL) with TCs still remains largely unknown and may be yet another piece of the puzzle in advancing our understanding of TC activity and intensity change in the Atlantic basin.

An elevated SAL occurs during the late spring and summer (during the Atlantic hurricane season) over extensive portions of the North Atlantic Ocean between the Sahara Desert, the West Indies, and the United States (Prospero and Carlson, 1972; Dunion and Velden, 2004). These SAL outbreaks typically move westward off the northwest African continent every 3-5 days during the summer months and can reach as far west as the Caribbean, Central America, and Gulf of Mexico (Karyampudi and Carlson, 1988). Dunion and Velden (2004) suggested that there are several characteristics of these frequent outbreaks that can act to suppress TC formation:

i. Low to Mid-Level Dry and Increased Static Stability

The SAL contains dry and stable air that can diminish local convection by promoting convectively driven downdrafts in the TC environment. Significant arc clouds (hundreds of km in length) can be generated by these downdrafts. As they propagate away from the TC inner core, they help promote low-level outflow in the quadrant/semicircle of the TC in which they form. This outflow pattern suppresses the typical low-level inflow that is vital for TC formation and maintenance. SAL outbreaks sustain low humidity levels (~40-50% drier than the typical moist tropical atmosphere) for extended periods of time

(several days) and over great distances (1000s of km) as they traverse the North Atlantic (Dunion and Velden, 2004).

ii. Mid-Level Easterly Jet (Enhanced Vertical Wind Shear)

The SAL contains a mid-level easterly jet, which significantly increases the local vertical wind shear. The low-level circulations of TCs under the influence of this jet often race out ahead of their mid and upper-level convection, thereby decoupling the storm and weakening it. It is well known that vertical wind shear and mid-level dry air can negatively impact African Easterly Waves (AEWs) and TCs. However, what is less understood is how shear and dry air seem to act together against disturbances and how they can even act together in a nonlinear way to amplify the effects of both. Vertical wind shear can increase the entrainment of dry air by convection, which can, in turn enhance the detrimental impact of dry air on the environment.

iii. Mineral Dust

The mineral dust suspended within the SAL absorbs solar energy and subsequently releases longwave infrared energy. These thermal emissions act to warm the SAL and can re-enforce the tropical inversion that already exists in the tropical North Atlantic (Dunion & Velden, 2004). This warming helps to stabilize the environment and also limits vertical mixing throughout the SAL, allowing the SAL to maintain its distinctive characteristics. Saharan dust may even serve as effective cloud condensation nuclei (CCN) and increase cloud droplet number concentrations (Zipser et al., 2009). This can lead to an increase in both cloud optical depth and albedo because a greater number of

smaller droplets have a higher total surface area for a given mass of liquid water. This is known as the first indirect aerosol effect. In addition, the indirect aerosol effect can lead to lower precipitation efficiency. Increasing the cloud droplet number concentration decreases the average cloud droplet size. As a result, clouds will retain higher liquid water contents and have a longer lifetime. This is termed the second indirect effect. Zipser et al. (2009) also propose an enhancing effect whereby the increased cloud droplet number concentrations from increased CCN form smaller droplets. These droplets are then transported to higher altitudes before freezing. The conversion between states provides latent heat to higher altitudes in the storm, potentially enhancing convection. In short, the African mineral dust suspended in the SAL may alter microphysical and radiative properties of clouds and the environment in which TCs are embedded and hence influence AEW formation and TC activity and intensity change. SAL interaction with TC, however, still remains largely unknown

The same method used to analyze SST in the previous section was also used to study dust via aerosol index (AI) comparisons. The AI comparisons use data from the aforementioned OMI for the hurricane season (as defined by the NHC). The results from the AI analyses, for the entire season, are shown in Figure 22 for 2005 and 2006. Following the same format used to display the SST analyses, the figure panel contains four images, each showing a different threshold AI value. In all of the AI figures, panels A, B, C, and D correspond to the AI threshold values 0.0, 1.0, 1.5, and 2.0, respectively. The probability that the AI exceeds the given threshold for each respective image is displayed by the color contours. Color contours shows the probabilities; light blue

greater than and equal to 10%, blue 20%, dark green 30%, purple 40%, red 50%, light green 60%, orange 70%, brown 80%, and yellow 90% POE values, respectively. POE contours, again similar to the SST analysis, increment by 10% with each color. Note that normally, an AI value greater than or equal to 1.5 is the minimum value considered to be associated with dust storms. Therefore these values can be used to identify Saharan dust storm activity.

Difference images for the entire hurricane season were created for the AI analyses. These images were computed by subtracting the 2006 AI POE values from the 2005 AI POE values at the exact same location. In this subtraction, zero values are accounted for so they do not distort the calculation. For visual simplicity, difference images only display two colors – red indicates higher POE values present in 2006 (i.e., less dust in 2006 than 2005) and blue indicates greater POE values present in 2005 (i.e., more dust in 2006 than 2005). These images provide a way to compare the overall probability distributions for AI values at the same location for the same threshold value. Therefore, the combination of information provided by the POE contours and difference images can display information regarding the extent of aerosols across the Atlantic, probability of the AI to occur in an exact spot, and a comparison between years.

Several general observations can be made from these figures. In general, the extent of the dust storms was greater during the 2006 season than the 2005 season. For most of the images, comparing the extents of the POE contours shows the dust reaching further across the Atlantic in 2006 than in 2005. Table 2 shows the approximate horizontal

extent for the dust in each threshold category for the seasonal images and for each individual month.

Figure 22 shows the POE contours for the 2005 and 2006 seasons. By comparing the extent of the POE contours, it is clear that higher POE values extended further across the Atlantic in 2006 than in 2005. The top four panels of Figure 22 show AI POE values greater than or equal to 10% extending to approximately 60°W, 58°W, 46°W, and 28°W for each of the threshold values of 0.0, 1.0, 1.5, and 2.0, respectively. Figure 22 also shows 2006 AI POE contours extending to approximately 70°W, 68°W, 50°W, and 39°W for each of the aforementioned threshold values. From the seasonal extents, it is evident that the reach of the aerosols during the hurricane season is greater in 2006 than in 2005. Not only is the horizontal extent of the aerosols larger in 2006 but the coverage in the north/south direction is greater as well. In the 2005 season, six TCs begin within the extent of the dust when the threshold is 1.0, three when the threshold is 1.5, and none when the threshold is 2.0. Out of ten named TCs in the 2006 season, four TCs form within the AI threshold of 1.0, two within the threshold of 1.5, and one within the threshold of 2.0.

From this point forward the zeroth AI threshold will be neglected and only the 1.0, 1.5, and 2.0 thresholds will be considered. The purpose of the zeroth threshold is to show the POE for all AI values in order to verify the distribution with published OMI images. As previously mentioned, AI values between zero and one are not associated with dust storms. AI values greater than or equal to the 1.0 threshold have significance and AI values greater than or equal to 1.5 and 2.0 are associated with dust storms. For this

reason, panel A (AI threshold=0.0) will be shown in the differences for completeness but excluded from the discussion.

At first glance, the difference image for the entire season appears cluttered. When examining the results on monthly basis (Figures 24, 26, 28, 30, 32, and 34), figures from the latter part of the season (i.e., Oct, Nov) show scatter along the northern edge of the image. This is perhaps backscatter from sea salt spray and is not associated with dust. Therefore, in the analysis, we ignore this. However, this scatter shows up in the seasonal difference images and makes them more difficult to interpret. As a result, only panels C and D showing the 1.5 and 2.0 AI thresholds will be considered when looking at the seasonal images.

In Figure 23, panel C shows a larger portion of the area of interest, the region in which the SAL moves across the Atlantic, experienced greater POE values in 2006 than the exact same location in 2005. The central to eastern portion of the MDR predominantly shows, as indicated by the blue, a higher likelihood of AI values greater than 1.5 in 2006 than 2005. Red indicates regions where a higher occurrence is present in 2006. There are a few sporadic areas in the Atlantic where red is seen, but the dominant presence of blue across the Atlantic clearly shows a higher occurrence of dust in 2006 than 2005. Note however, that the presence of dust over the entire 2005 season was greater than the presence in the 2006 season to the northwest of Morocco south through the western portion of Africa and just north of the eastern edge of the MDR. Additionally, in the western Atlantic, approximately in the middle of the MDR, there is a mixture of red and blue. However, by the time the dust reaches Cuba and the southern part of Florida, the

differences show that there were higher occurrences of dust reaching this area in 2006 than in 2005. Panel D of Figure 23 distinctly shows 2006 having a predominantly higher occurrence of AI values greater than 2.0. Overall, this shows a higher likelihood of occurrence of aerosol index values greater than 1.5 and 2.0 – thresholds indicating the presence of Saharan dust – in 2006. Breaking down the entire season into shorter, monthly timescales will provide a closer look at these features as each month portrays a different likelihood of occurrence.

Figure 24 shows the AI POE for the month of June. In June, two storms formed in 2005 and one storm formed in 2006 however none formed within the presence of dust in either year. It is quite clear from the figures that, for June, the dust extended further across the Atlantic in 2006 than in 2005. Compare the two B panels in Figure 24. Purple, red and several light green spots present in 2005 signify a probability greater than or equal to 40%, 50%, and 60%, respectively. In the same area, red, light green, and orange colors representing probabilities greater than or equal to 50%, 60%, and 70% respectively are present over a larger area. This obvious difference is distinctly seen on the June difference image shown in Figure 25. Blue indicates a greater occurrence of AI thresholds being met in 2006. Panels C and D obviously show the prominence of dust in 2006 as compared to 2005. The distribution of differences in panels B, C, and D indicate that dust was present up to 65% more often in 2006 than in 2005.

On the other hand, July was quite a bit different from June. In both years, aerosols reached their furthest extent across the Atlantic. This far-reaching presence can be seen in Figure 26. Figure 27 shows that, within this region of greatest aerosol extent, the

locations where more dust is present in one year versus another year are rather intermixed. Areas are either dominantly red or blue showing that there were differences in the likelihood of occurrence within this large extent. When all the areas are combined, there is a slightly higher occurrence of dust in panels C and D for 2006. Five storms occurred during this month in 2005: Cindy, Dennis, Emily, Franklin, and Gert. Before Hurricanes Dennis and Emily, Hurricane Audrey in 1957 held the record for the strongest hurricane to occur before the month of August (Storm World, p. 143). Dennis first broke this record with a minimum pressure of 930 hPa which was then surpassed by Emily at 929 hPa. Dennis resulted in $2.23 billion in damages in the US and $31.7 billion in Jamaica (converted into US currency) (NHC, TCR: Dennis). Dennis and Emily both formed along the southern edge of the MDR. Dennis formed on the periphery of the 10% contour for the AI threshold of 1.0 and Emily formed within the 10% contour for the AI threshold of 1.5. July of 2006 had two storms: The first, a TC not originally named during the season and the second, Tropical Storm (TS) Beryl. Neither of these storms formed within regions where any of the AI thresholds were reached. Overall, July showed the greatest horizontal and north/south reach of the aerosols for both seasons with a slightly higher occurrence in 2006.

August, Figure 28, shows similar results to those seen in July with the exception being the extent of the aerosols is not as vast. Panel B shows the extent of the curves reaching Cuba in both 2005 and 2006. The probabilities show that the extent is greater in the north/south direction in 2006 as compared to 2005 but similar in the east/west compass extent for both years. Contrary to what would be expected considering previous research

efforts, the differencing shows more aerosols present in 2005 than in 2006 in the MDR. During August, five TCs formed in 2005 and three in 2006. Two of the five TCs produced in 2005 formed just barely within the 10% contour for the AI threshold of 1.5. One of the three TCs forming in 2006 developed just inside the 10% contour of the same AI threshold.

Overall, September shows aerosols extending to the middle of the MDR in panels B and C of Figure 30 but not reaching far beyond the western coast once the threshold is raised to 2.0 in panel D. Figure 31 shows a slightly greater horizontal extent in 2006 for the AI thresholds of 1.5 and 2.0. Panel C of Figure 31 shows broader north/south coverage of the aerosols in 2005 for the 1.5 threshold. The difference image also shows that it is a mixed month between one season having greater probabilities than the other. Panel D of Figure 31 makes it appear that 2006 had a greater presence of aerosols over the 2.0 threshold than September of 2005, but the differences are too small (i.e., less than one in ten chance that 2006 POE values were greater than 2005) to be significant. The coverage of the aerosols significant enough to be associated with dust has decreased in extent for both years. This is also the month in which the majority of 2006 storms form – all four reaching hurricane strength. These four storms form just outside the reach of the lowest 10% contour for the AI threshold of 1.5. In 2005, of the five storms that occur, one forms on the periphery of the 10% contour for the same AI threshold.

Compared to September, less dust is present during the months of October and November in both years. There is less Saharan dust present in 2006 than 2005 in panels C and D of Figure 32 displaying October POE values. However, it is a mute point by this time since

the dust barely reaches into the Atlantic in the 1.5 and 2.0 thresholds. Seven storms form during this period in 2005, none of which form within the reach of the Saharan dust. The 2006 season ends as Hurricane Isaac dies out on October 2nd. The 2005 season continued with three storms forming in November and one at the end of December before ending on January 6th.

Overall more aerosols are present in 2006 than 2005. This confirms the findings of Kim and Lau (2007) where they found an increase in atmospheric dust in 2006. Contrary to the expectation when this research began – that more aerosols would be consistently be greater in 2006 than in 2005 – it appears that the presence of dust is different in each time period. The seasonal difference shows a higher probability for AI values of 1.5 or 2.0 present in 2006. June also shows a very clear difference in the disparity between aerosols in 2005 and 2006. However, July and August, despite the larger extent present in July, show only a slight tendency towards a greater presence of dust in 2006. September shows a decreased occurrence of dust in 2005 and 2006 and both seasons also experience similar magnitudes of dust present. It is this month, where 2006 seems to get a reprieve from higher dust content, that the majority of the 2006 storms form. By October and November the passage of dust storms has decreased. In October there is a higher likelihood of aerosols over western Africa into the first third of the MDR in 2005. Despite this, seven storms form in 2005 but they develop in regions where dust is not present. For 2006, the impact of El Nino comes into play by the months of October and November. The CPC report indicates that, even in active seasons, El Nino suppresses activity late in the season over the Caribbean Sea and western tropical Atlantic.

When combining information on the presence of Saharan dust and initiation points from each of the months, one particular observation stands out. Across each of the months it has been noted that no storms, in either the 2005 or 2006 seasons, formed within contour intervals greater than 30% for the AI threshold of 1.5 nor within the 10% contour interval for the AI threshold of 2.0. This appears to indicate that once a certain threshold of dust is present, TC genesis and development may be suppressed. In specific case studies, Dunion and Velden (2004) observed that once a forming storm was able to escape the presence of the SAL, indicated here by AI values greater than 1.5 or 2.0, it was able to intensify. Dunion and Velden (2004) identified Hurricanes Cindy and Floyd of 1999 and Hurricanes Erin and Felix of 2001 as storms that intensified into major hurricanes (as defined by the Saffir-Simpson scale) once escaping the influence of the SAL. This could indicate the suppressant role, as suggested by several articles, of dust as storms are able to form once they are away from the influence of the dust.

Despite the potential for development based upon other known conditions, Saharan dust appears to impact the developmental environment of the TCs. From section 5.2 it is known that SST values were great enough to support TC formation and development in the tropical Atlantic, Gulf of Mexico, and Caribbean Sea. From AI data two results are evident. First, more dust was present in 2006 than in 2005. Second, TCs tended not to form until out of, or almost out of, the reach of Saharan dust. There are, however, other factors known to play a role in the development of TCs. These factors are the amount of moisture available to the storm and vertical wind shear present in the atmosphere. The following section will look at moisture availability.

Table 2: Approximate Horizontal Extent of AI POE: The approximate horizontal extent of AI POE contours were determined directly from the AI POE images.

Approximate Horizontal Extent of AI POE				
	AI = 0.0	**AI = 1.0**	**AI = 1.5**	**AI = 2.0**
June 2005	58°W	58°W	45°W	30°W
June 2006	80°W	75°W	60°W	52°W
July 2005	75°W	75°W	65°W	51°W
July 2006	85°W	85°W	80°W	52°W
August 2005	66°W	66°W	54°W	45°W
August 2006	79°W	79°W	55°W	32°W
September 2005	59°W	59°W	46°W	28°W
September 2006	60°W	60°W	51°W	29°W
October 2005	50°W	46°W	60°W	60°W
October 2006	55°W	55°W	28°W	17°W
November 2005	45°W	39°W	23°W	-
November 2006	55°W	40°W	27°W	-
Season 2005	60°W	58°W	46°W	28°W
Season 2006	70°W	68°W	50°W	39°W

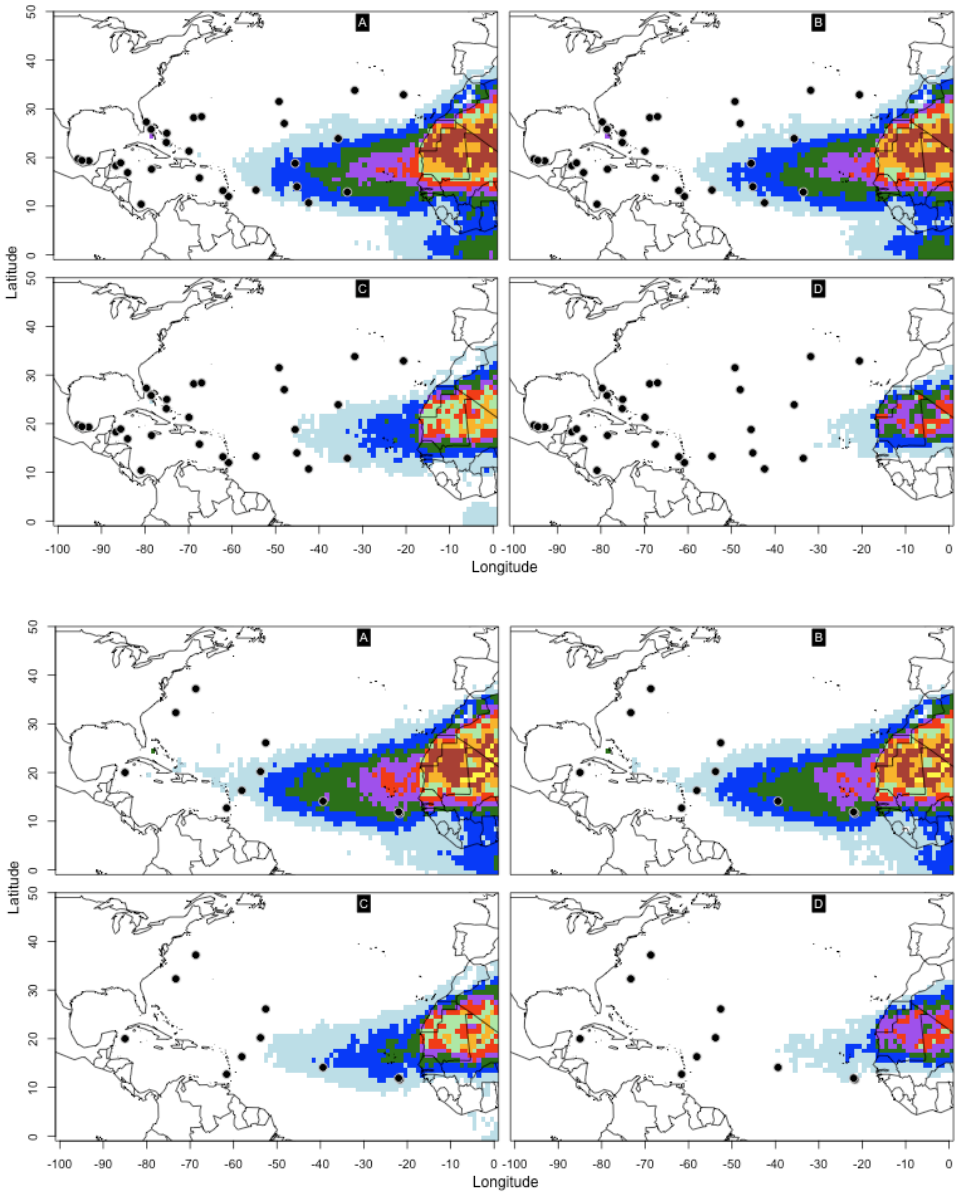

Figure 22: Seasonal Aerosol Index (AI) Probability of Exceedance (POE): Displays the AI analyses for year 2005 (top four panels) and year 2006 (bottom four panels) hurricane seasons. Each figure displays initial location of TCs (black dots) and the calculated POE values (color contours) for 0.0 (Fig. A), 1.0 (Fig. B), 1.5 (Fig. C), and 2.0 (Fig. D) AI threshold values. Color contours shows the probabilities; light blue greater than and equal to 10%, blue 20%, dark green 30%, purple 40%, red 50%, light green 60%, orange 70%, brown 80%, and yellow 90% POE values, respectively.

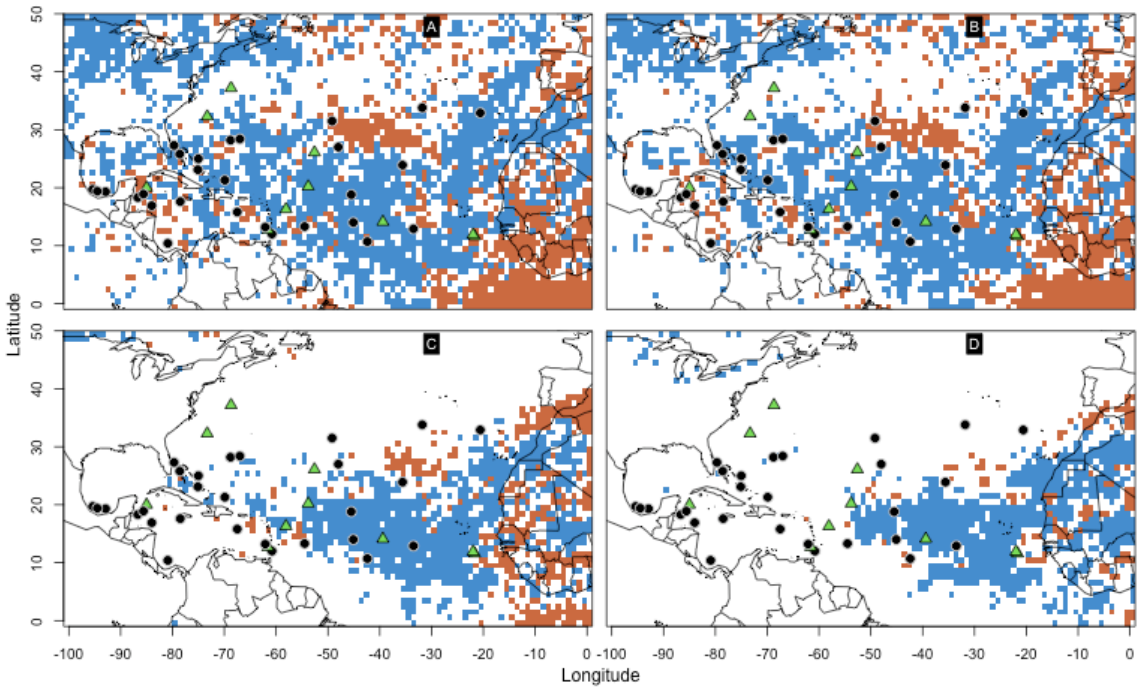

Figure 23: Seasonal AI POE Differences (2005-2006): Each of the four panels, A, B, C, and D displays the POE differences for the AI threshold values of 0.0, 1.0, 1.5, and 2.0, respectively. Blue shows negative values (i.e., 2006 values are higher than 2005 values), while red shows positive values (i.e. 2005 values are less than 2006 values).

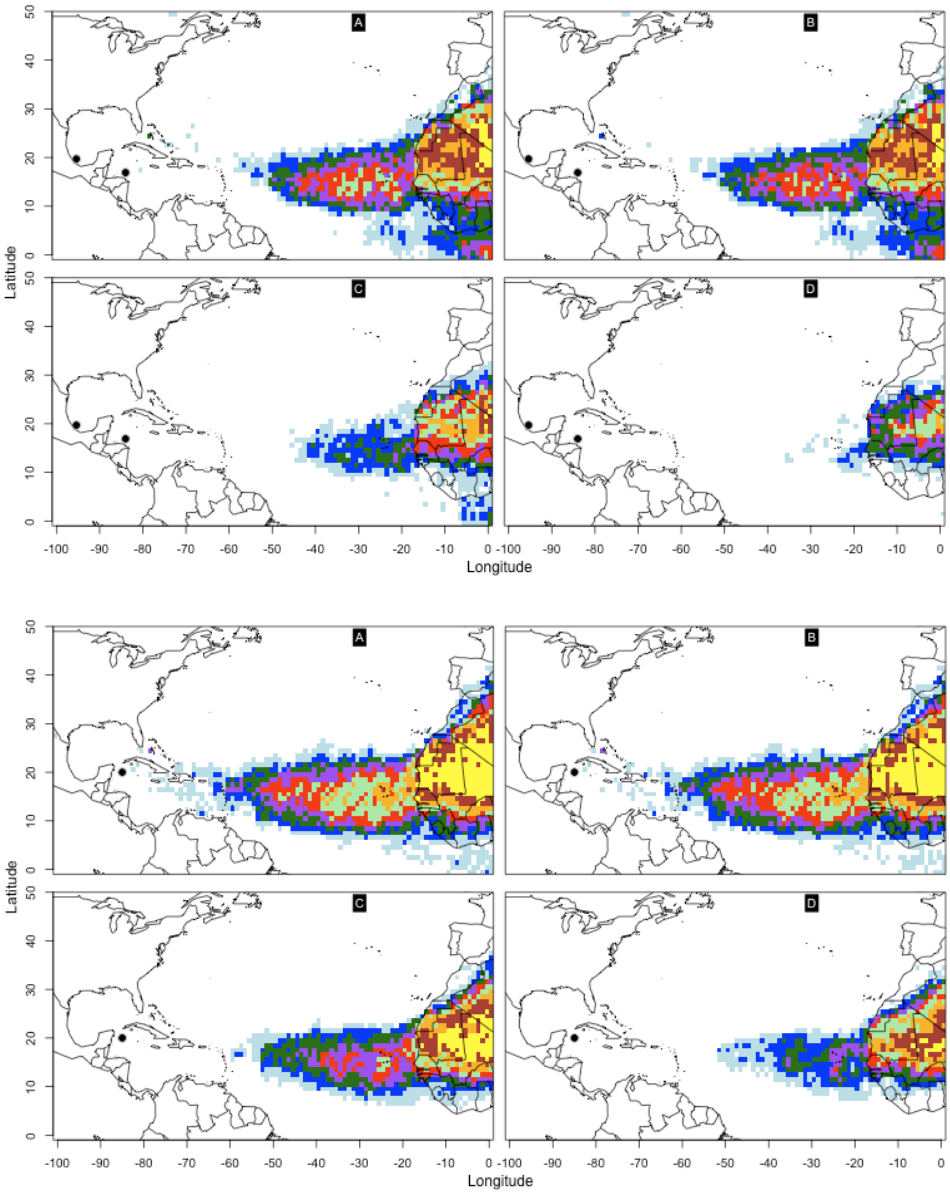

Figure 24: June AI POE: Same as Figure 22 except this displays the AI analyses for June of 2005 (top four panels) and June of 2006 (bottom four panels).

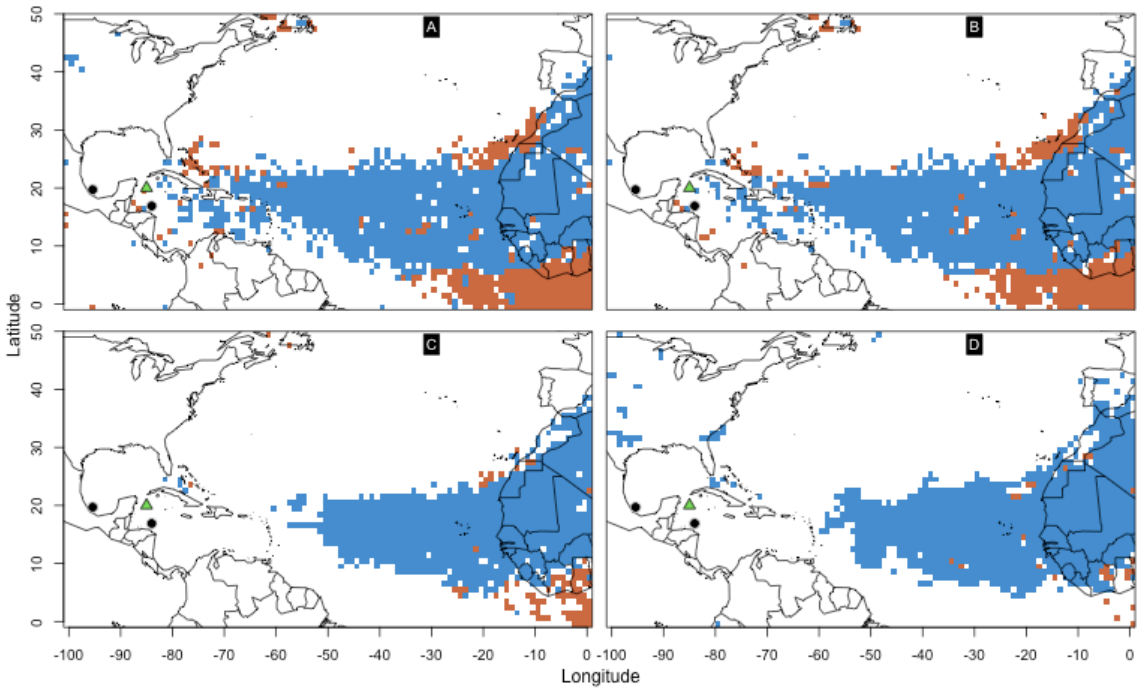

Figure 25: June AI POE Differences: Same as Figure 23 except this displays the difference between June of 2005 and June of 2006 AI analyses.

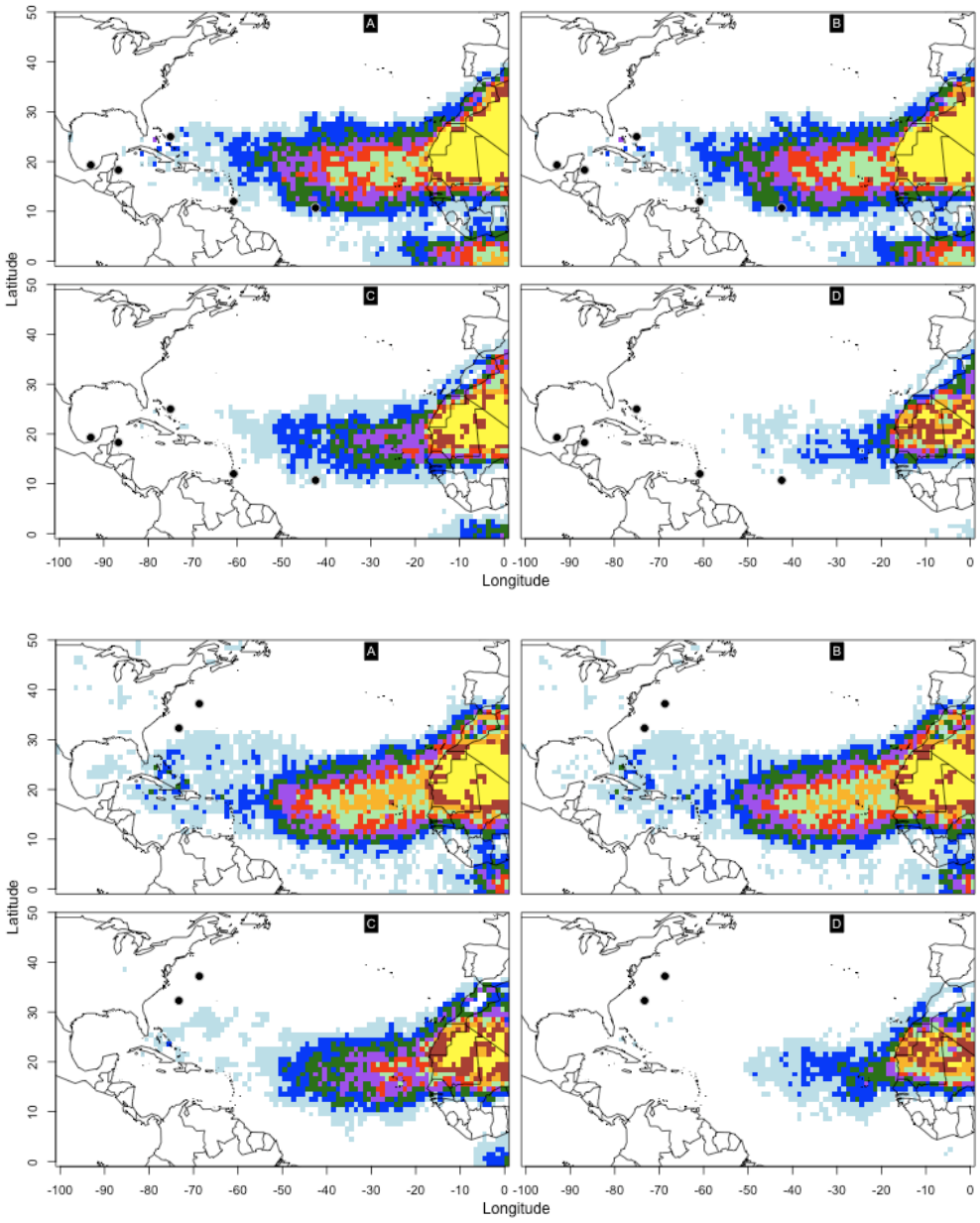

Figure 26: July AI POE: Same as Figure 22 except this displays the AI analyses for July of 2005 (top four panels) and July of 2006 (bottom four panels).

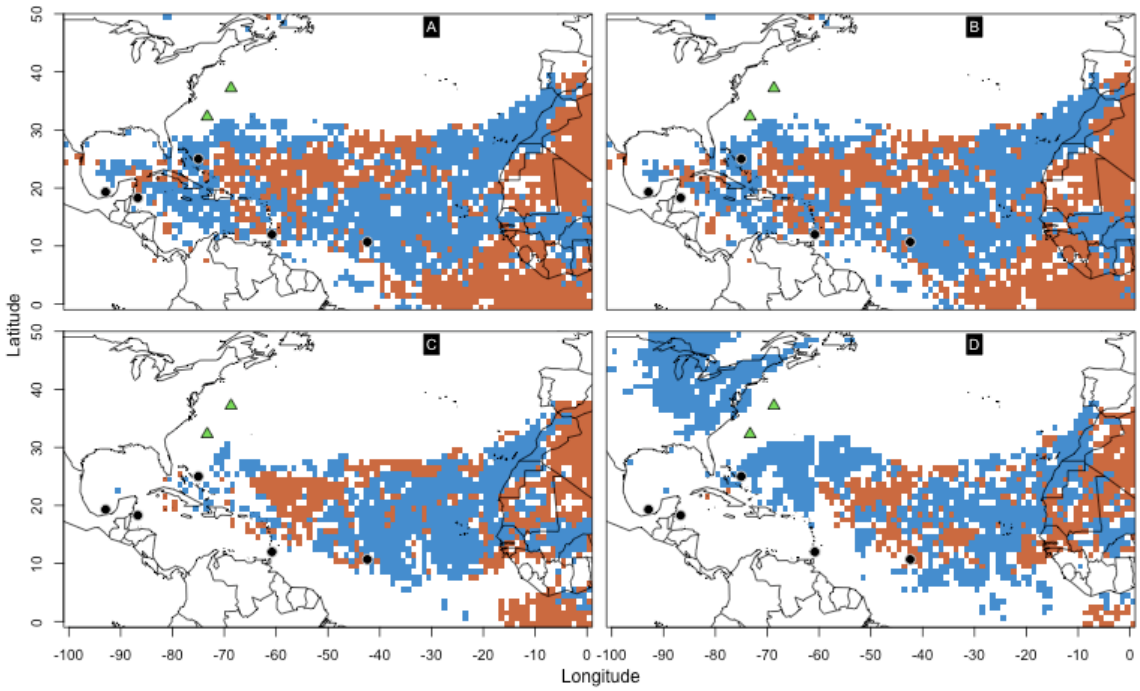

Figure 27: July AI POE Differences: Same as Figure 23 except this displays the difference between July of 2005 and July of 2006 AI analyses.

.

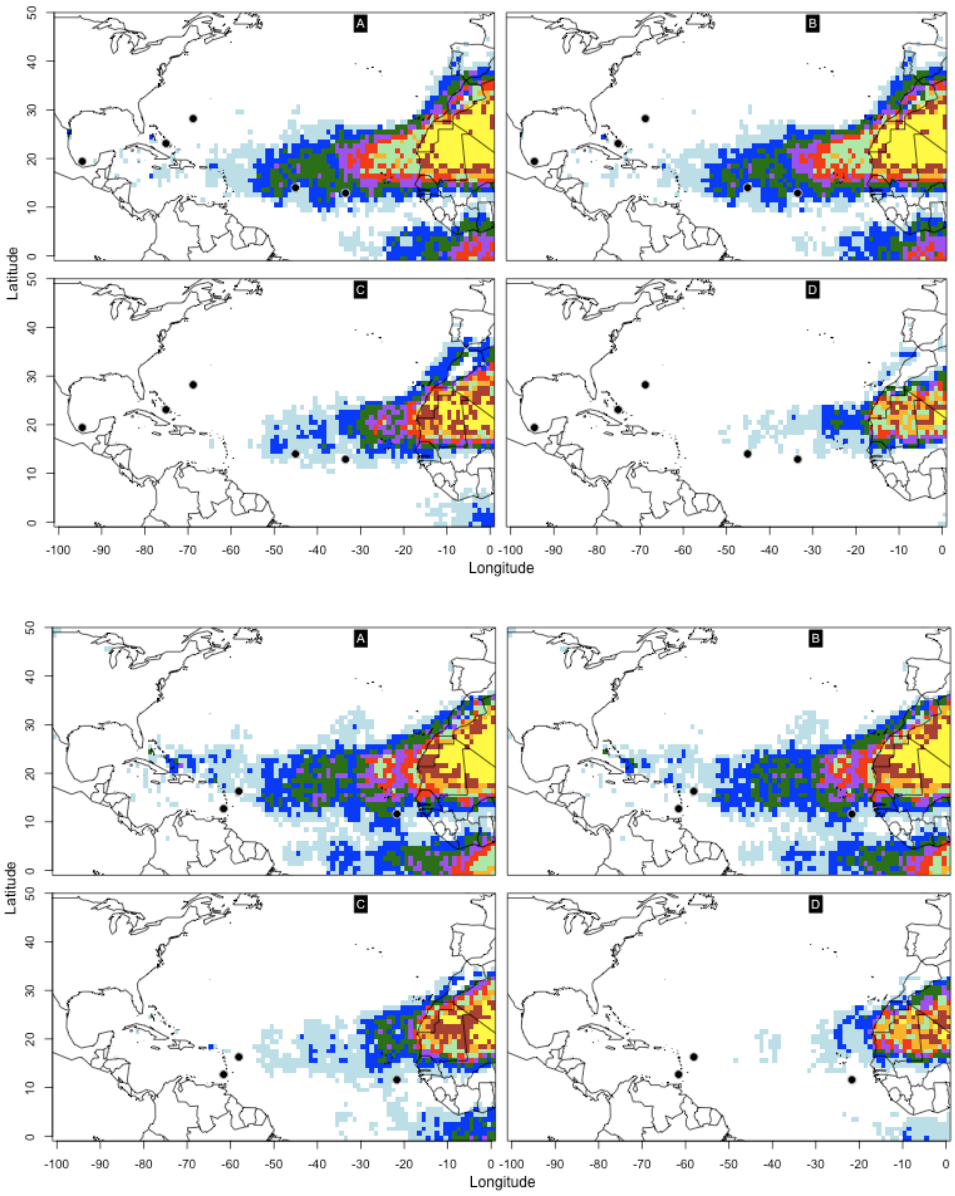

Figure 28: August AI POE: Same as Figure 22 except this displays the AI analyses for August of 2005 (top four panels) and August of 2006 (bottom four panels).

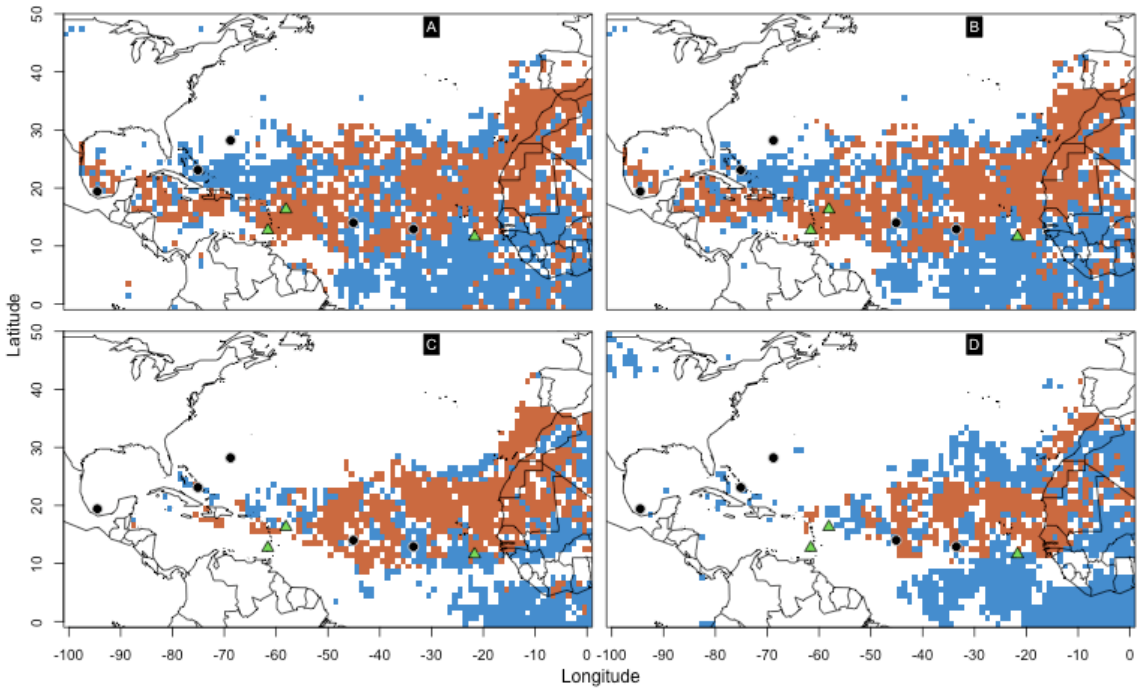

Figure 29: August AI POE Differences: Same as Figure 23 except this displays the difference between August of 2005 and August of 2006 AI analyses.

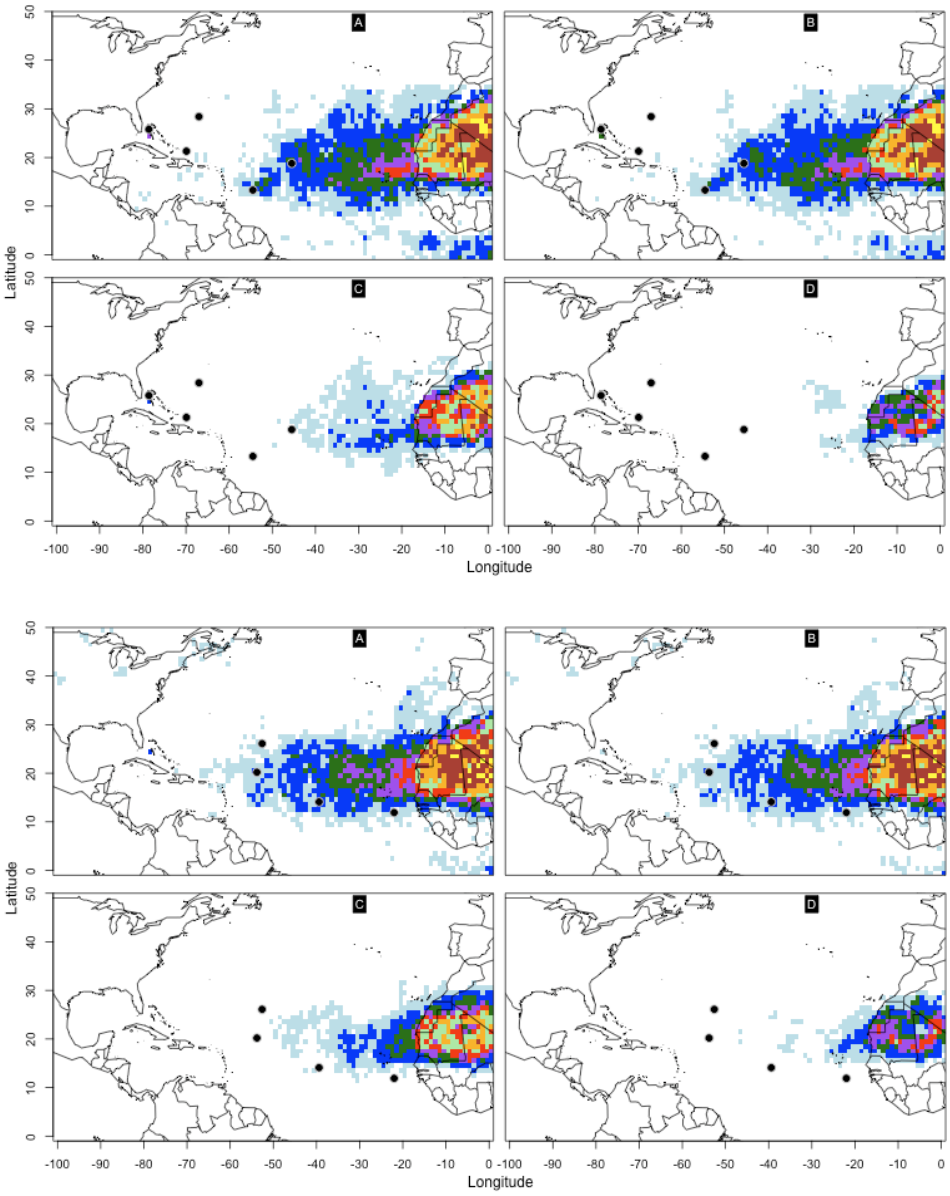

Figure 30: September AI POE: Same as Figure 22 except this displays the AI analyses for September of 2005 (top four panels) and September of 2006 (bottom four panels).

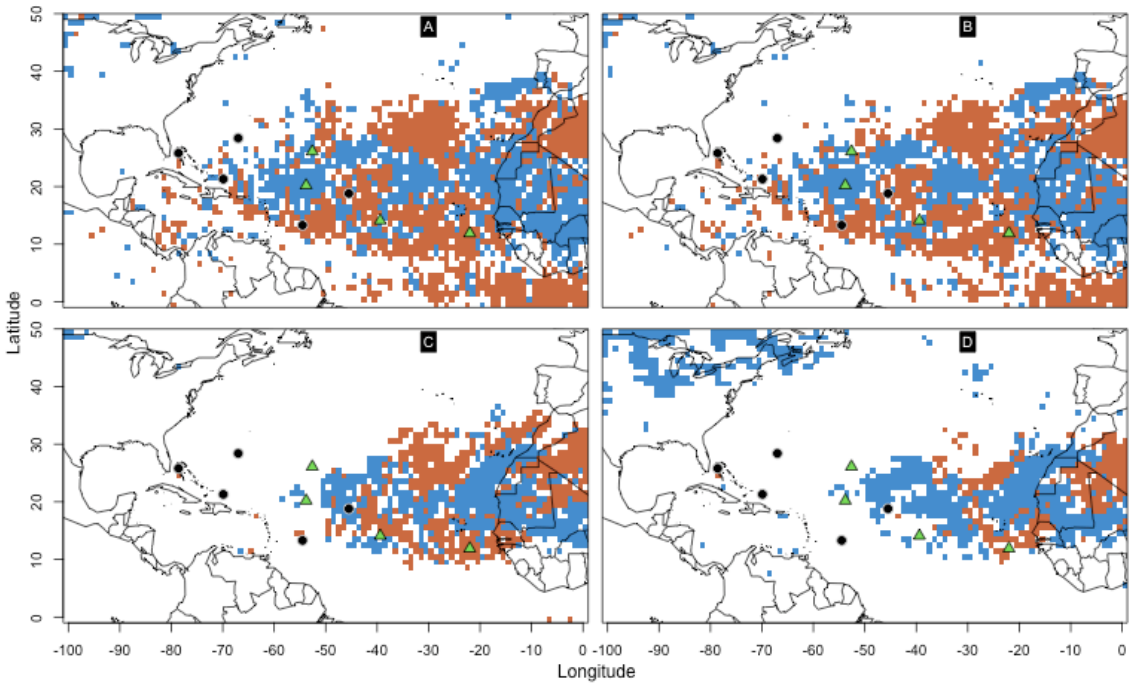

Figure 31: September AI POE Differences: Same as Figure 23 except this displays the difference between September of 2005 and September of 2006 AI analyses.

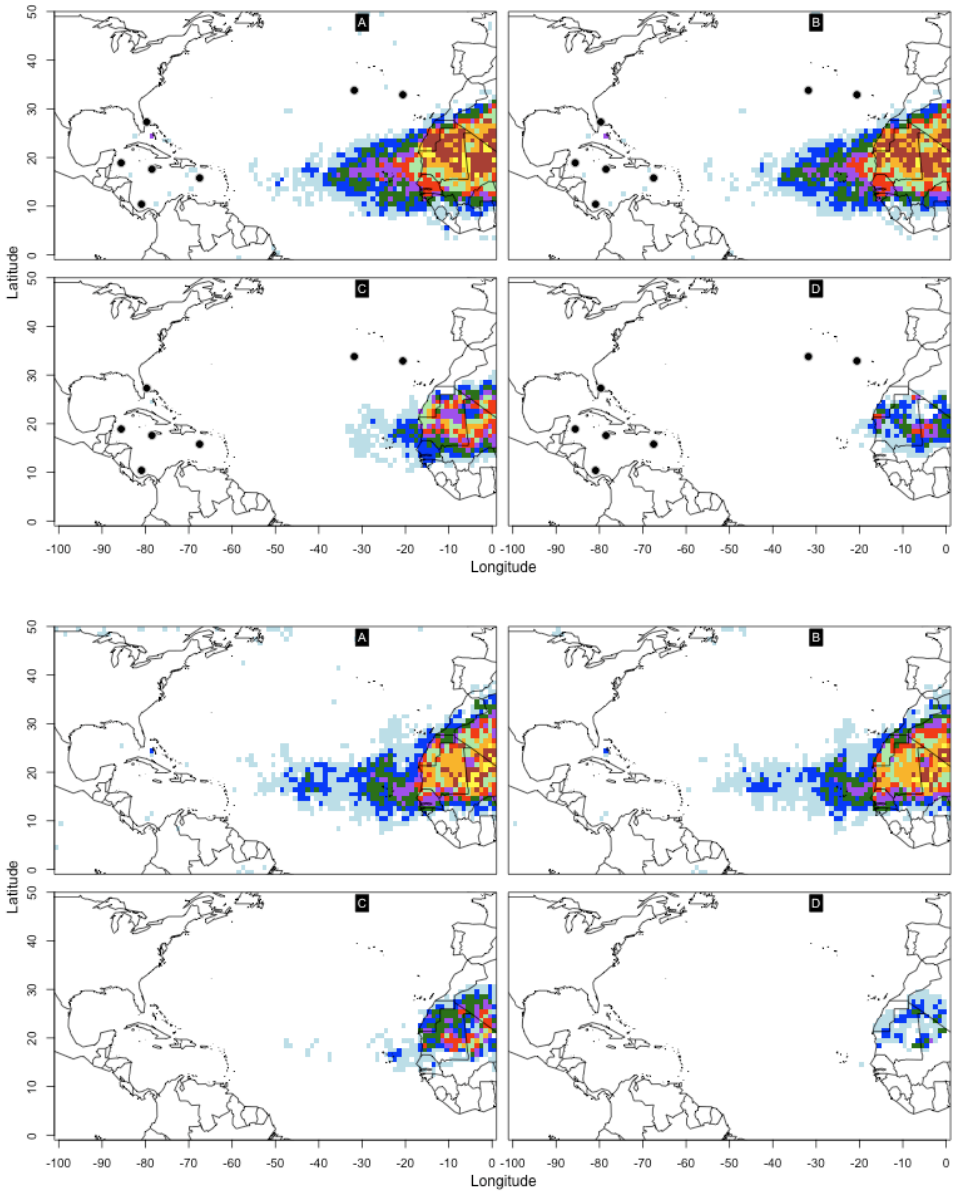

Figure 32: October AI POE: Same as Figure 22 except this displays the AI analyses for October of 2005 (top four panels) and October of 2006 (bottom four panels).

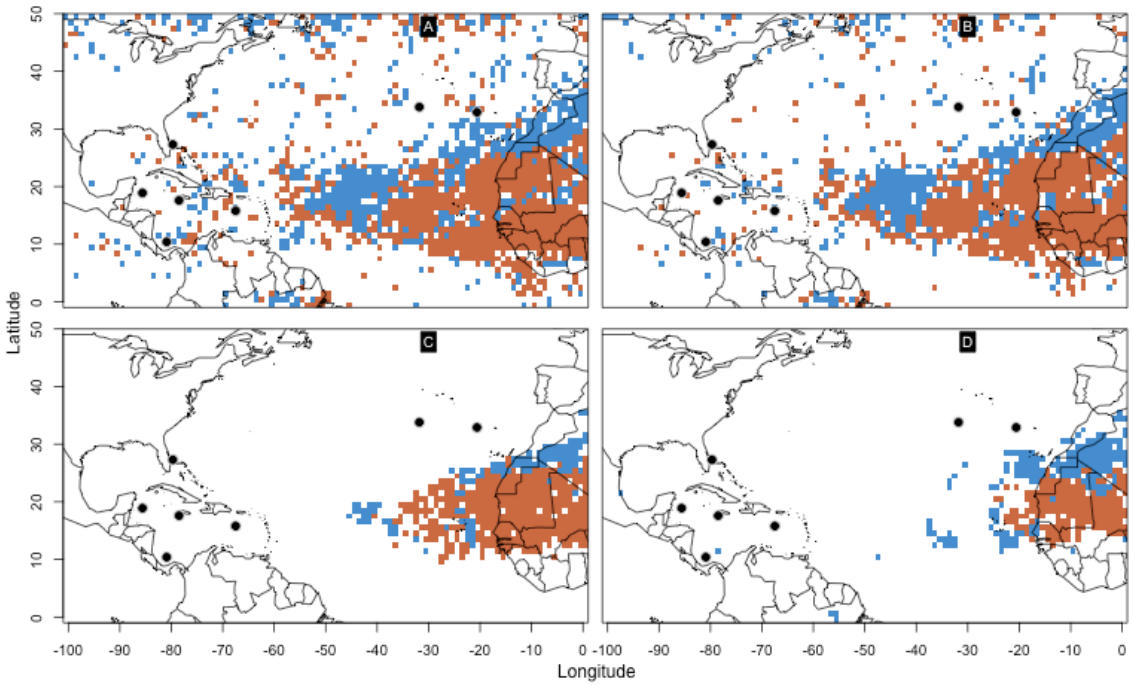

Figure 33: October AI POE Differences: Same as Figure 23 except this displays the difference between October of 2005 and October of 2006 AI analyses.

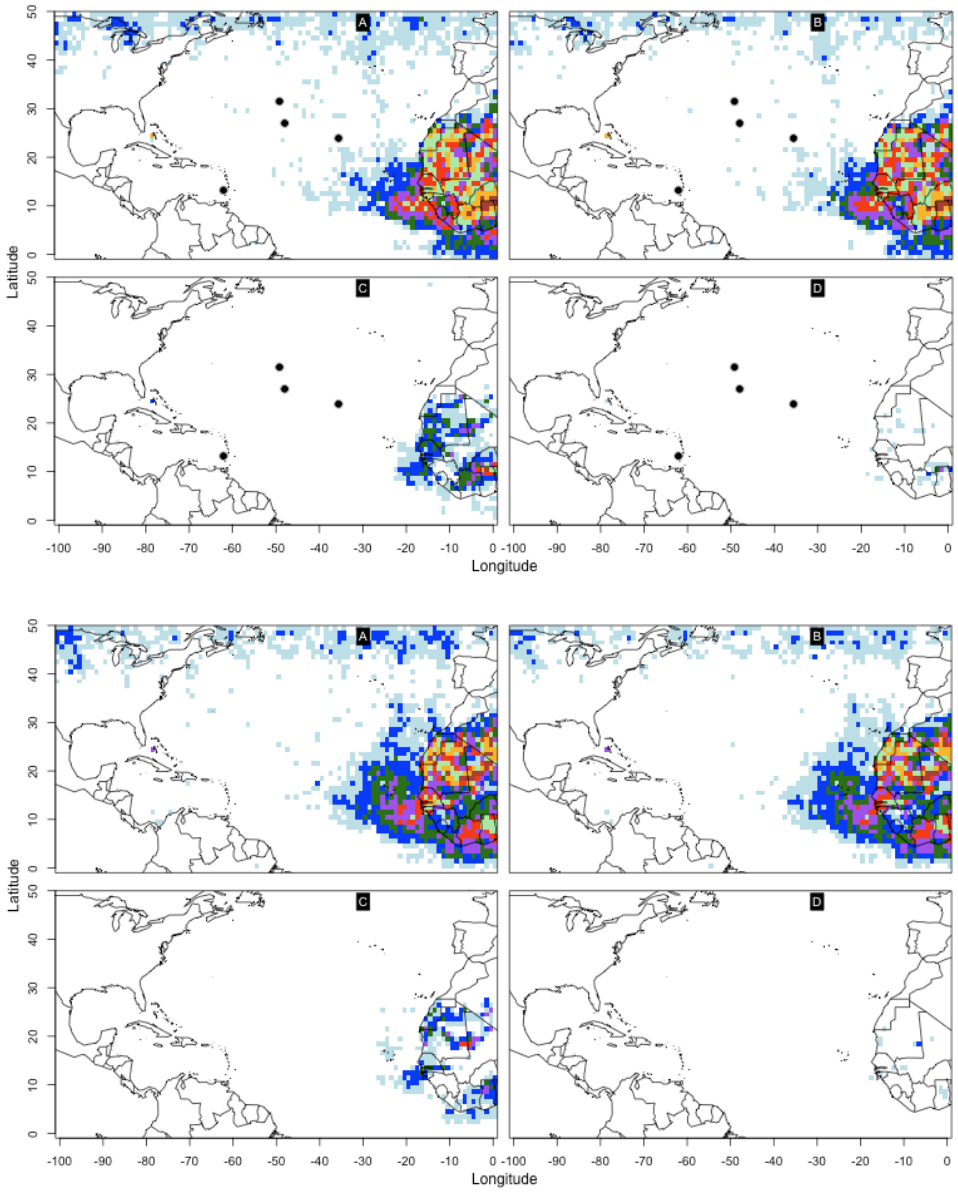

Figure 34: November AI POE: Same as Figure 22 except this displays the AI analyses for November of 2005 (top four panels) and November of 2006 (bottom four panels).

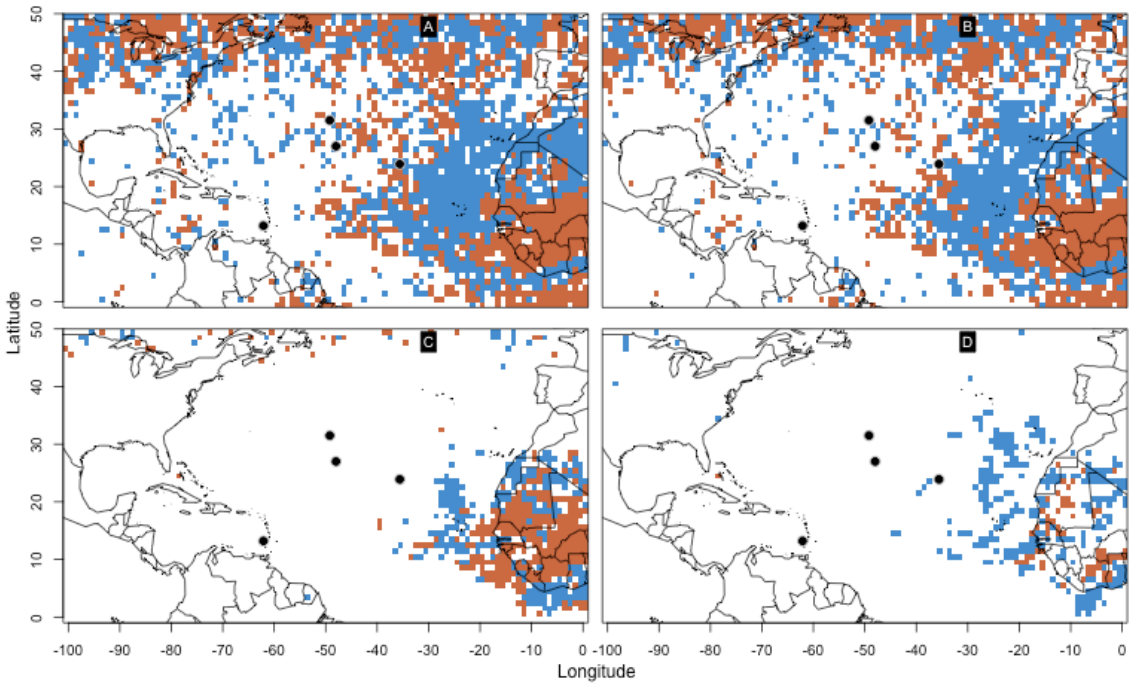

Figure 35: November AI POE Differences: Same as Figure 23 except this displays the difference between November of 2005 and November of 2006 AI analyses.

5.4 Moisture and Moist Instability Comparisons

As discussed in the previous sections, heat and energy for the a TC are gathered by the disturbance through contact with warm ocean waters. The winds near the ocean surface spiral into the disturbance's low-pressure area and hence rise vertically transporting heat and moisture to higher altitudes. As the moisture condenses into water drops, latent heat is released, contributing additional energy to power the storm. Bands of thunderstorms form and the storm's cloud tops rise higher into the atmosphere. Without this latent heat energy and mid-tropospheric moisture, the storm lacks the necessary energy to form and/or sustain itself. In this section, a time history of moisture profiles and a moist stability index will be analyzed.

Time history of moisture profiles are made from Skew-T data at the eight different points noted in Figure 5. The dew point depression ($T-T_d$) is calculated from the data and plotted from the 5th of July to the 31st of October. As explained in the methods, odd days are plotted during this period. This time frame was chosen for two reasons: (1) no NCEP data was available for June of 2005 and (2) historically, the majority of storms form during these peak months. To interpret the images, one can recognize that the higher the dew point depression value, the drier the air is in the atmosphere that day. The air is more moist when the difference between the temperature and dew point temperature is smallest. When the temperature is cooled to the dew point temperatures, the air becomes saturated. Therefore, the smaller the amount of cooling needed for the temperature to reach the dew point temperature, the greater the content of moisture in the air. Changes in dew point depression with height are evidenced by changes in color on a particular

day. Some portions of the atmosphere will be dry while other levels are moist on the same day.

From all the time history figures (Figures 36 - 43), one particular pattern can be noted. Recall the general shape and reach of the AI POE contours shown in Section 3. Now regard Figure 5 which displays the eight points for which Skew-T data was gathered for the time series. Note that Points 1 and 2 are generally within AI values greater than 1.5 or 2.0. From time to time, Point 3 is still within the edges of Saharan dust contours but Point 4 is consistently out of the reach of the dust. Similarly, Points 5 and 6 are normally within the boundary of the 1.5 AI threshold contours while Points 7 and 8 are usually free of dust. A trend in moisture content is evident when the dew point depression images, Figures 36-43, are compared. At Points 1, 2, 5, and 6, less moisture is present in the vertical time series. Values at Points 3 and 7 show more moisture available while Points 4 and 8 display significantly more moisture in the atmosphere. This trend is present in 2005 and 2006 but more obvious in Points 5 through 8 at 25°N than Points 1 through 4 at 15.75°N. The points within the influence of the Saharan dust display drier days while those beyond the reach of the Saharan dust show more moisture present in the column. Thus, as the presence of dust decreases, the amount of moisture in the atmosphere increases which adds support to Dunion and Velden's (2004) hypotheses on the influences of the SAL on the atmospheric conditions surrounding TCs. Couple this with the literature support for the importance of moisture in TCs, Saharan dust should be considered more carefully in order to improve computer modeling of TCs. Additionally, a comparison of Skew-T diagrams at Points 2 and 3 in 2005 and 2006 reconfirm this

trend between the points within and just outside the reach of the dust. This dry air is easily noticed on a Skew-T diagram by the nose-like shape created between the dew point and temperature lines on the diagram. Figure 44 shows an example of the Skew-T diagrams observed and this notable feature. A drier atmosphere is seen in the region where dust is present while a more moist atmosphere is apparent in the regions where dust is not present.

When points between years are compared (i.e., panel A is compared to panel B for Figures 36-43) similarities and differences are found. Point 1 in 2006 had a few drier days but, on the whole, both are comparable. Point 3 is more moist in 2005 than 2006 which is in line with AI observations in that area. Point 4 is moist in both years. At Points 4 and 7, 2005 has more moisture present than 2006 however moisture in the atmosphere at Point 8 is quite similar between the years.

Calculated values of the moist stability index (MSI) are shown in Figure 45 for Points 1-4 and in Figure 46 for Points 5-8. Green bars represent MSI values for 2005 and blue bars denote MSI values for 2006. Negative values indicate a stable environment and positive values an unstable environment. One general conclusion from these figures is that the 2006 season was more stable than the 2005 season because more negative values, indicating stability, are present in 2006. Additionally, there are several regions in which each season differs dramatically – 2005 being highly or consistently positive with the 2006 being negative.

In conclusion, these results show that points within the aforementioned AI contours have drier vertical moisture profiles than points outside the reach of the dust. Points 1-4 at a

latitude of 15.75°N are comparable in moisture content for both years while points at 25°N show more moisture in the atmosphere in 2005 across the Atlantic, but similar moisture amounts off the southeastern coast of Florida in both years. Also recall that September was the most active period for 2006. The moisture profiles show that, generally, moisture content in 2006 was on par with observed moisture in the atmosphere in 2005. The moist stability index shows more instability in the atmosphere in 2005 as compared to 2006. Section 5.5 will look into the time history of wind profiles to understand another important environmental condition – vertical wind shear.

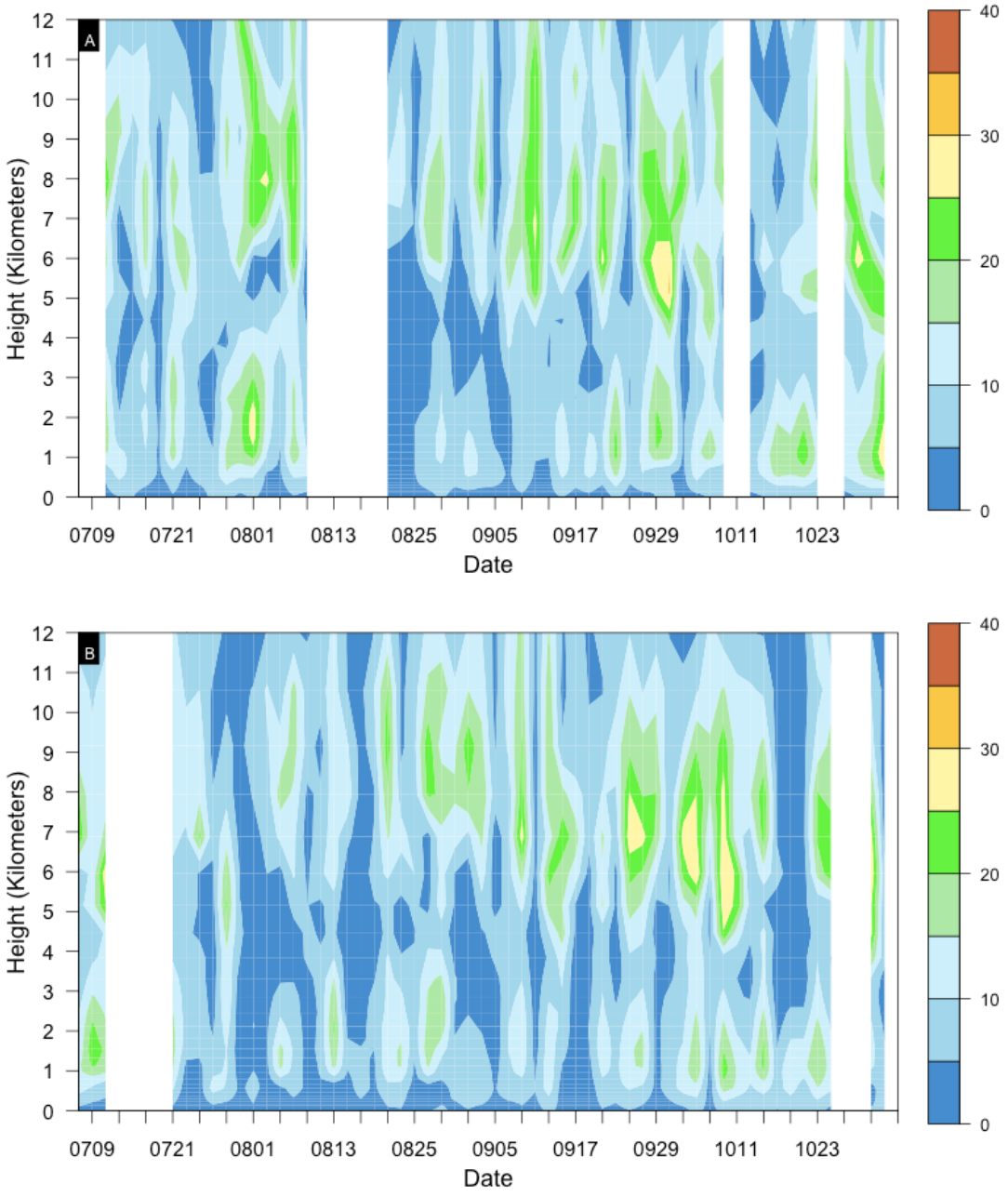

Figure 36: Dew Point Depression at Point 1: Displays the dew point depression ($T-T_d$) at Point 1 shown in Figure 5. Panels A and B show the time history of dew point depression vertical profiles (July-October) for the 2005 and 2006 seasons.

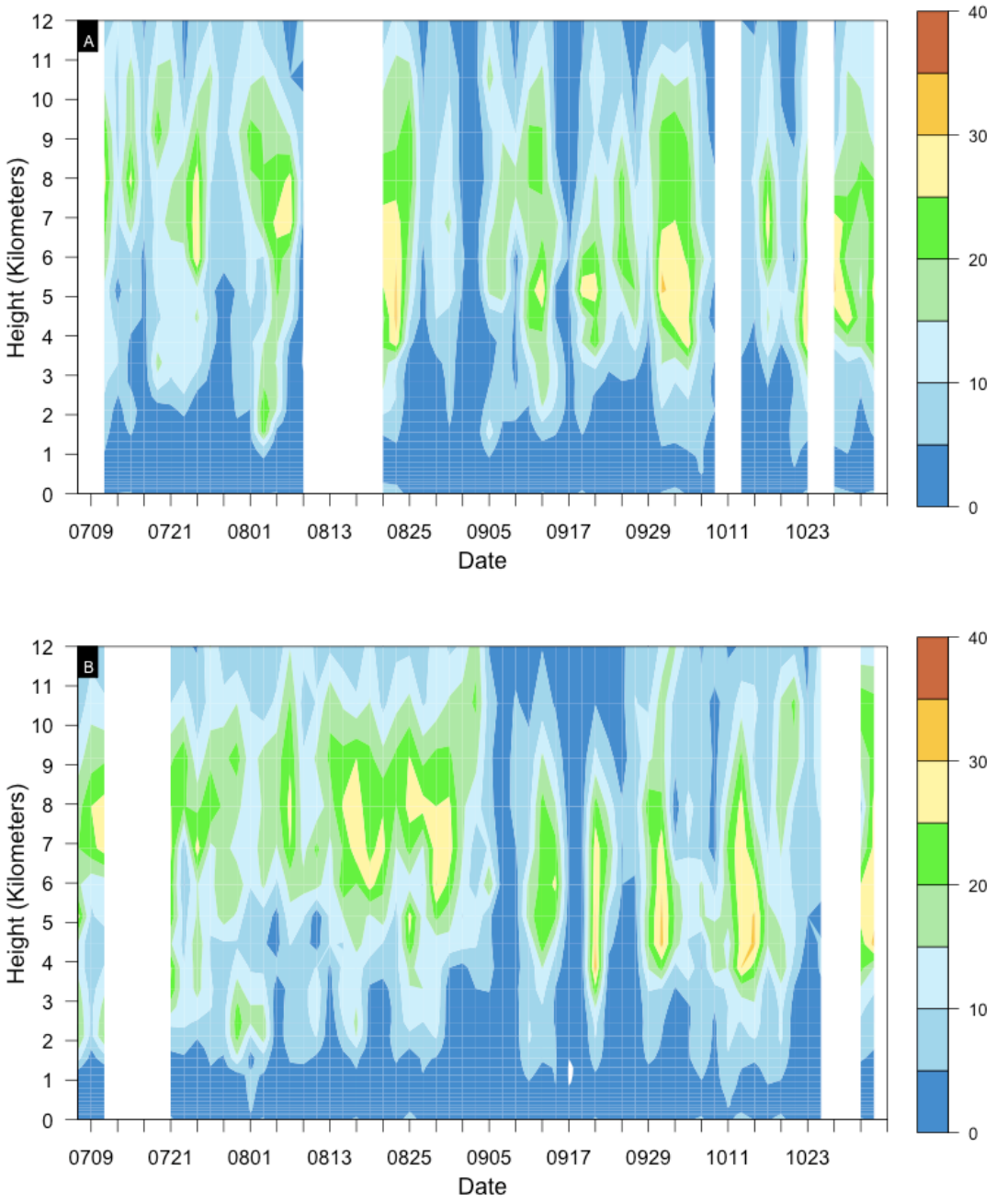

Figure 37: Dew Point Depression at Point 2: Same as Figure 36 except at Point 2 shown in Figure 5.

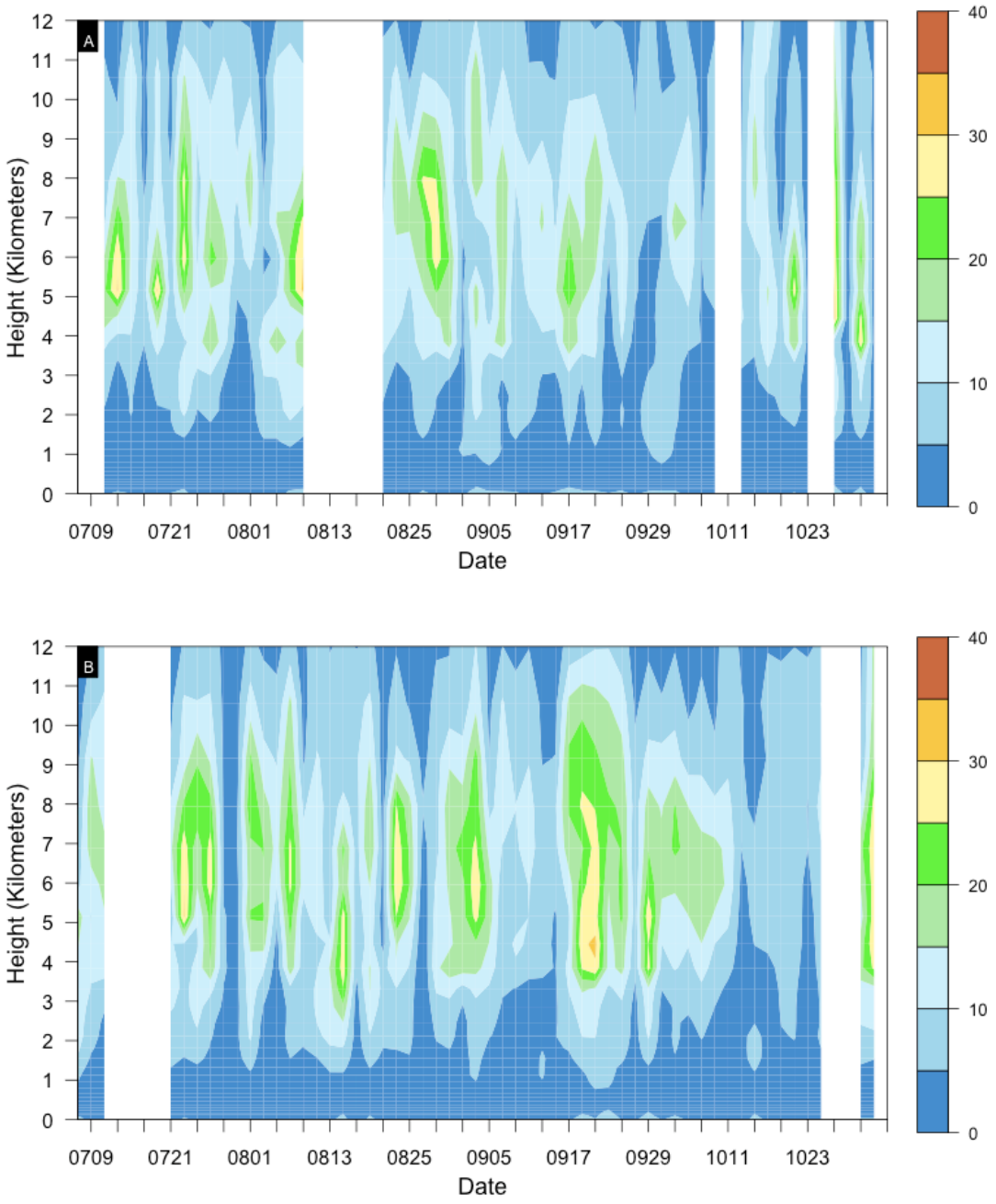

Figure 38: Dew Point Depression at Point 3: Same as Figure 36 except at Point 3 shown in Figure 5.

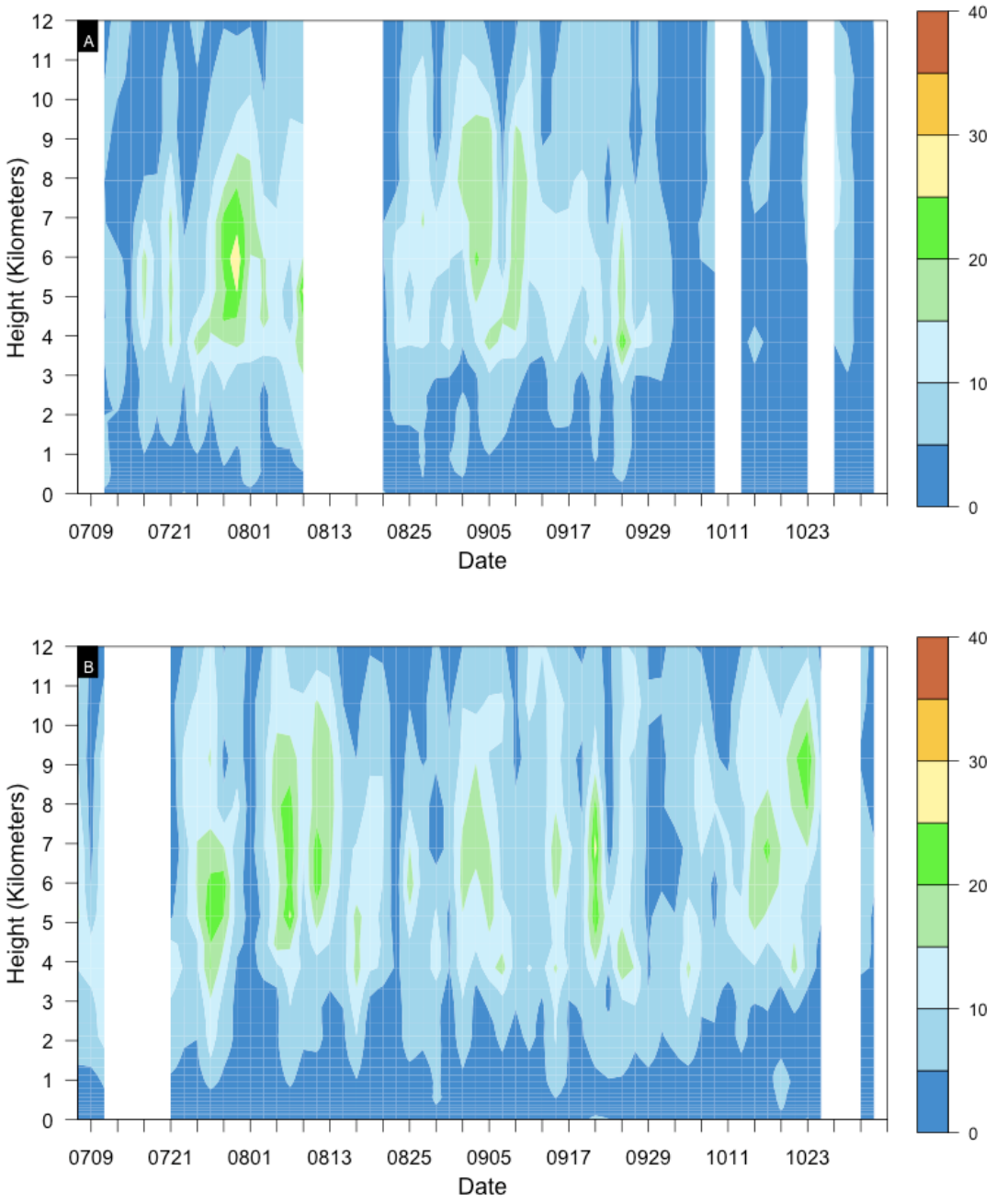

Figure 39: Dew Point Depression at Point 4: Same as Figure 36 except at Point 4 shown in Figure 5.

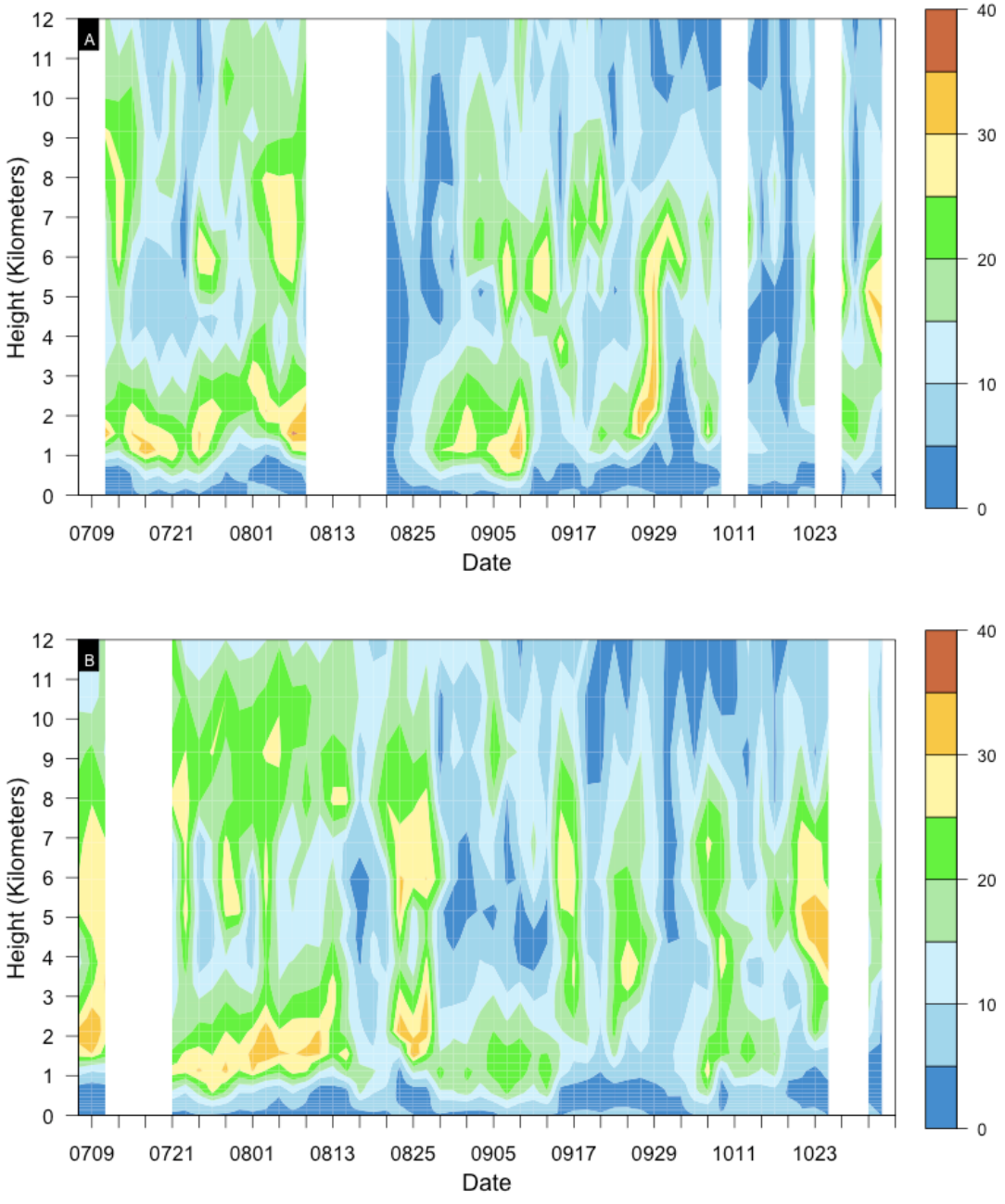

Figure 40: Dew Point Depression at Point 5: Same as Figure 36 except at Point 5 shown in Figure 5.

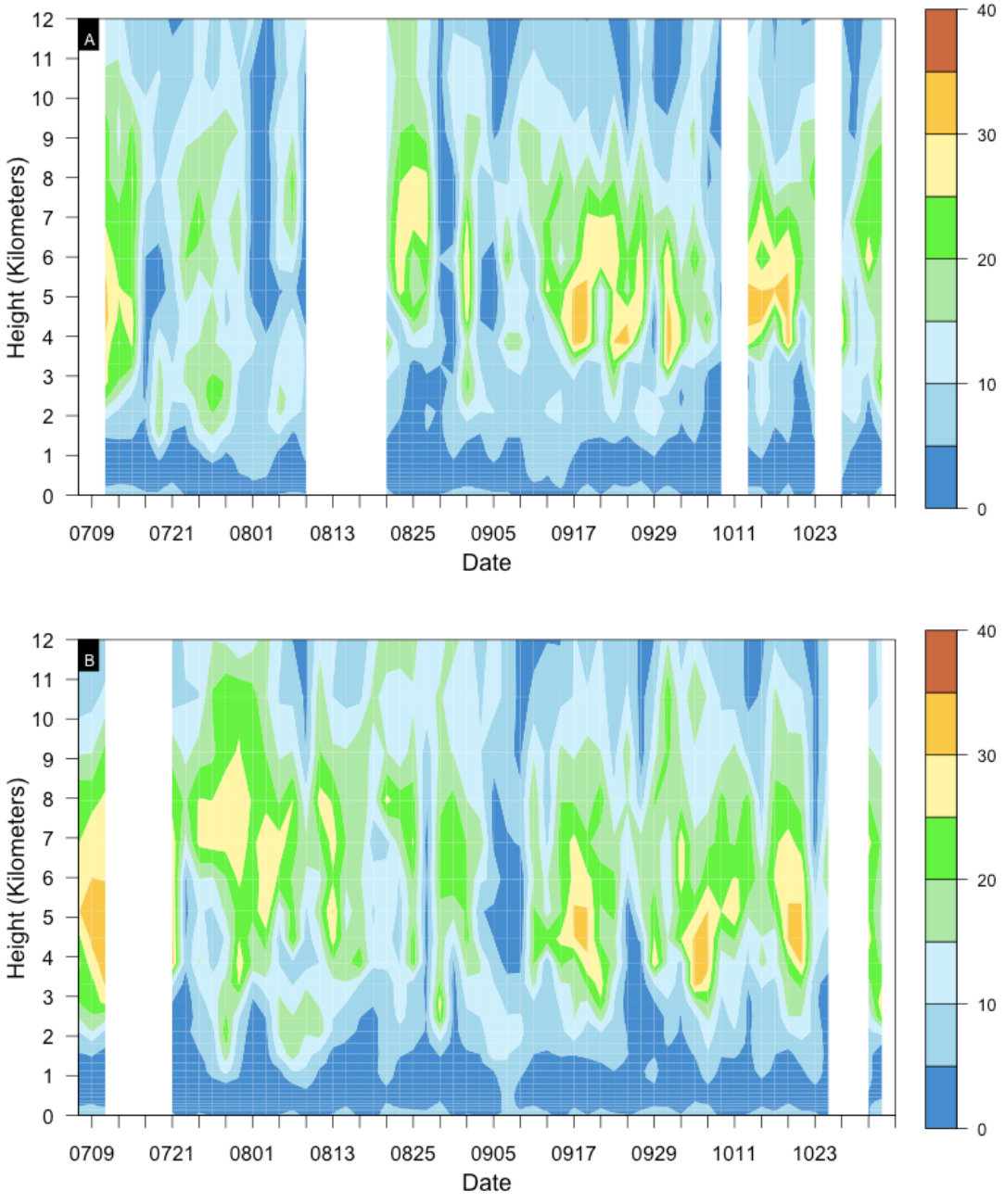

Figure 41: Dew Point Depression at Point 6: Same as Figure 36 except at Point 6 shown in Figure 5.

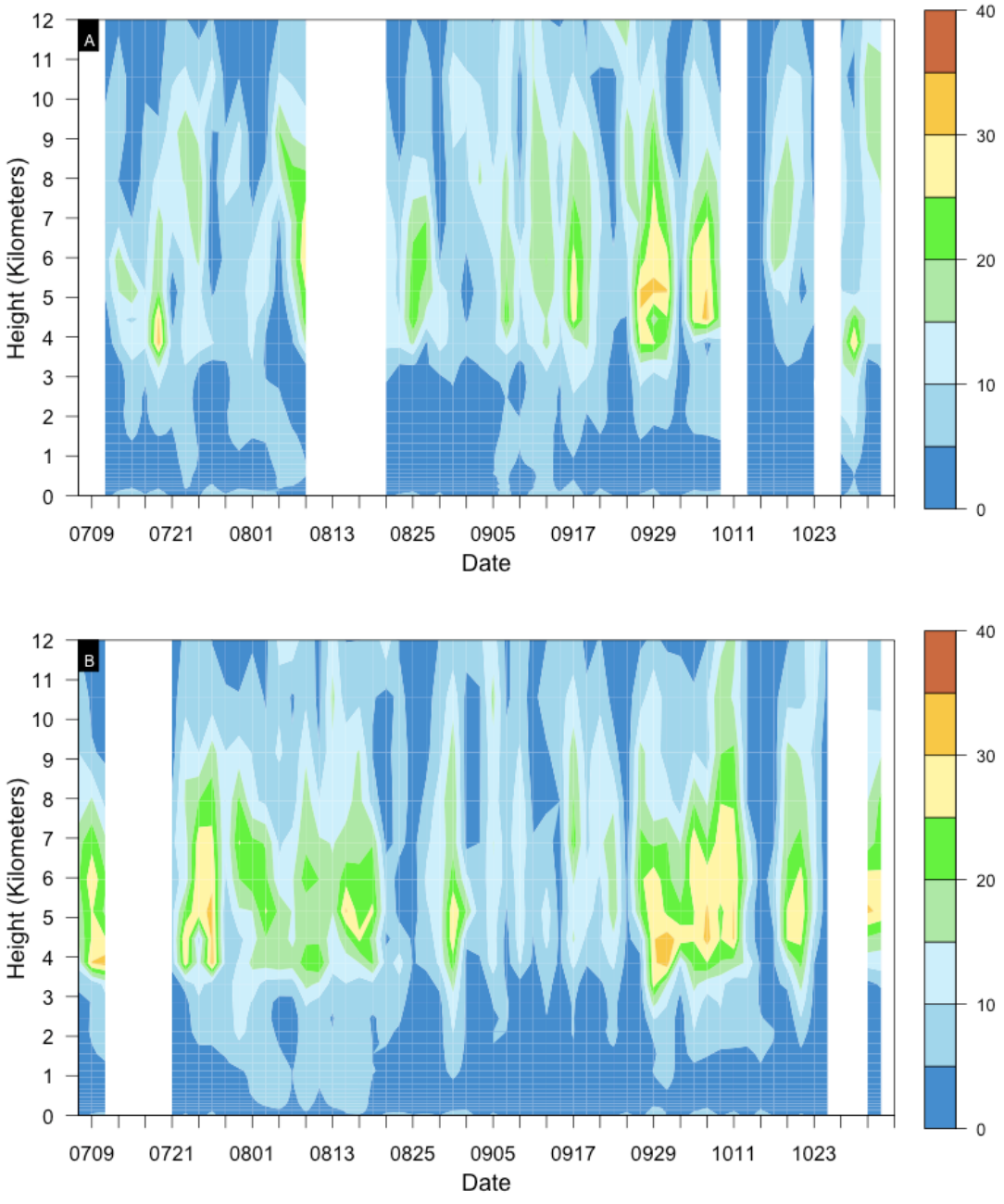

Figure 42: Dew Point Depression at Point 7: Same as Figure 36 except at Point 7 shown in Figure 5.

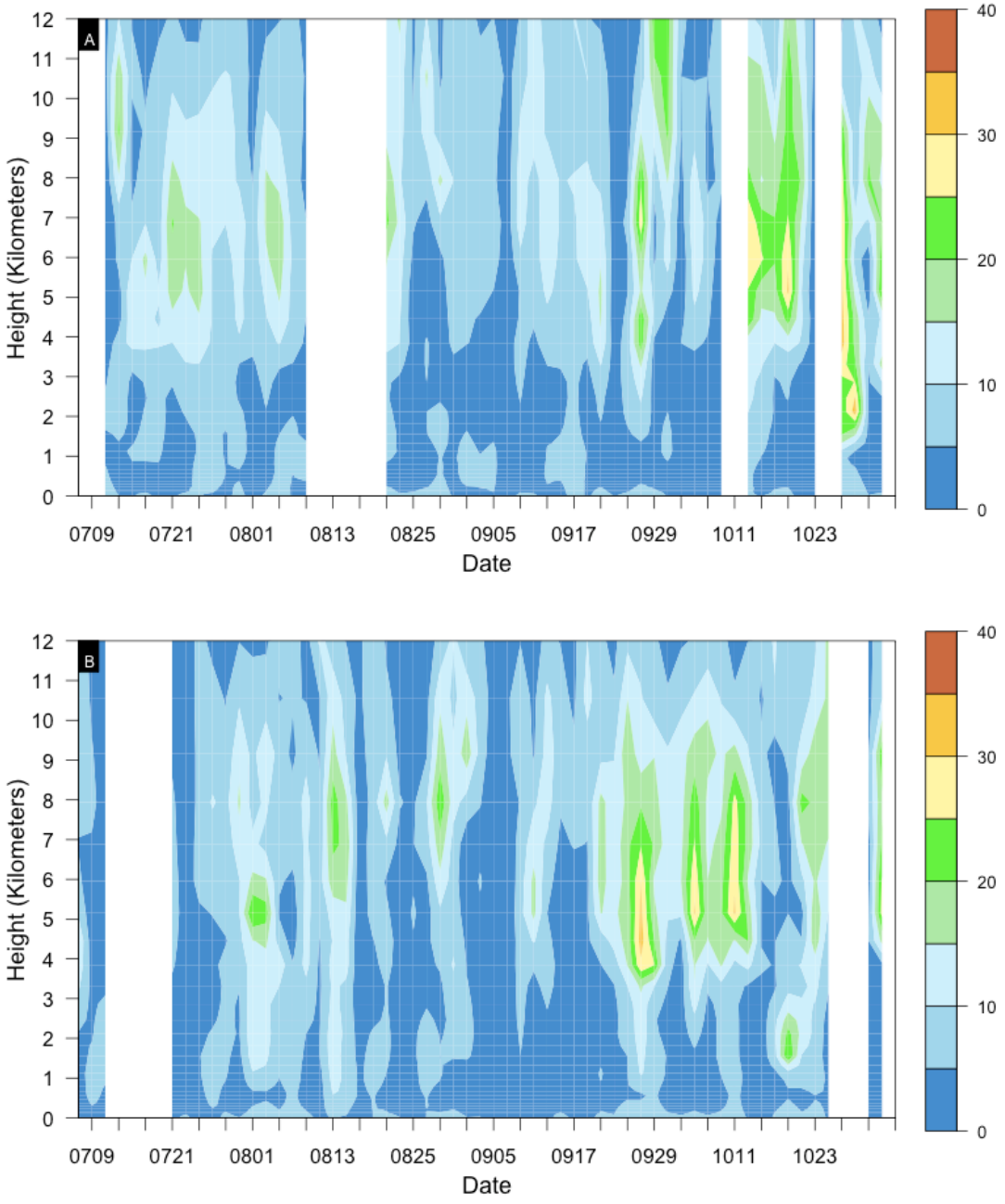

Figure 43: Dew Point Depression at Point 8: Same as Figure 36 except at Point 8 shown in Figure 5.

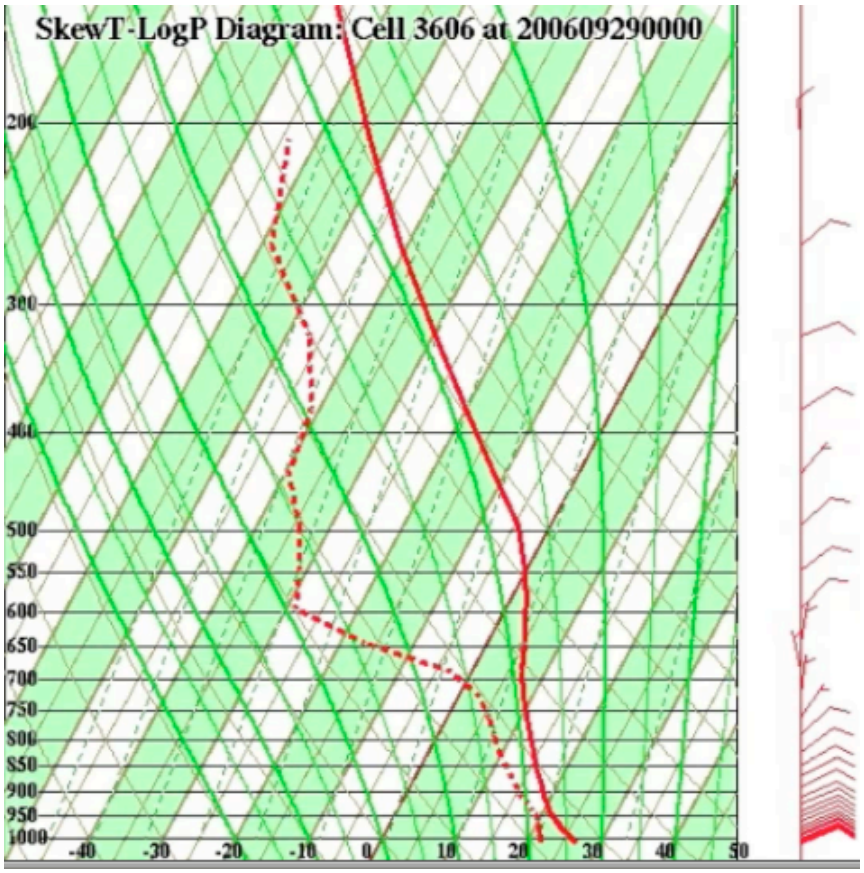

Figure 44: Example Skew-T Diagram: Skew-T diagram at Point 2 in 2006 showing a region of dry air in the mid-troposphere as the difference between the temperature (T) and dew point temperature (T_d) increases.

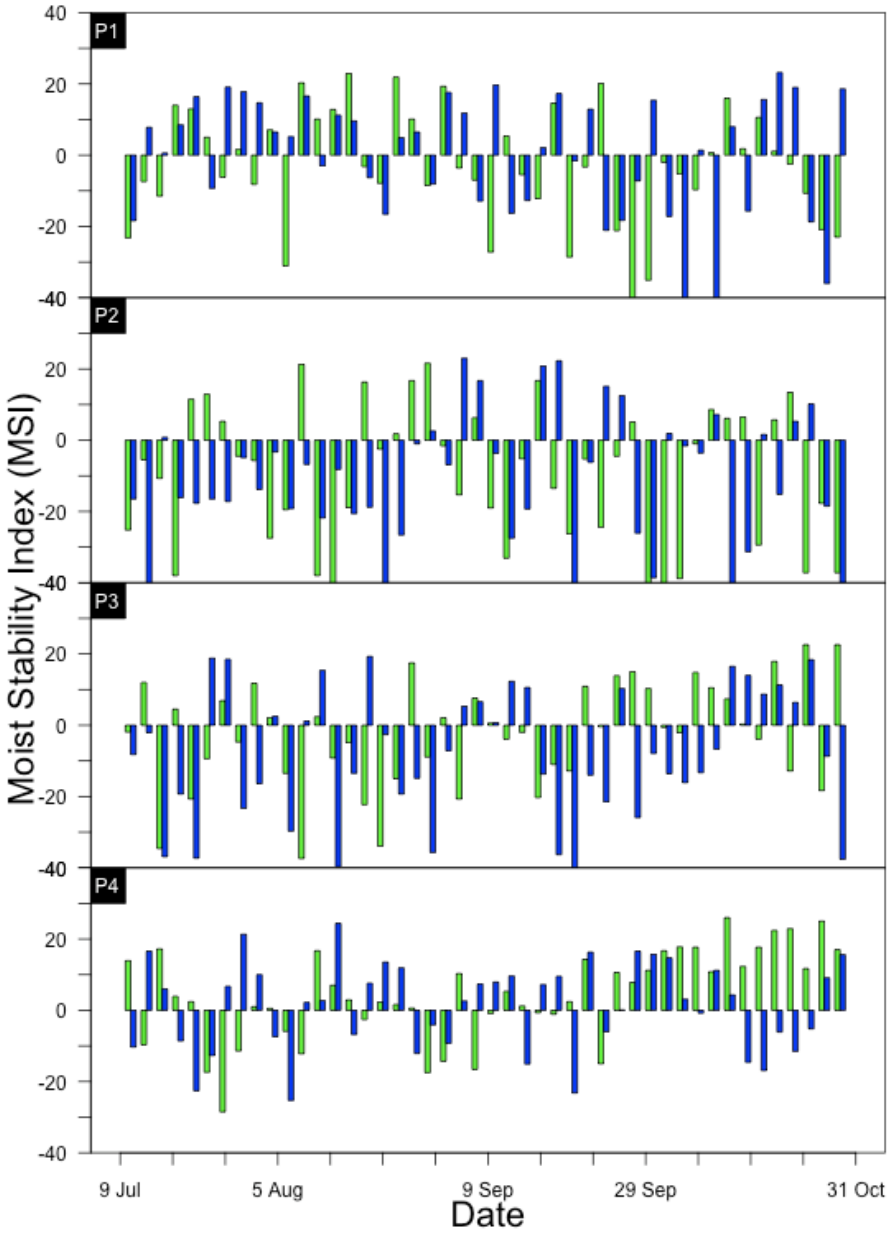

Figure 45: Moist Stability Index: Points 1-4: The time history of Moist Stability Index (MSI) at Points 1-4 shown in Figure 5. MSI values from 2005 are shown in green and 2006 values are shown in blue.

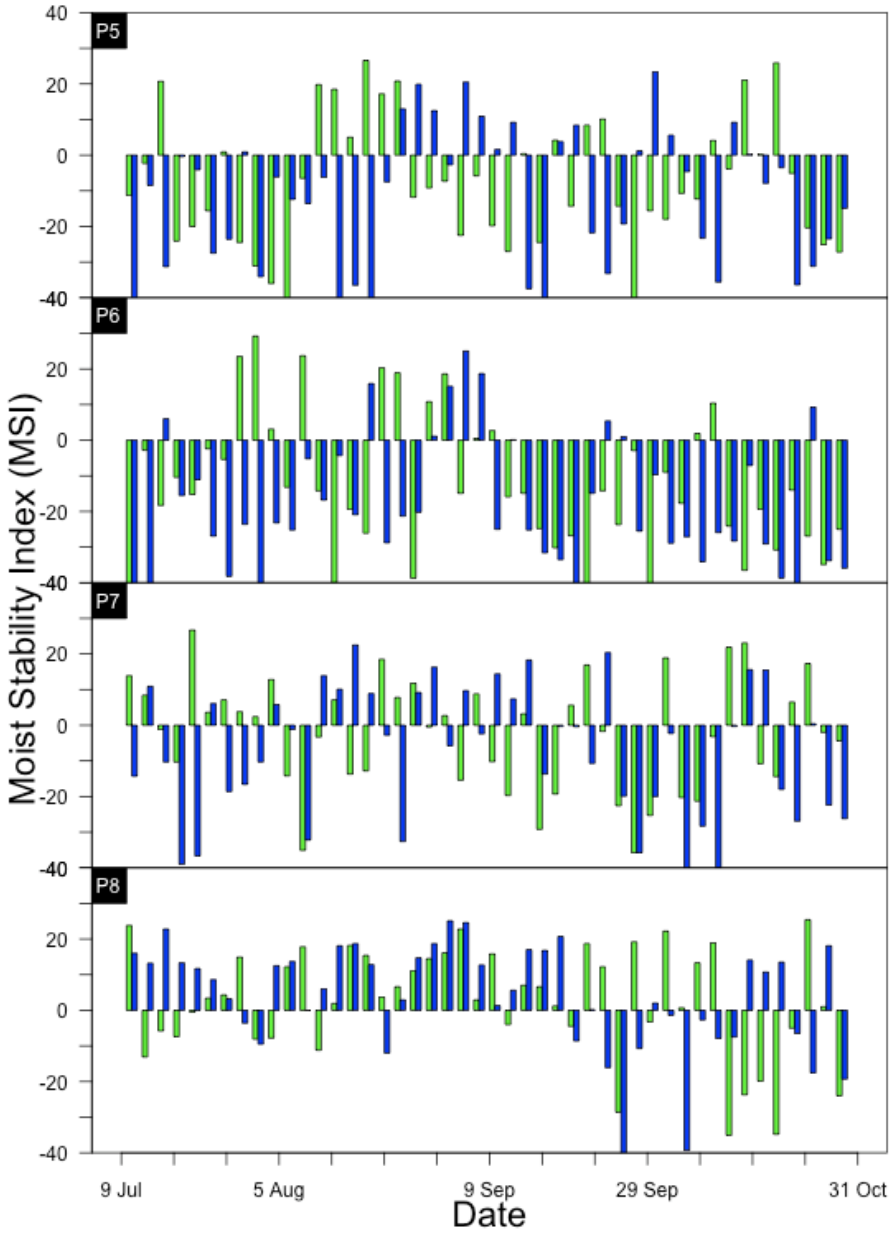

Figure 46: Moist Stability Index: Points 5-8: The time history of Moist Stability Index (MSI) at Points 5-8 from Figure 5. MSI values from 2005 are shown in green and 2006 values are shown in blue.

5.5 Wind Shear Comparisons

A continuation of the storm circulation is vital to the development and intensification of a TC. As surface winds take on heat and moisture from the ocean surface, they have to be able to rise to higher altitudes in the storm. However, if the winds at these high levels remain relatively light (little or no wind shear) and there is enough moisture present in the mid-troposphere, the storm can remain intact and continue to strengthen. Light upper level winds allow raised moisture to be "fanned out" to other parts of a TC. If winds aloft are too strong (i.e., greater than 15 m/s), the upper and lower portions of the disturbance can be cut off from each other at which point the infusion of moisture and heat from warm ocean water into the disturbance halts. If this occurs, the low pressure system is cut off from its primary energy source. Several different methods were used to observe vertical wind shear between 2005 and 2006. Wind barbs, speed shear, and directional shear are plotted for each point in Figures 47-70. Figures 71-73 display vertical wind shear calculated between three different levels: 850-250 hPa (troposphere), 700-400 hPa (mid-troposphere), and 850-500 hPa (low-troposphere).

Figures 47-70 show a trend similar to that seen in the vertical moisture profiles. Points inside the AI contours show more changes in speed and direction with height while points outside the AI contours display a more consistent speed and direction above the marine boundary layer or show weaker wind speeds throughout the entire column. This trend can also be seen between Points 1, 2, 5, and 6 and Points 3, 4, 7, and 8 in the 700-400 hPa and 850-500 hPa vertical wind shear calculations. Wind information on Skew-T diagrams at Points 2 and 3 for both years shows this trend as well.

The vertical wind shear calculations (Figures 71-73) show both years experiencing relatively low shear environments in the mid and lower troposphere, even considering the aforementioned trend. In general, the lowest wind shear values were found in the lower atmosphere. Stronger wind shear values were evident in the mid-troposphere but the values were still, mostly, under the 15 m/s threshold. Vertical wind shear values were largest when calculated for the whole troposphere. In September, the most active month for 2006, wind shear values were close to the same magnitude in both years for the 700-400 hPa and 850-500 hPa calculations. The 850-250 hPa calculations in this month show slightly lower wind shear values in 2006 as compared to 2005 at some of the points. However, once October begins, 2006 wind shear values are higher than 2005 values at most points.

Results from 500 hPa wind barbs indicated that the pattern of easterly winds coming off the west coast of Africa may have played a critical role in determining the strength of 2005 hurricane season. These winds helped strengthen tropical low-pressure systems moving westward from the African coast. They also steered the low-pressure systems westward toward the low-shear, warm-water environment of the MDR, where they transformed into tropical storms and hurricanes. Observations from NCEP wind barb fields at 500 hPa show higher amplitude easterly waves and more storms breaking off these waves in 2005. In 2006, the midlevel easterly jet is much stronger. The SAL is associated with a strong midlevel easterly jet which has the potential to increase low-level vertical wind shear (Dunion and Velden, 2004). This strong midlevel easterly jet

appeared to decrease the number of opportunities available for storm development in 2006.

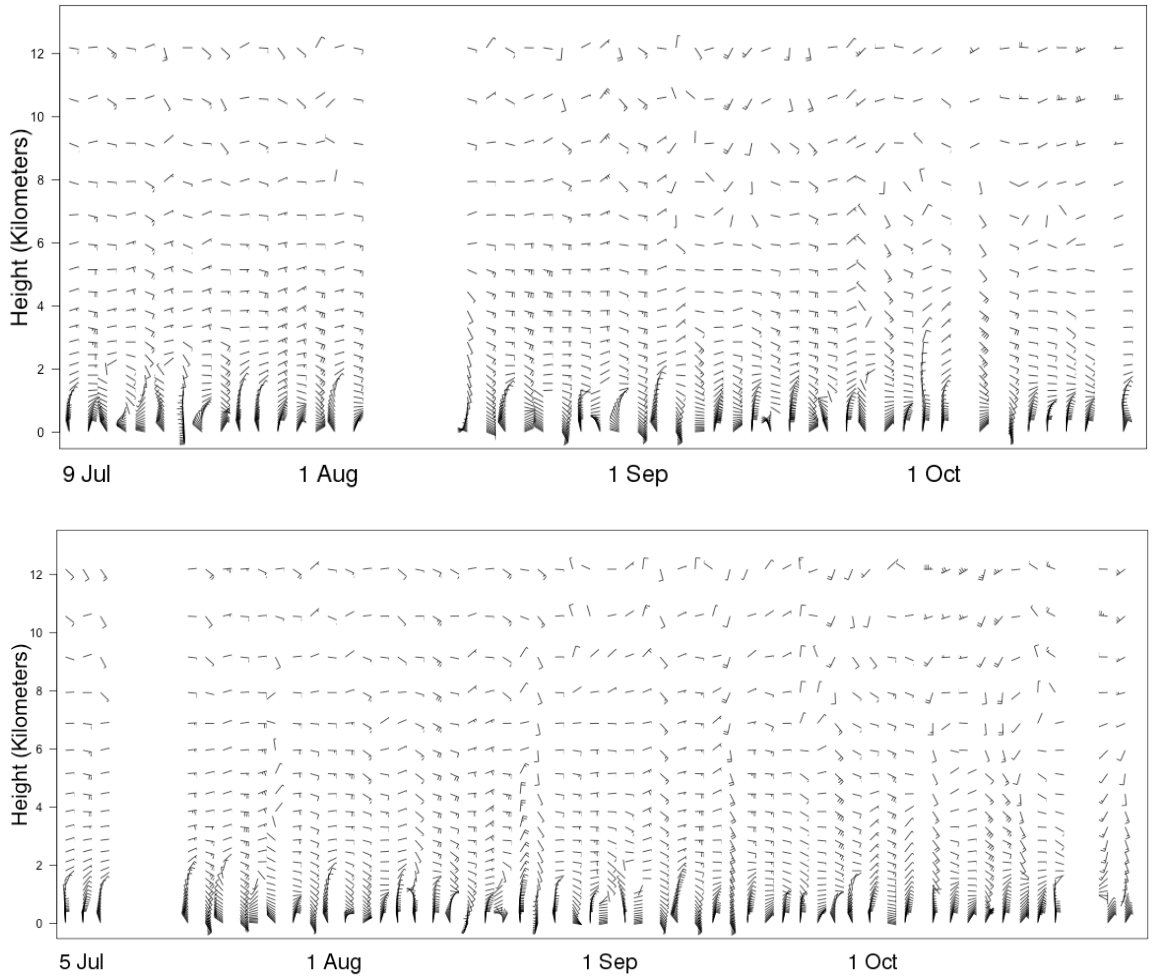

Figure 47: Time Series: Wind Barbs at Point 1: Shows the vertical profile in time (July-October) of the wind speed and direction at Point 1 from Figure 5 for 2005 (top panel) and 2006 (bottom panel).

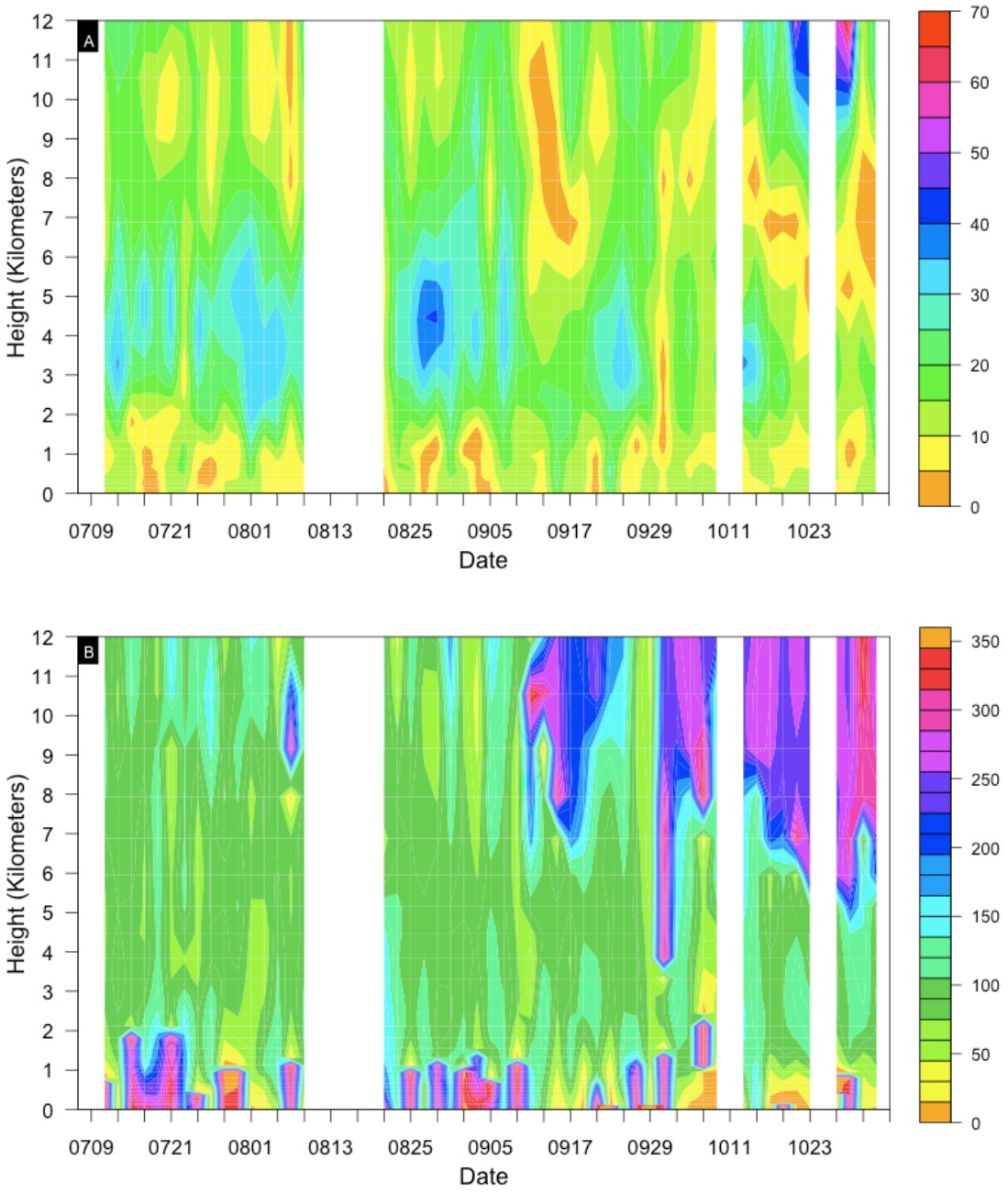

Figure 48: Time Series: Speed and Directional Shear at Point 1 in 2005: Shows the vertical profile in time (July-October) of the wind speed (Panel A) and direction (Panel B) in 2005 at Point 1 from Figure 5. Wind speeds are in knots.

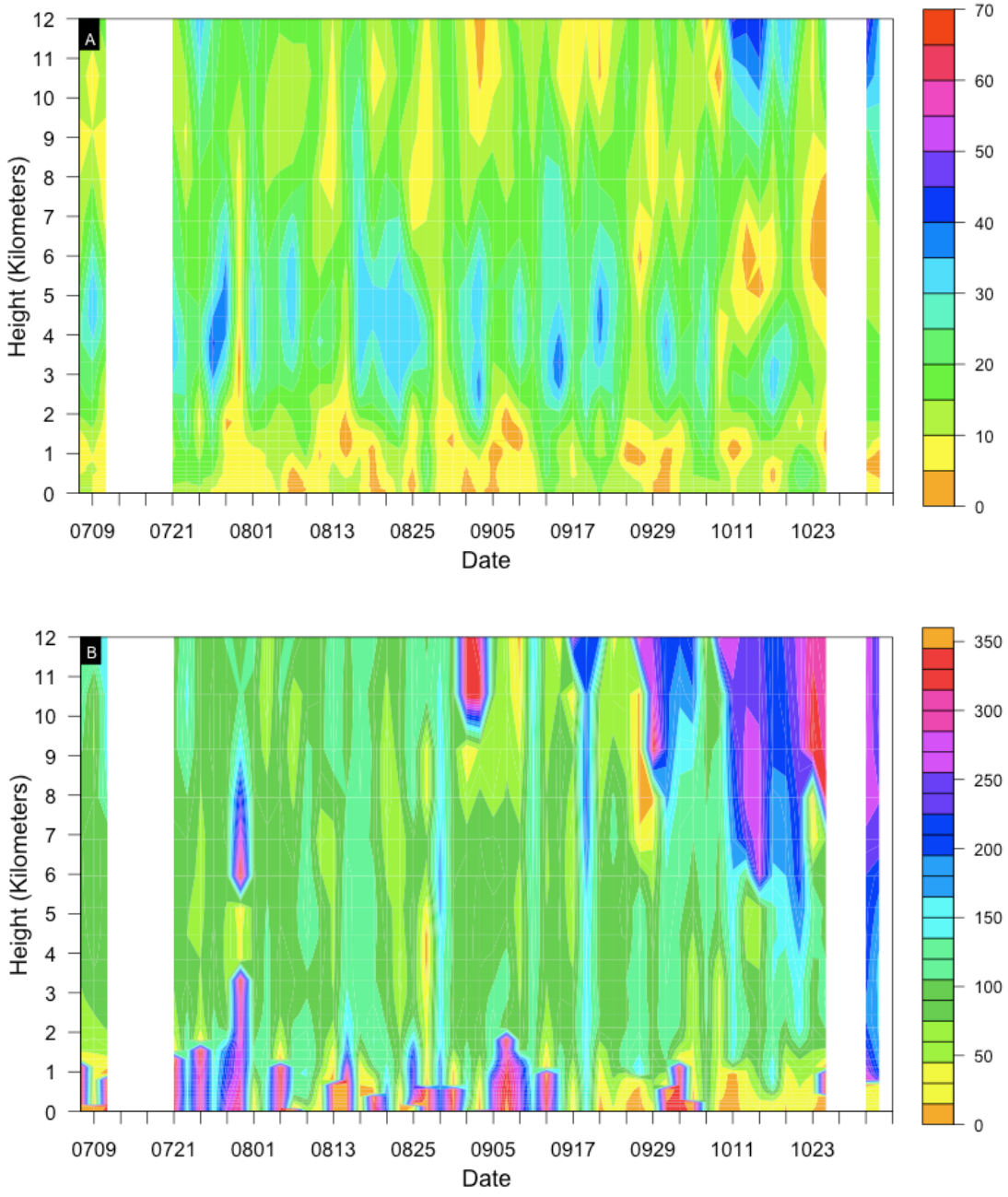

Figure 49: Time Series: Speed and Directional Shear at Point 1 in 2006: Shows the vertical profile in time (July-October) of the wind speed (Panel A) and direction (Panel B) in 2006 at Point 1 from Figure 5. Wind speeds are in knots.

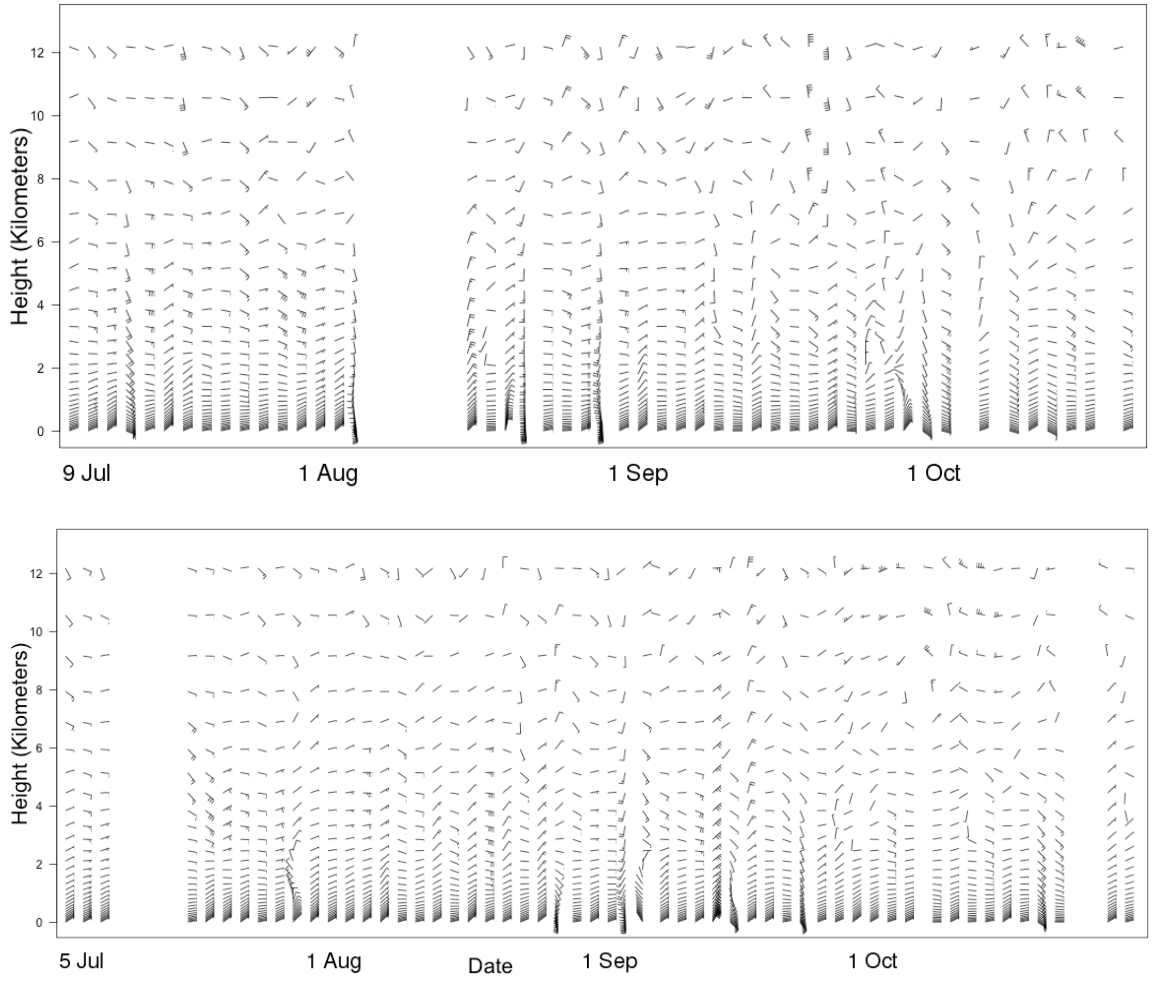

Figure 50: Time Series: Wind Barbs at Point 2: Same as Figure 53 except at Point 2 from Figure 5.

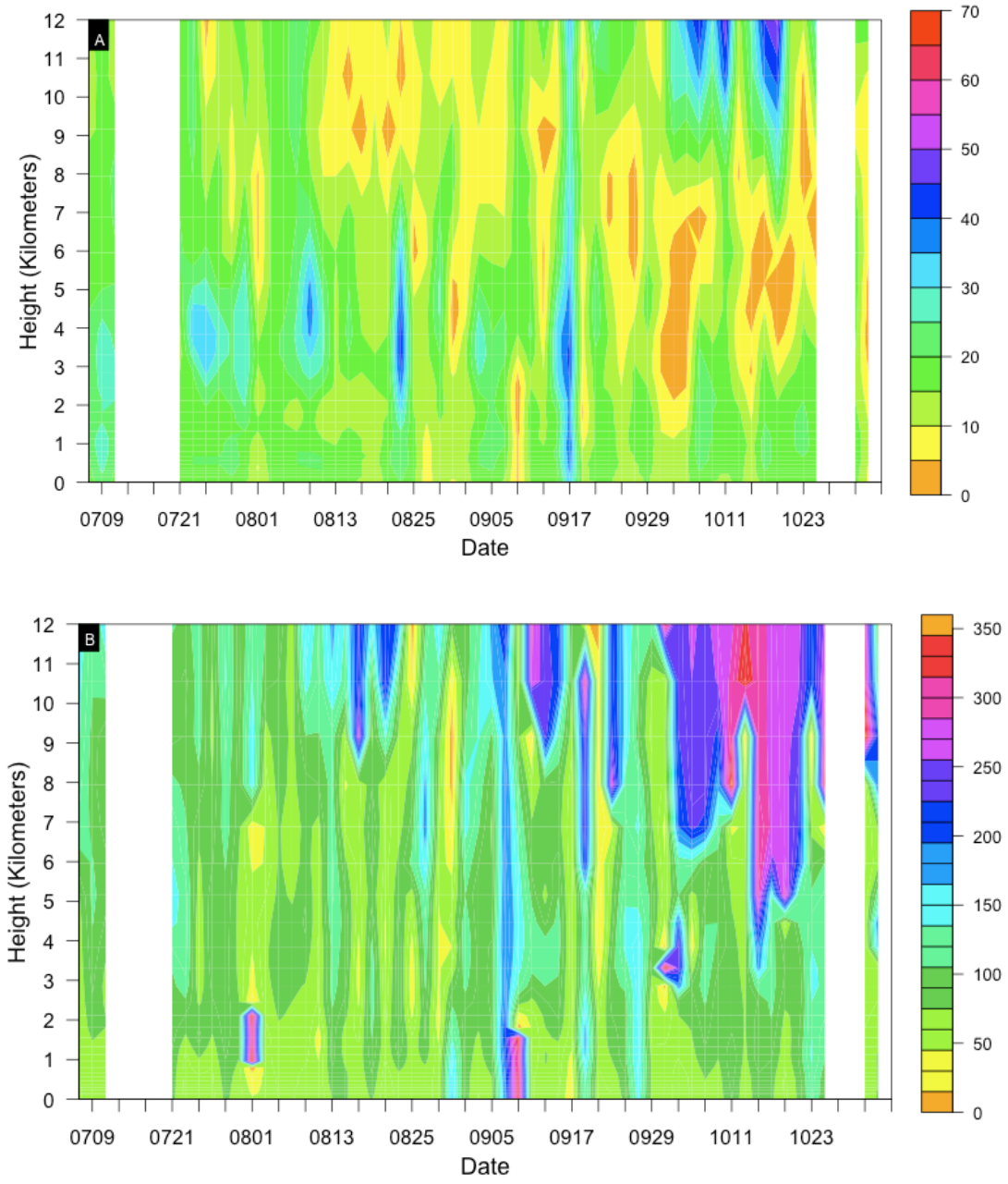

Figure 51: Time Series: Speed and Directional Shear at Point 2 in 2005: Same as Figure 55 except for Point 2 from Figure 5.

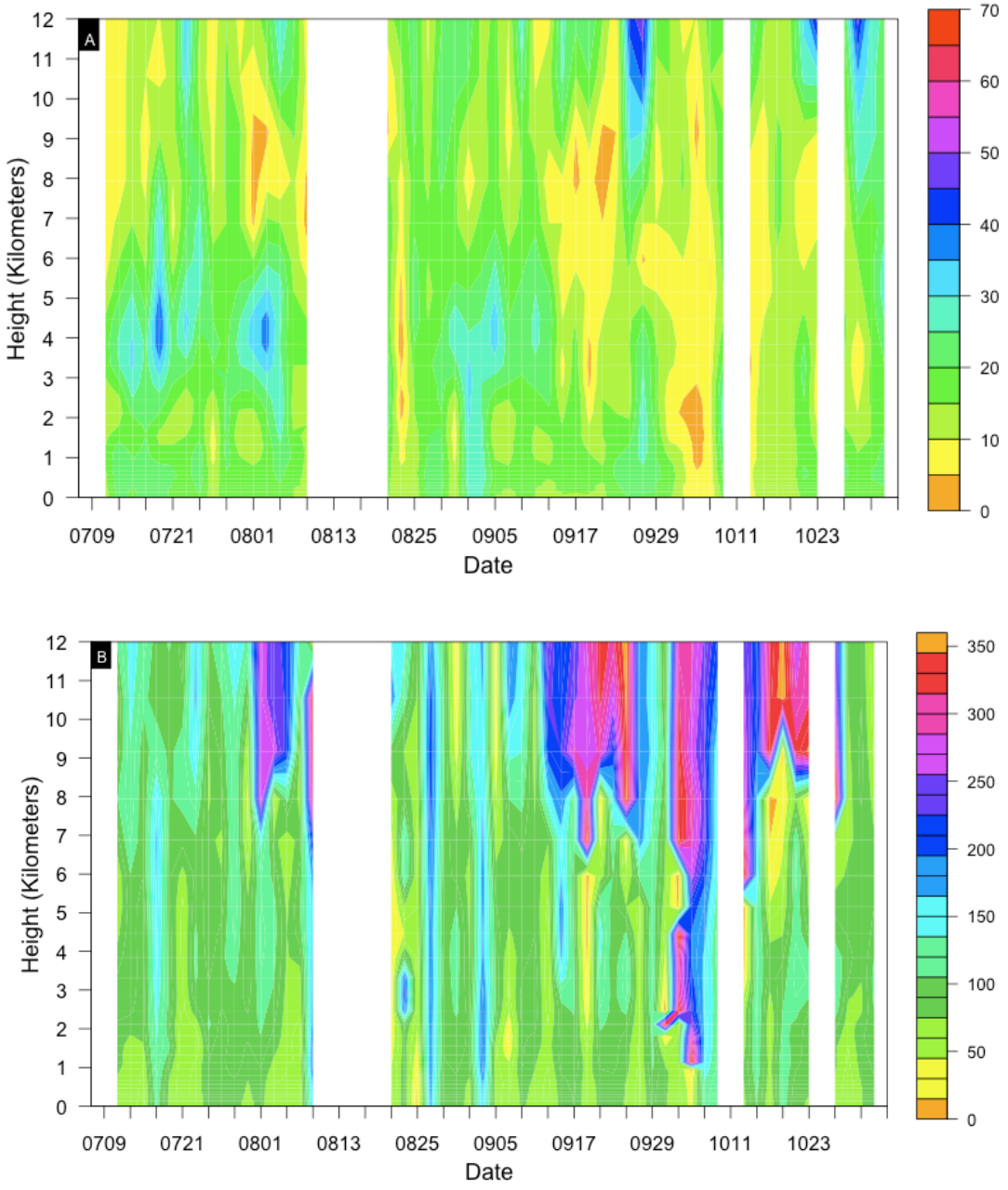

Figure 52: Time Series: Speed and Directional Shear at Point 2 in 2006: Same as Figure 54 except at Point 2 from Figure 5.

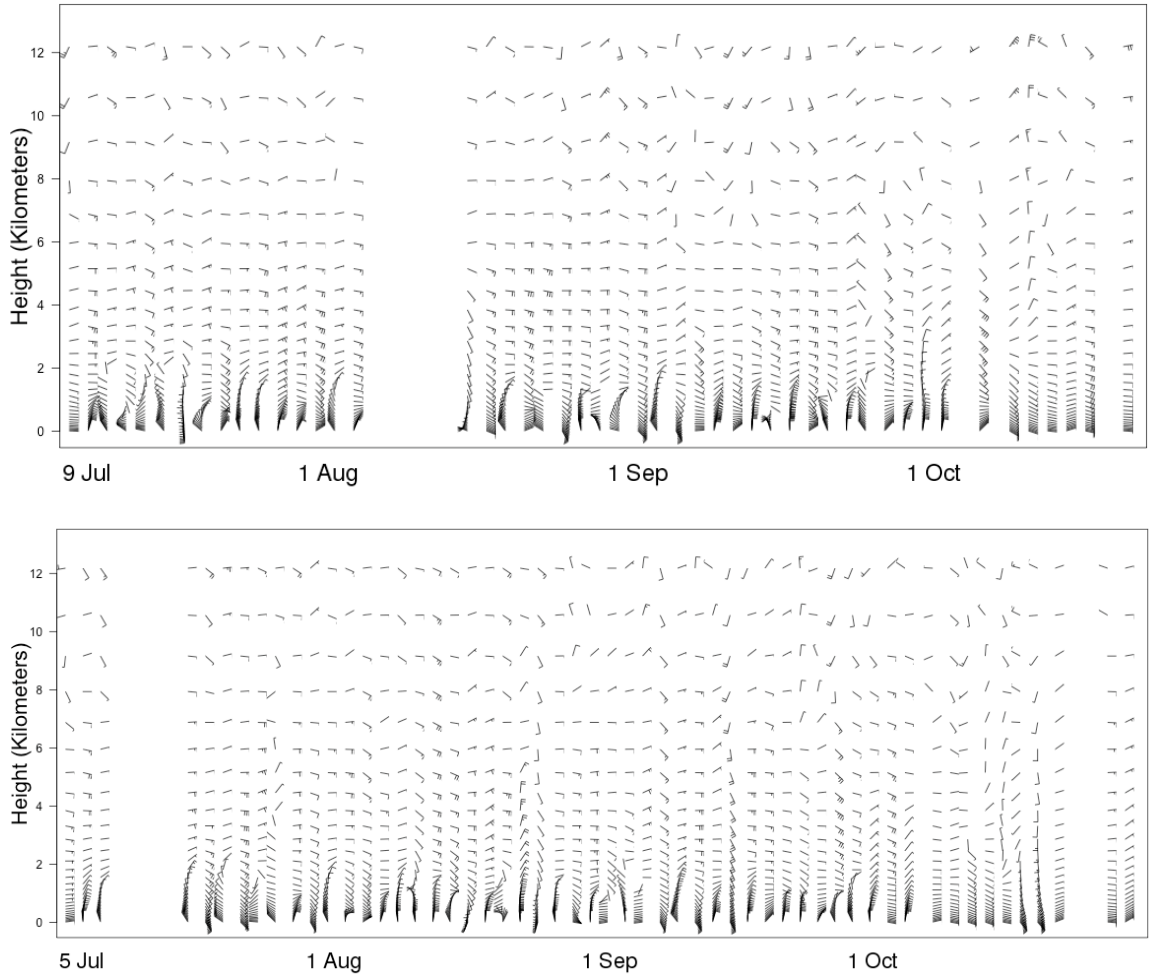

Figure 53: Time Series: Wind Barbs at Point 3: Same as Figure 53 except for Point 3 from Figure 5.

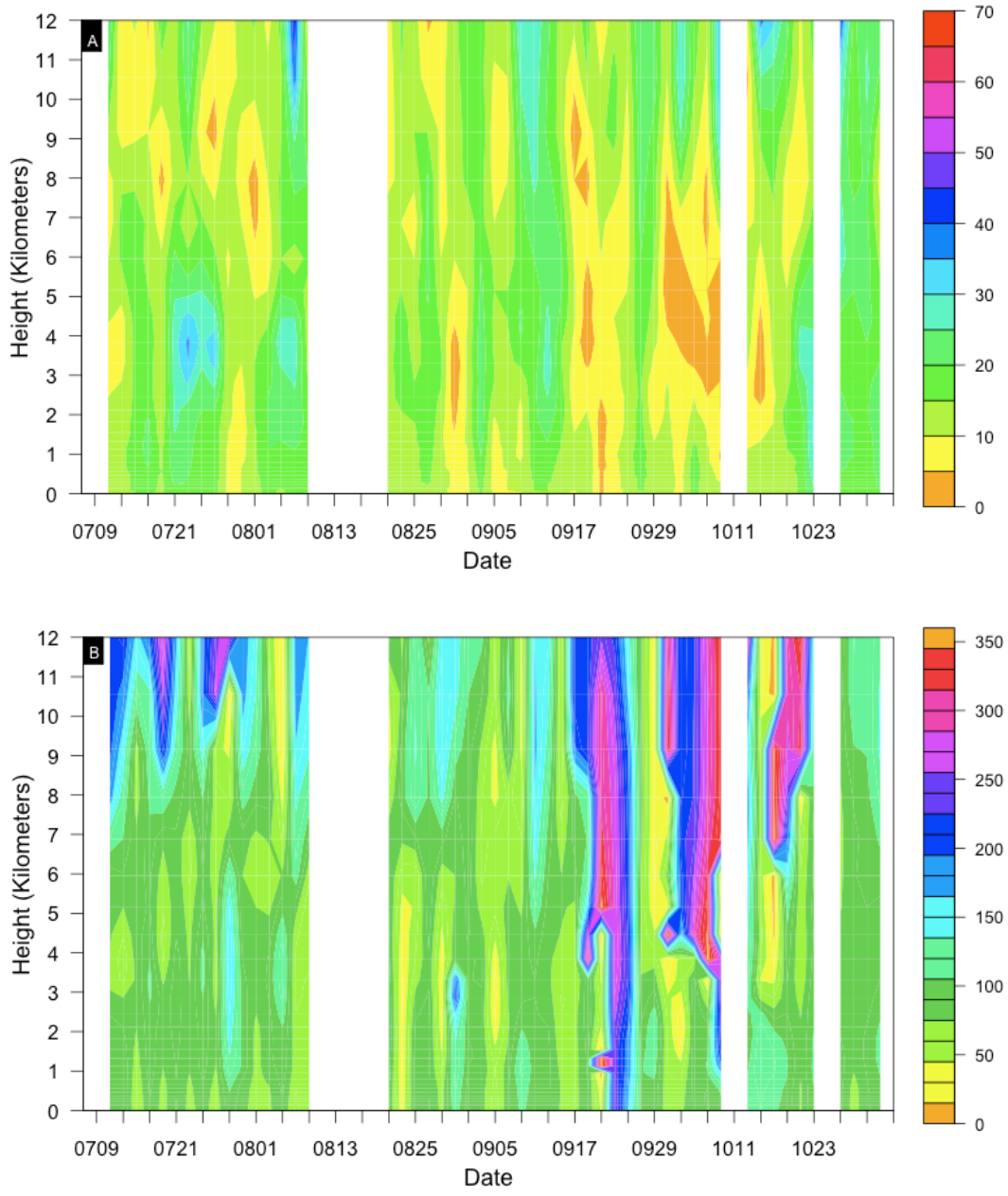

Figure 54: Time Series: Speed and Directional Shear at Point 3 in 2005: Same as Figure 54 except at Point 3 from Figure 5.

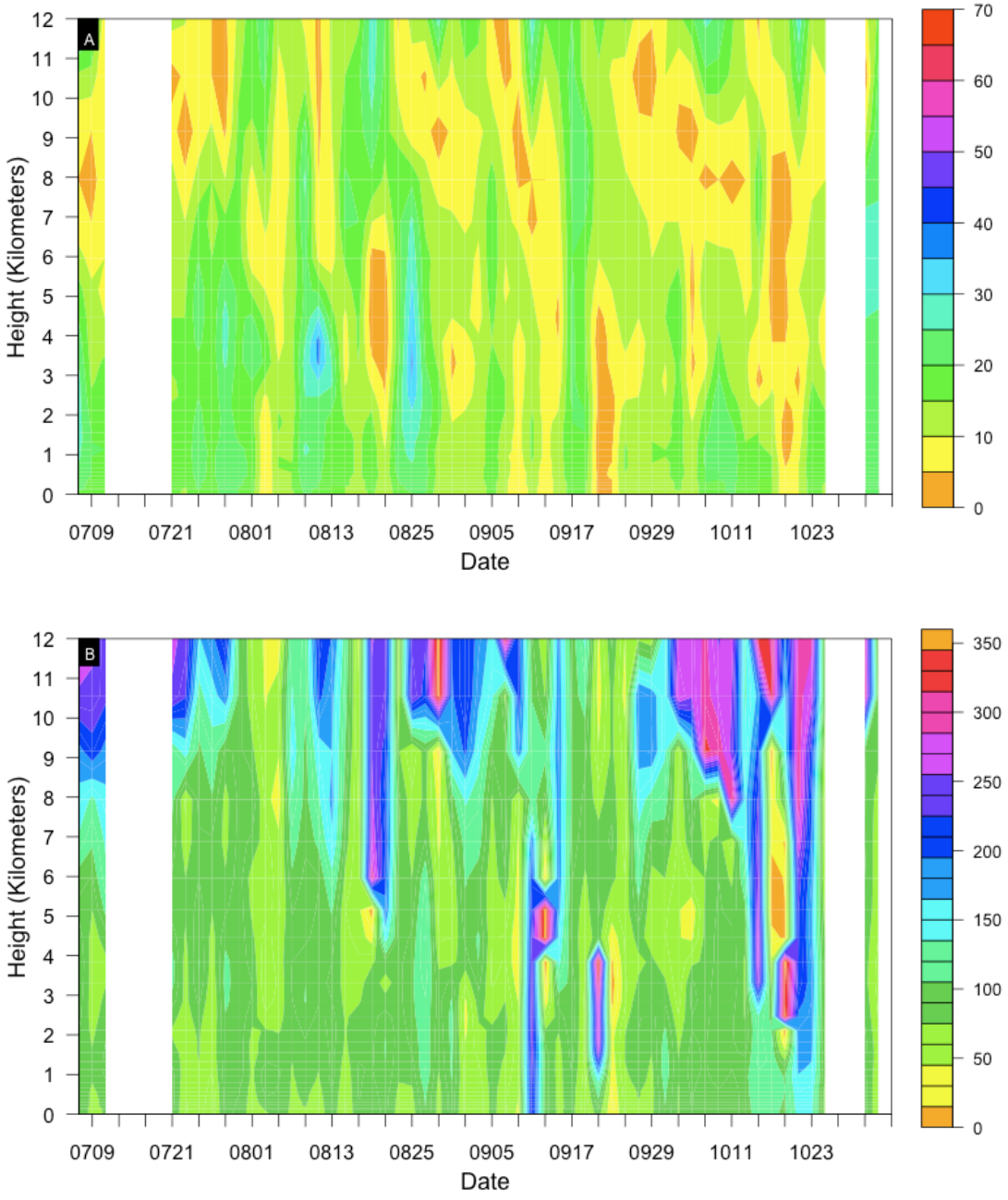

Figure 55: Time Series: Speed and Directional Shear at Point 3 in 2006: Same as Figure 55 except for Point 3 from Figure 5.

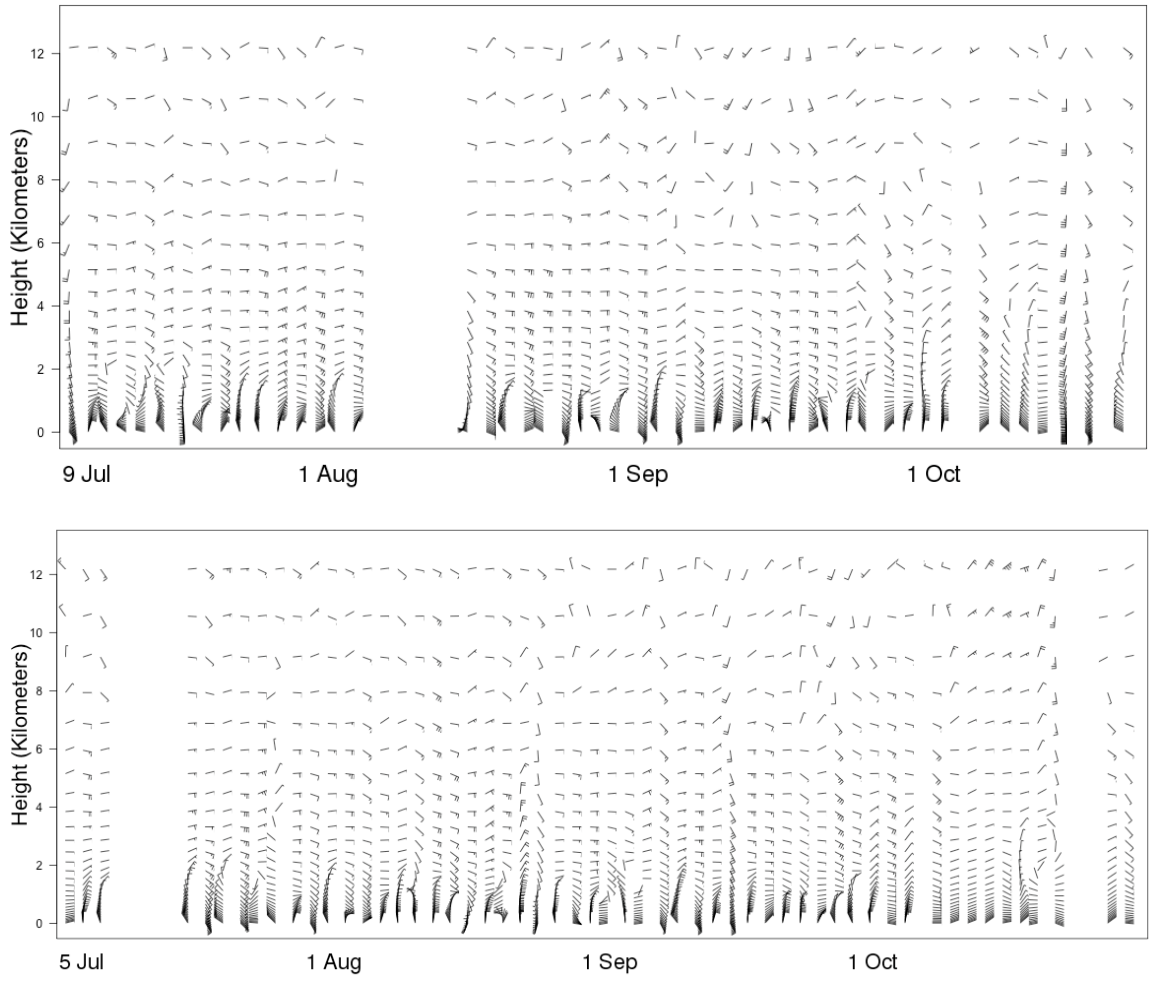

Figure 56: Time Series: Wind Barbs at Point 4: Same as Figure 53 except for Point 4 from Figure 5.

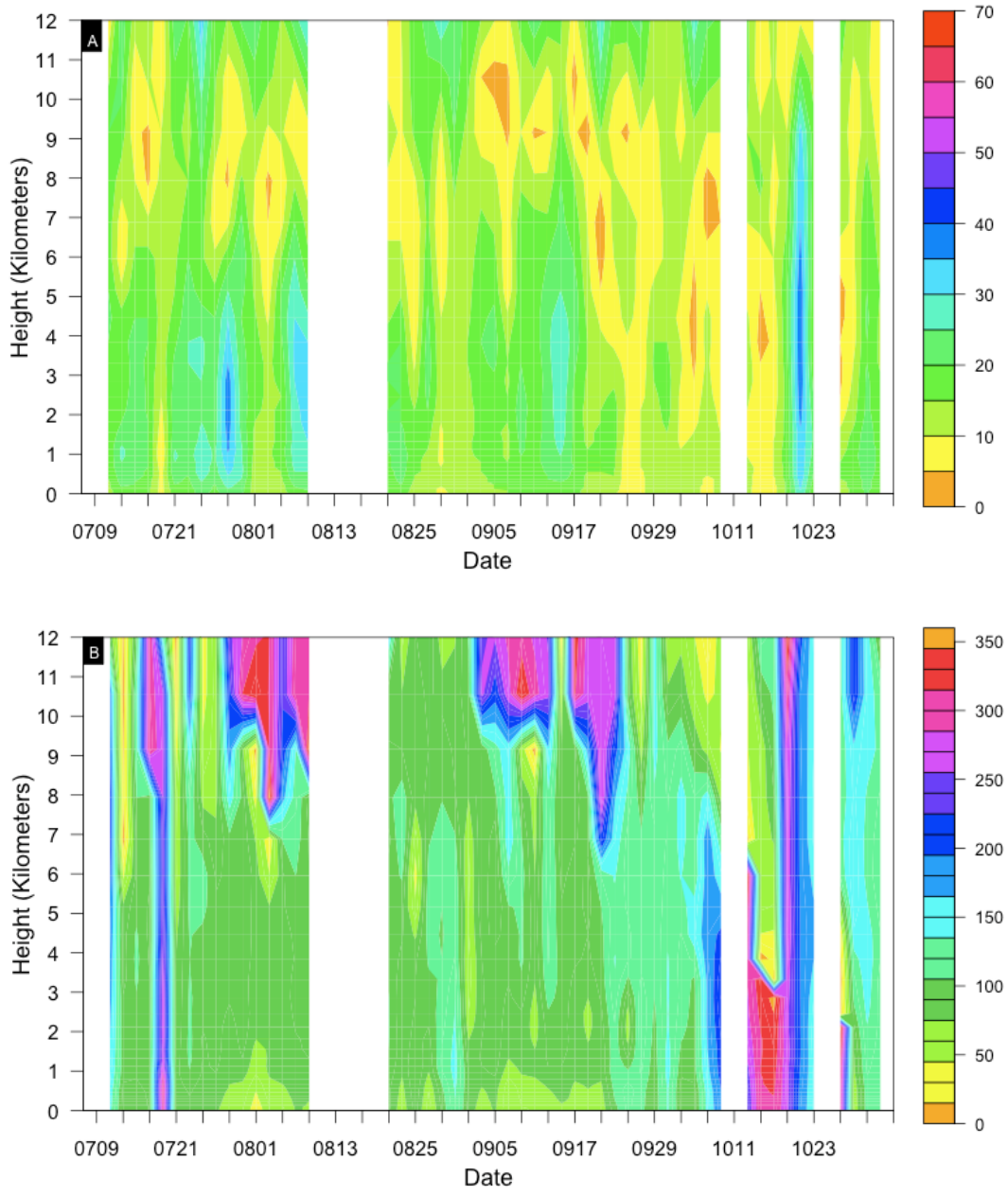

Figure 57: Time Series: Speed and Directional Shear at Point 4 in 2005: Same as Figure 54 except at Point 4 from Figure 5.

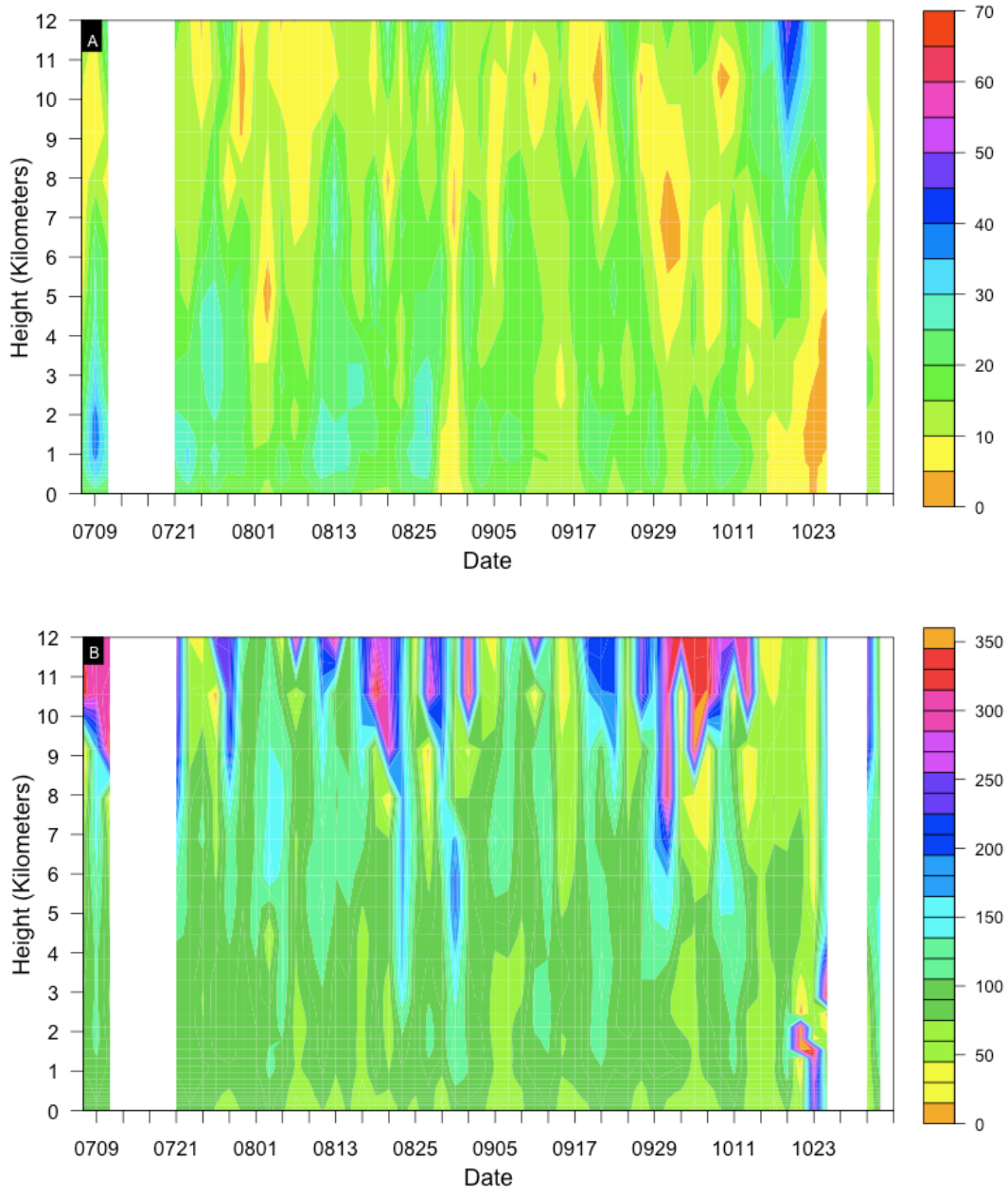

Figure 58: Time Series: Speed and Directional Shear at Point 4 in 2006: Same as Figure 55 except for Point 4 from Figure 5.

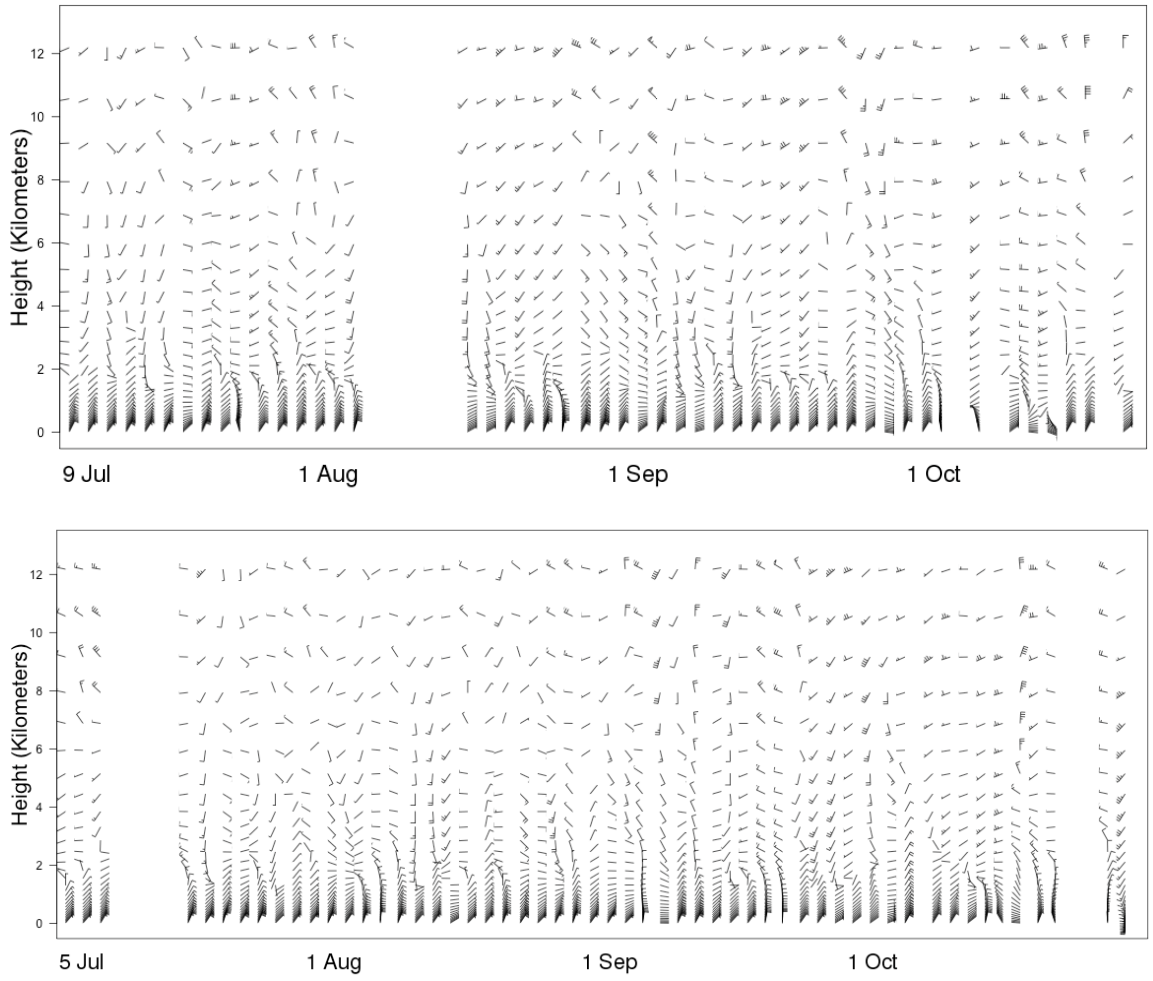

Figure 59: Time Series: Wind Barbs at Point 5: Same as Figure 53 except for Point 5 from Figure 5.

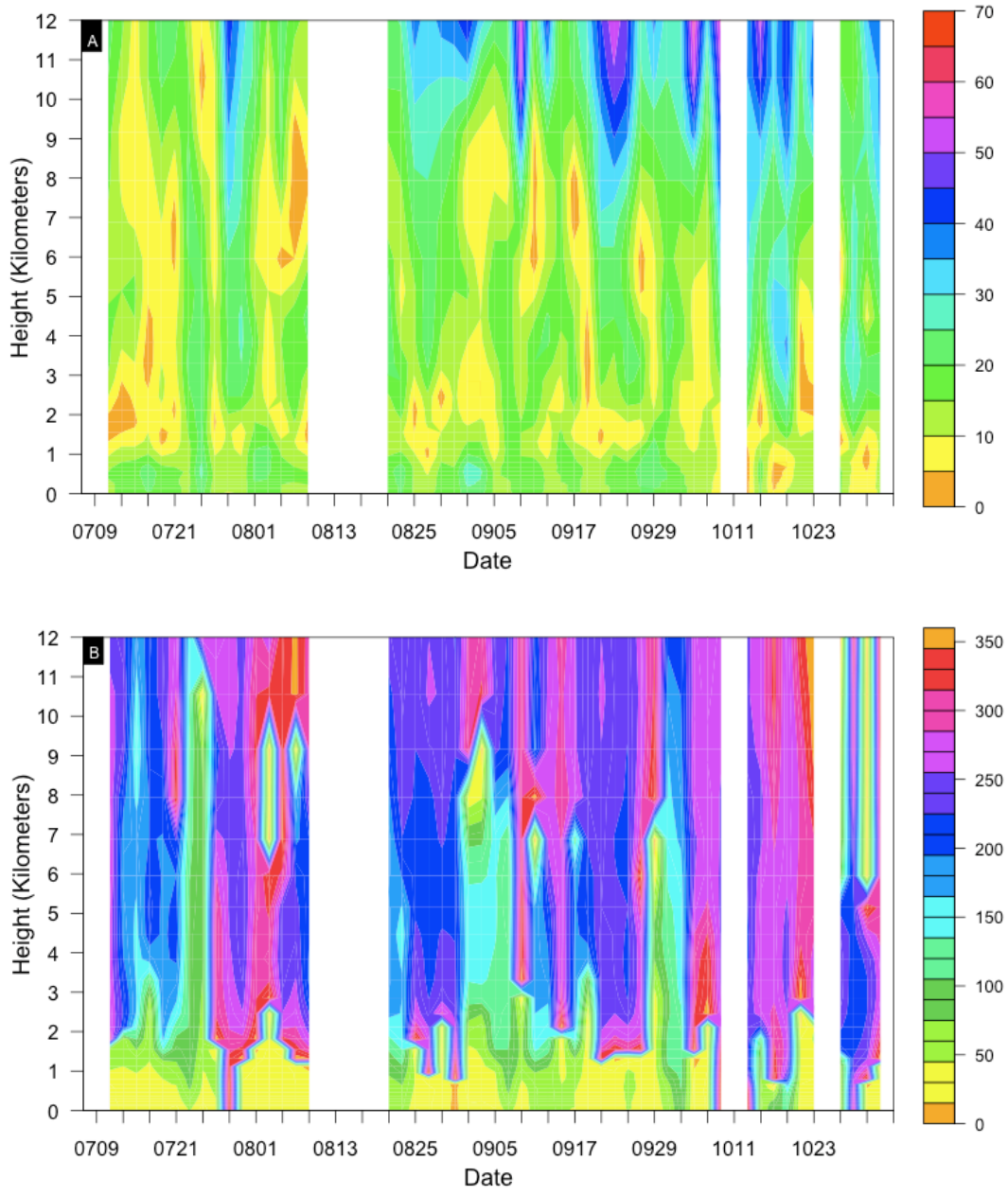

Figure 60: Time Series: Speed and Directional Shear at Point 5 in 2005: Same as Figure 54 except at Point from Figure 5.

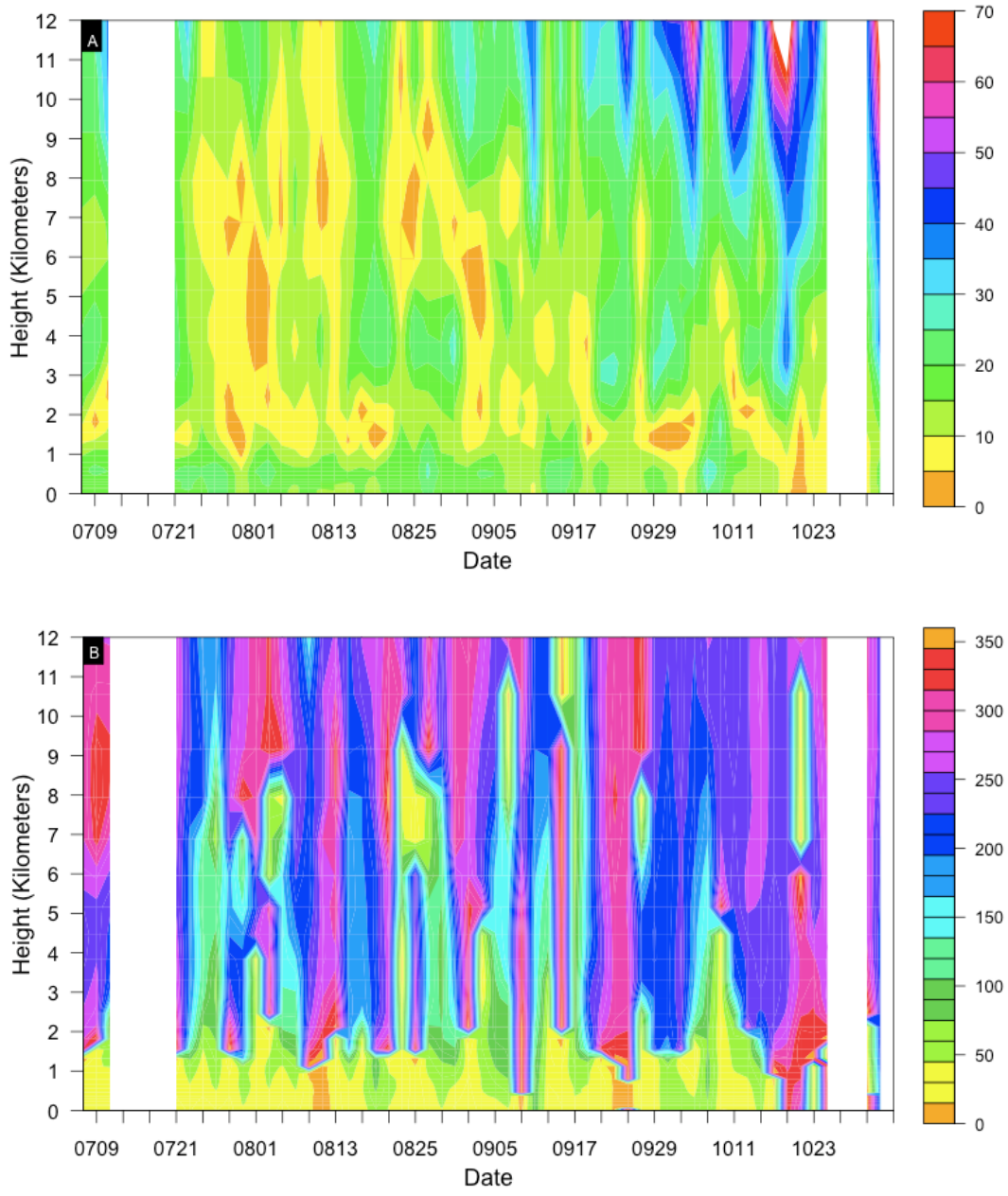

Figure 61: Time Series: Speed and Directional Shear at Point 5 in 2006: Same as Figure 55 except for Point 5 from Figure 5.

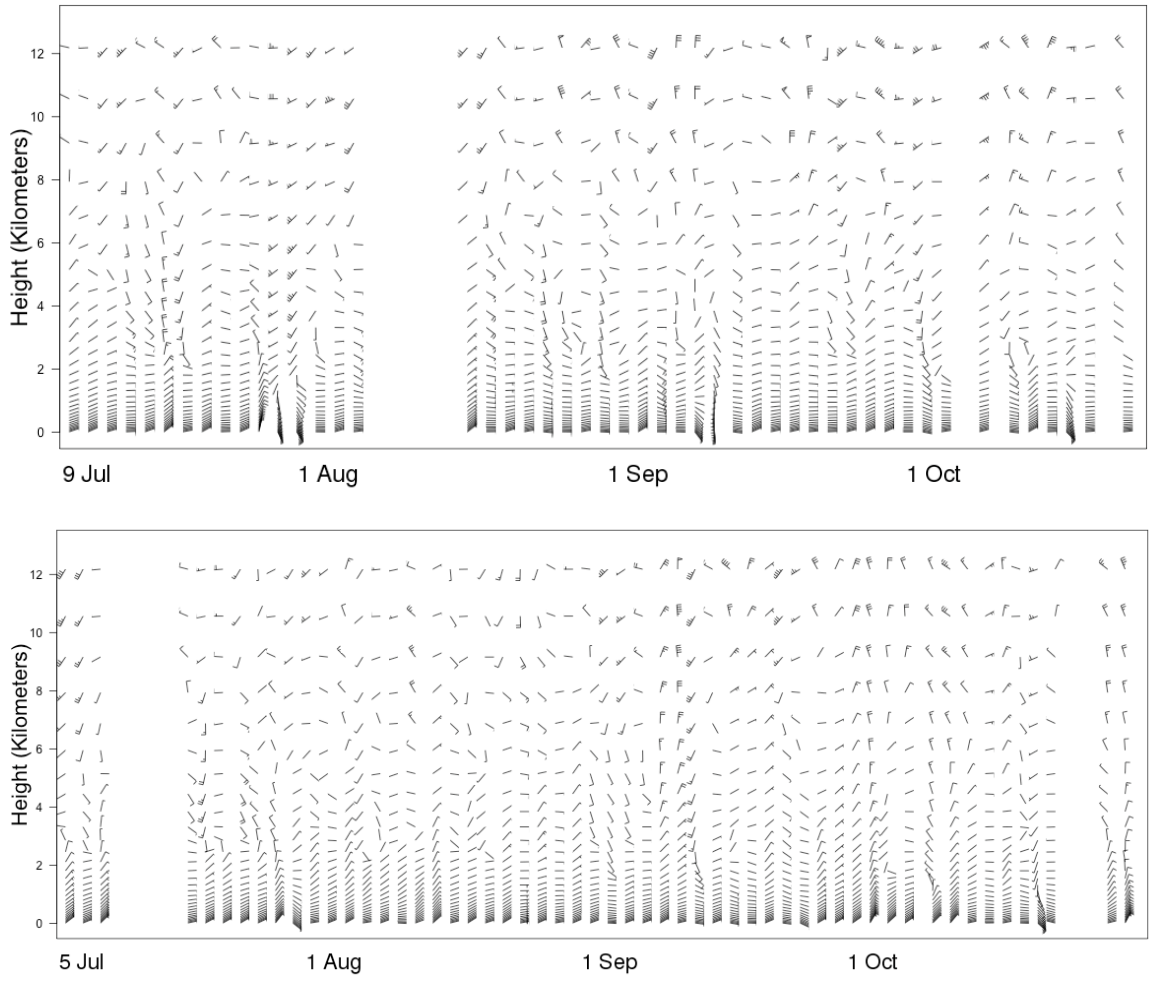

Figure 62: Time Series: Wind Barbs at Point 6: Same as Figure 53 except for Point 6 from Figure 5.

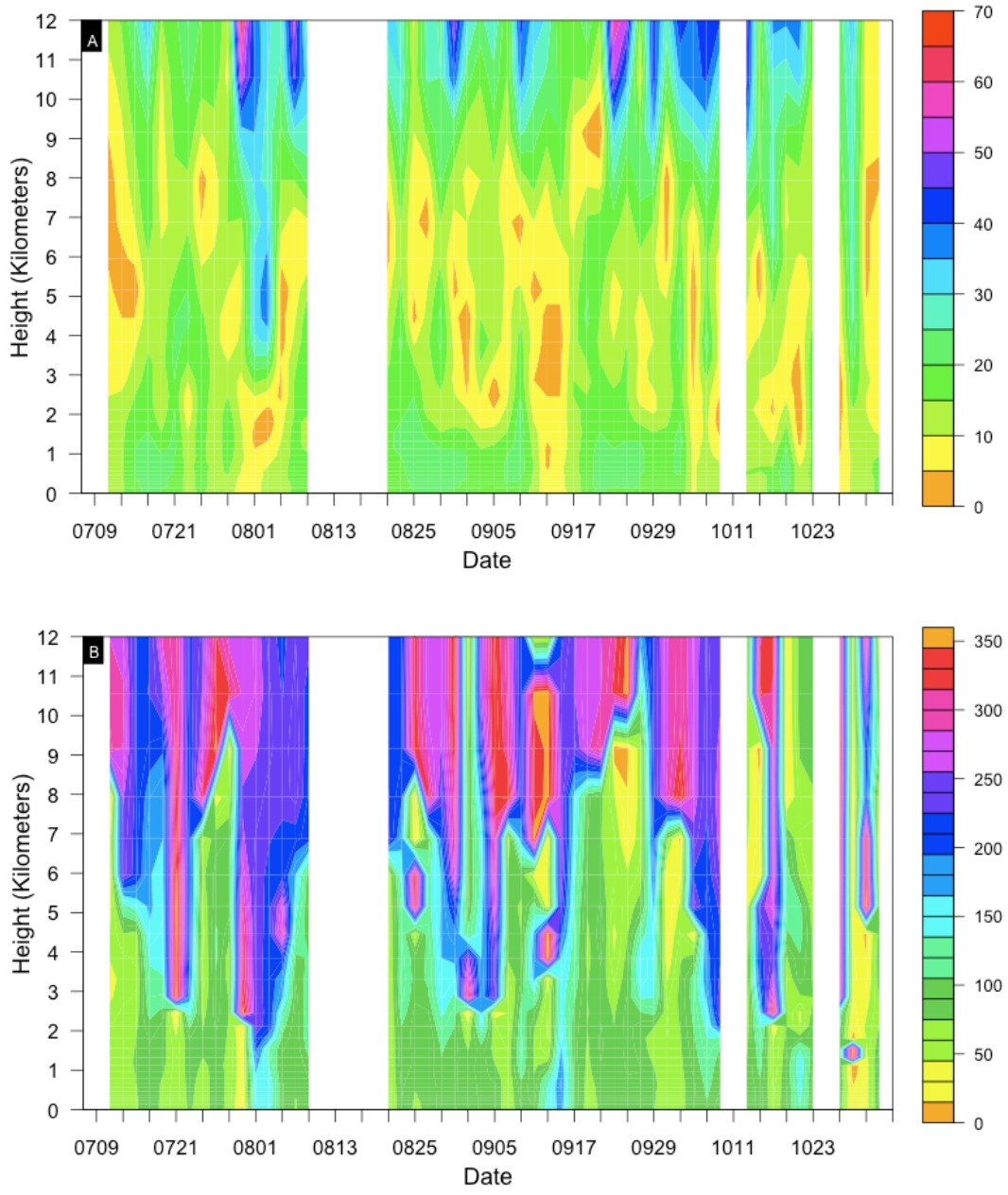

Figure 63: Time Series: Speed and Directional Shear at Point 6 in 2005: Same as Figure 54 except at Point 6 from Figure 5.

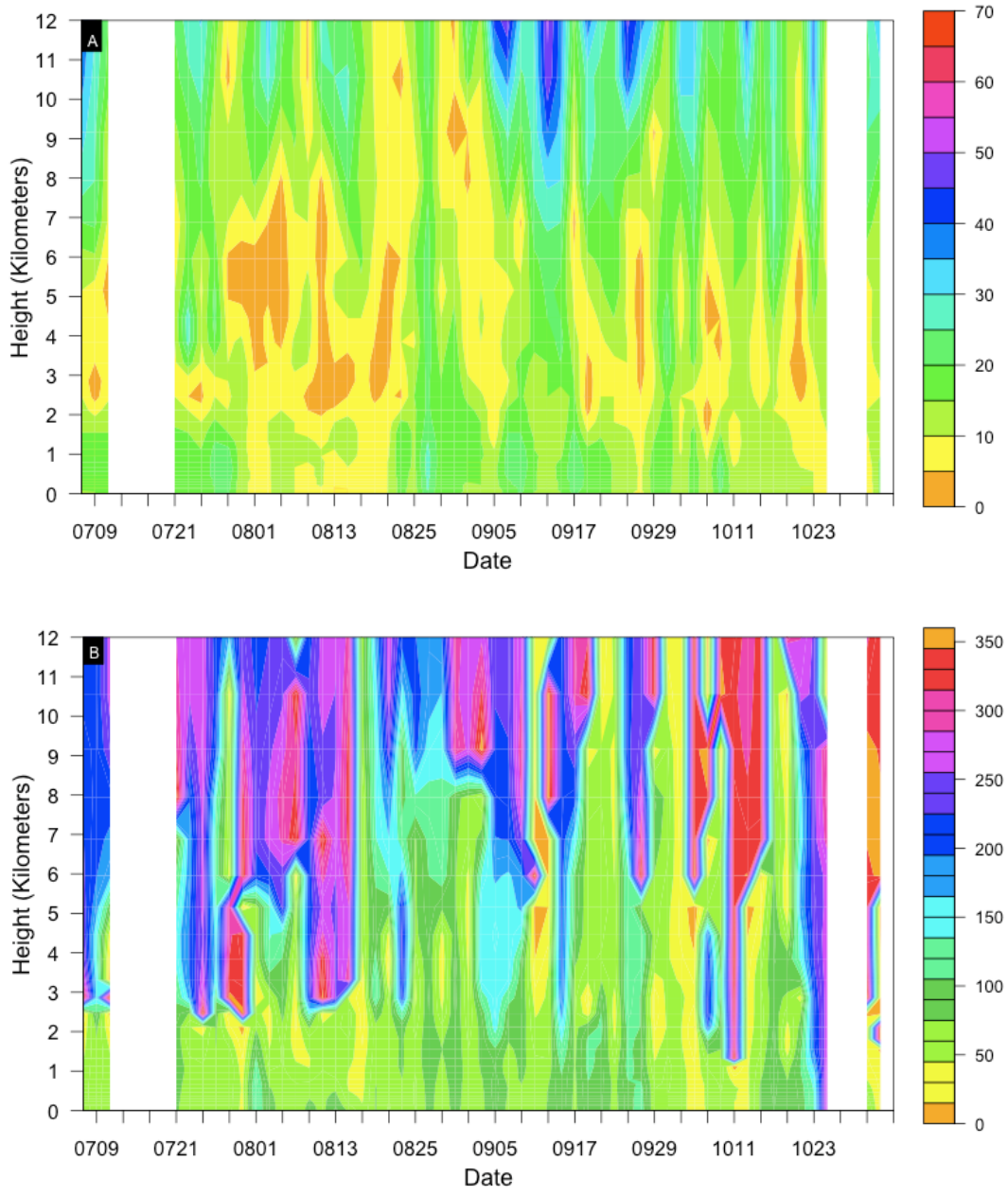

Figure 64: Time Series: Speed and Directional Shear at Point 6 in 2006: Same as Figure 55 except for Point 6 from Figure 5.

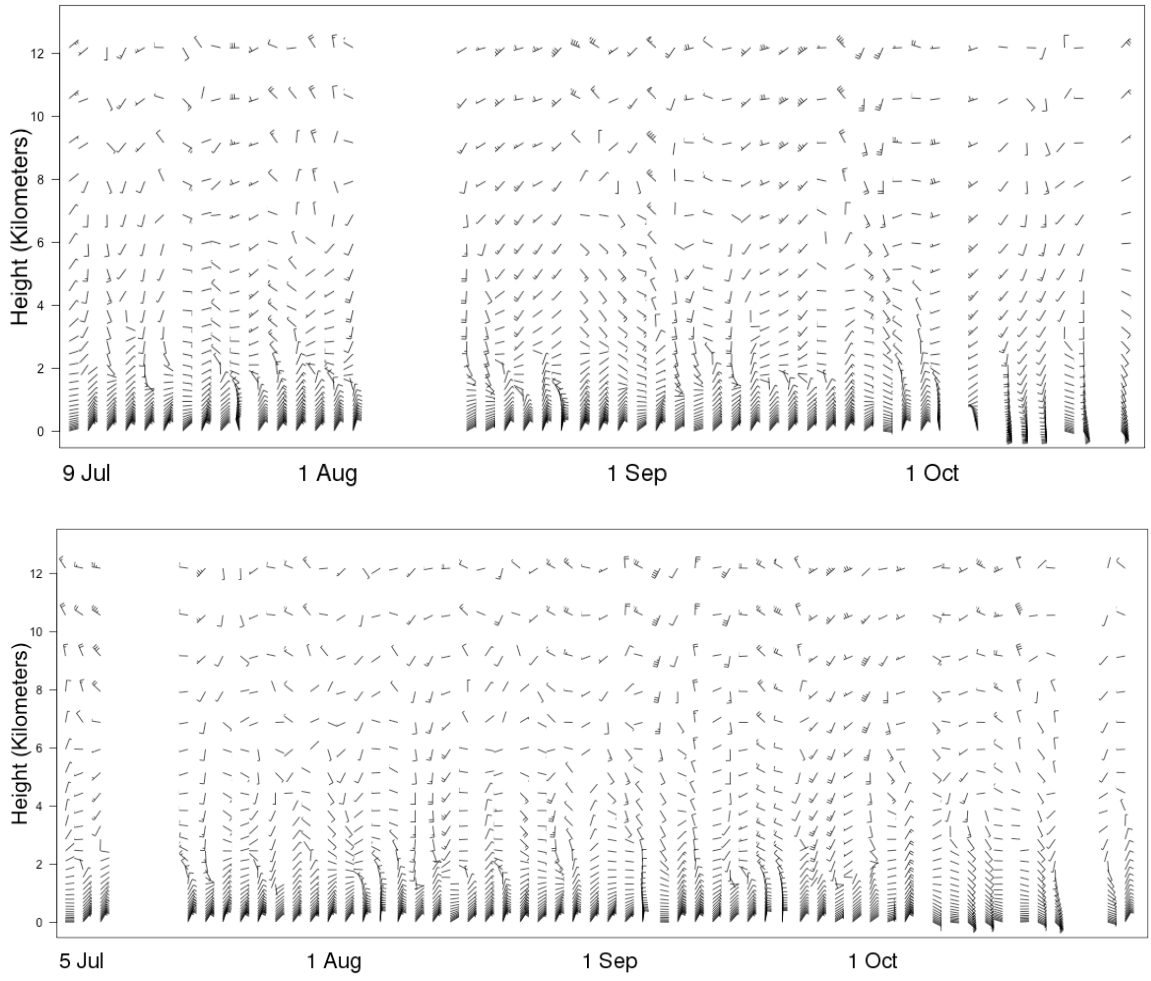

Figure 65: Time Series: Wind Barbs at Point 7: Same as Figure 53 except for Point 7 from Figure 5.

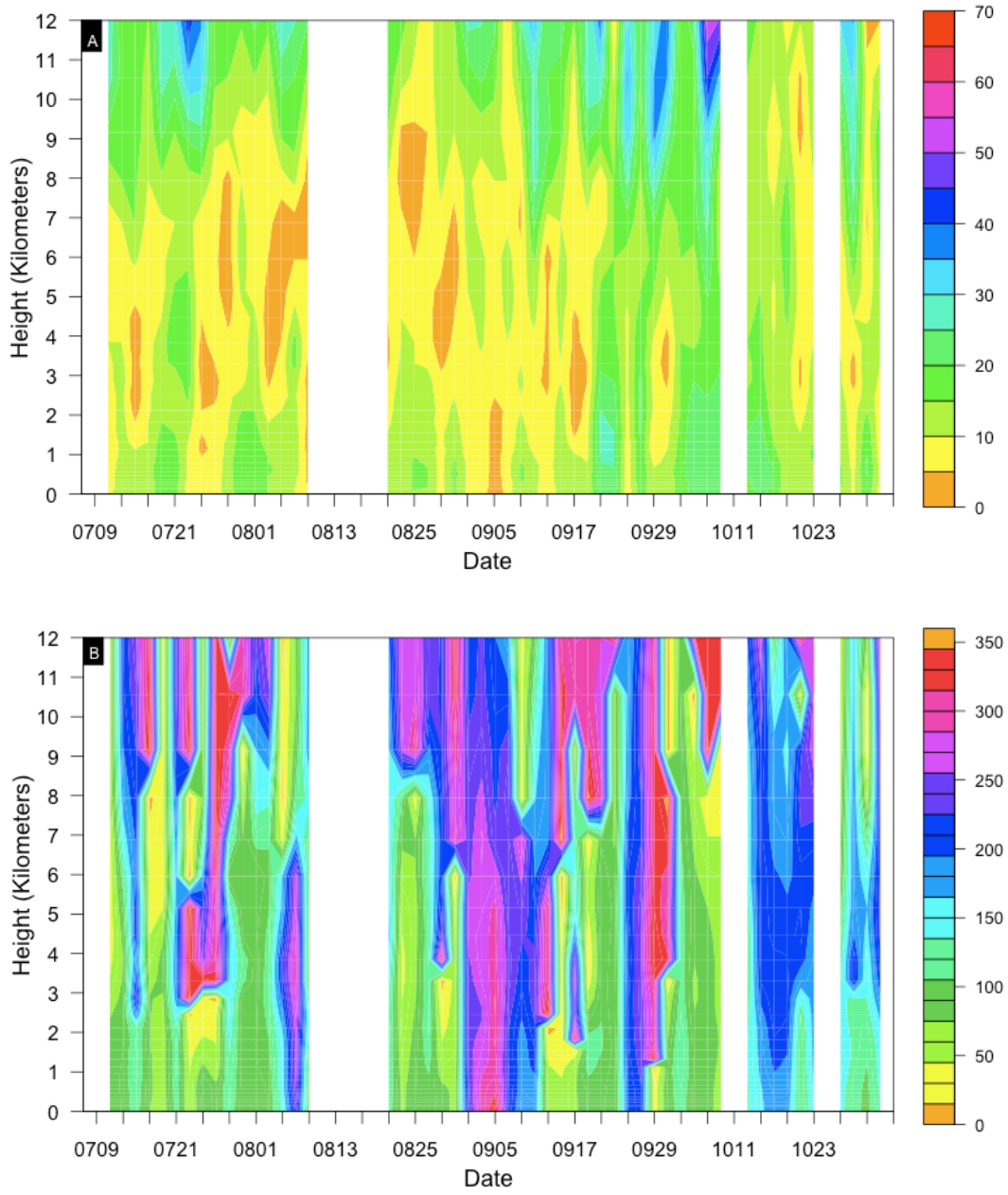

Figure 66: Time Series: Speed and Directional Shear at Point 7 in 2005: Same as Figure 54 except at Point 7 from Figure 5.

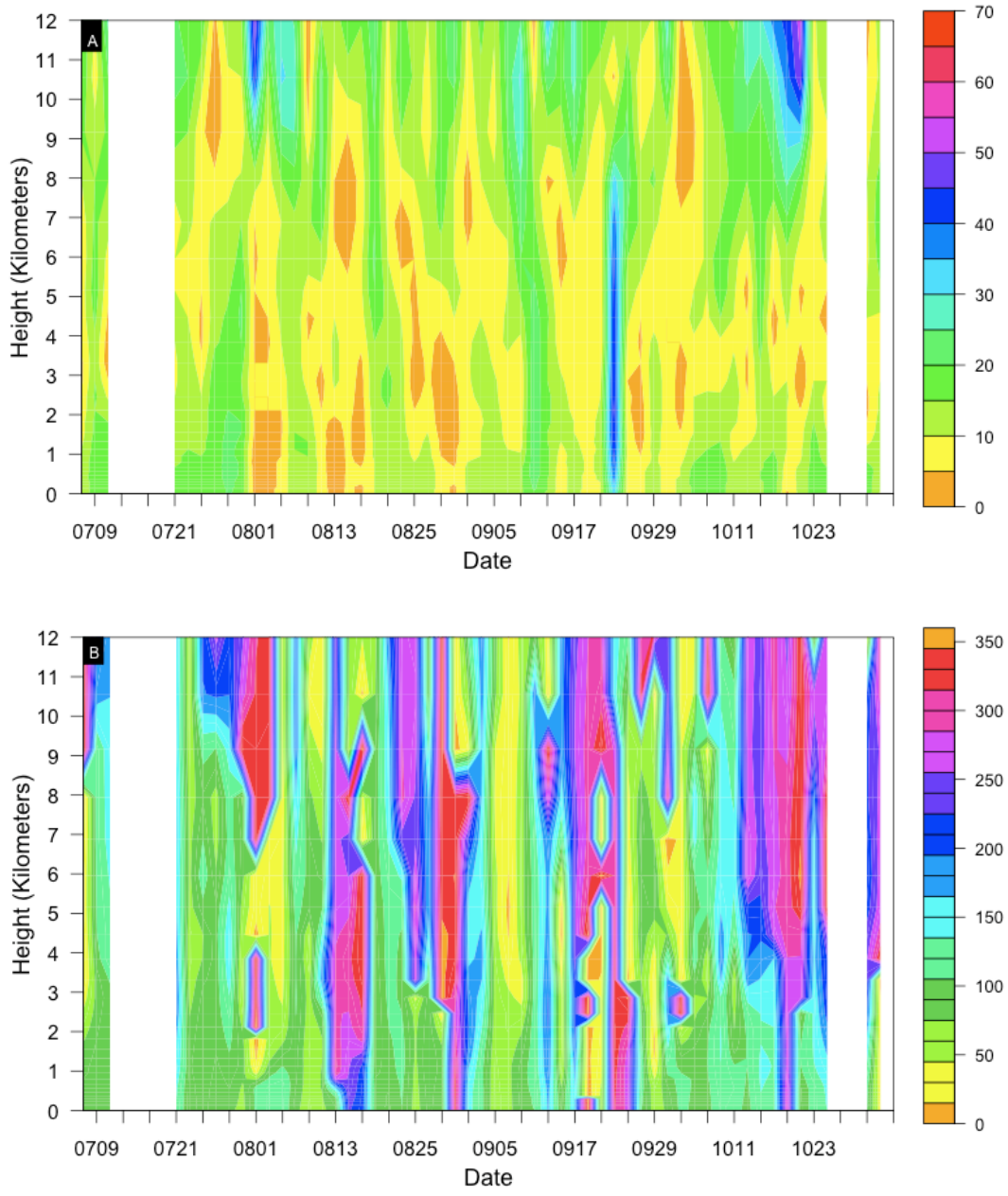

Figure 67: Time Series: Speed and Directional Shear at Point 7 in 2006: Same as Figure 55 except for Point 7 from Figure 5.

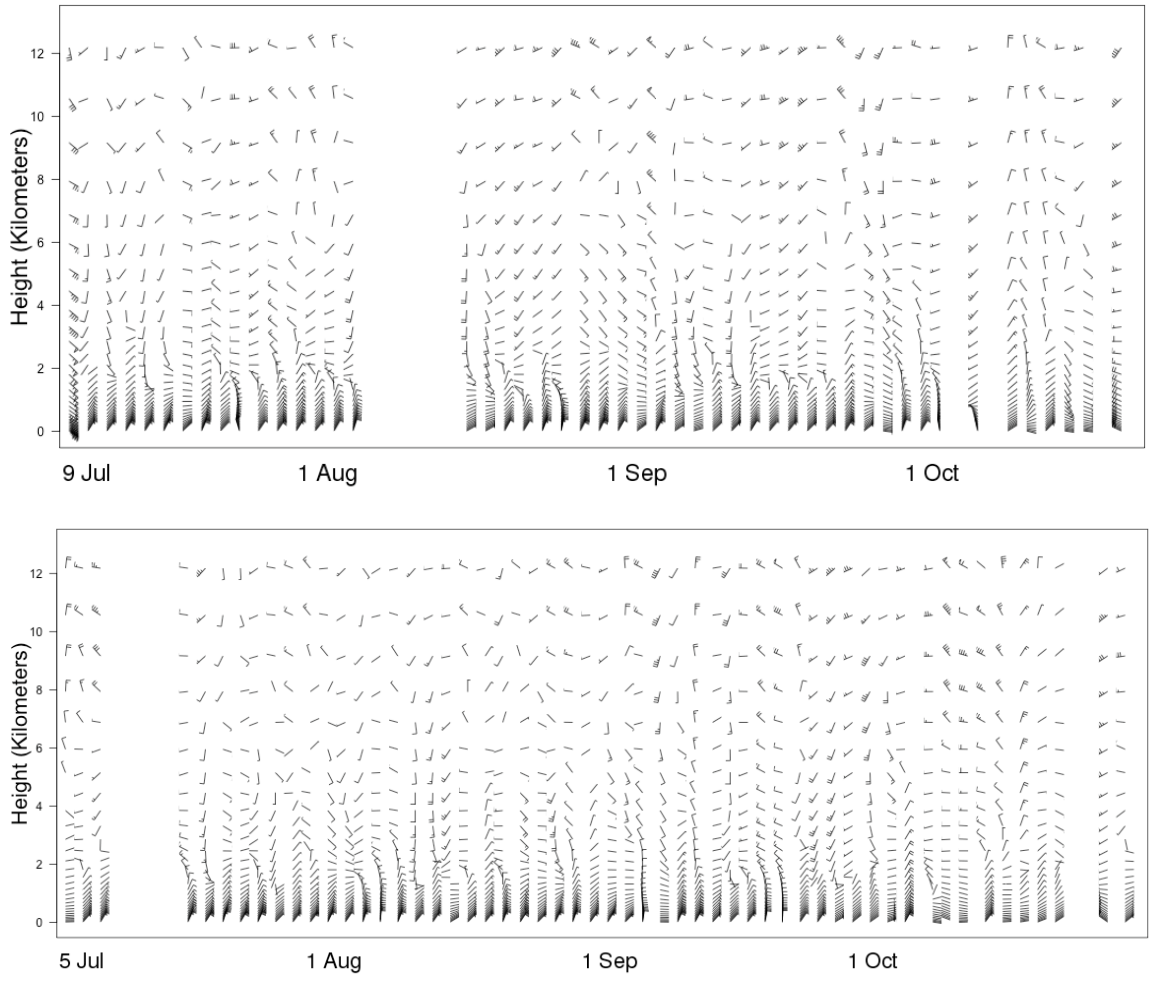

Figure 68: Time Series: Wind Barbs at Point 8: Same as Figure 53 except for Point 8 from Figure 5.

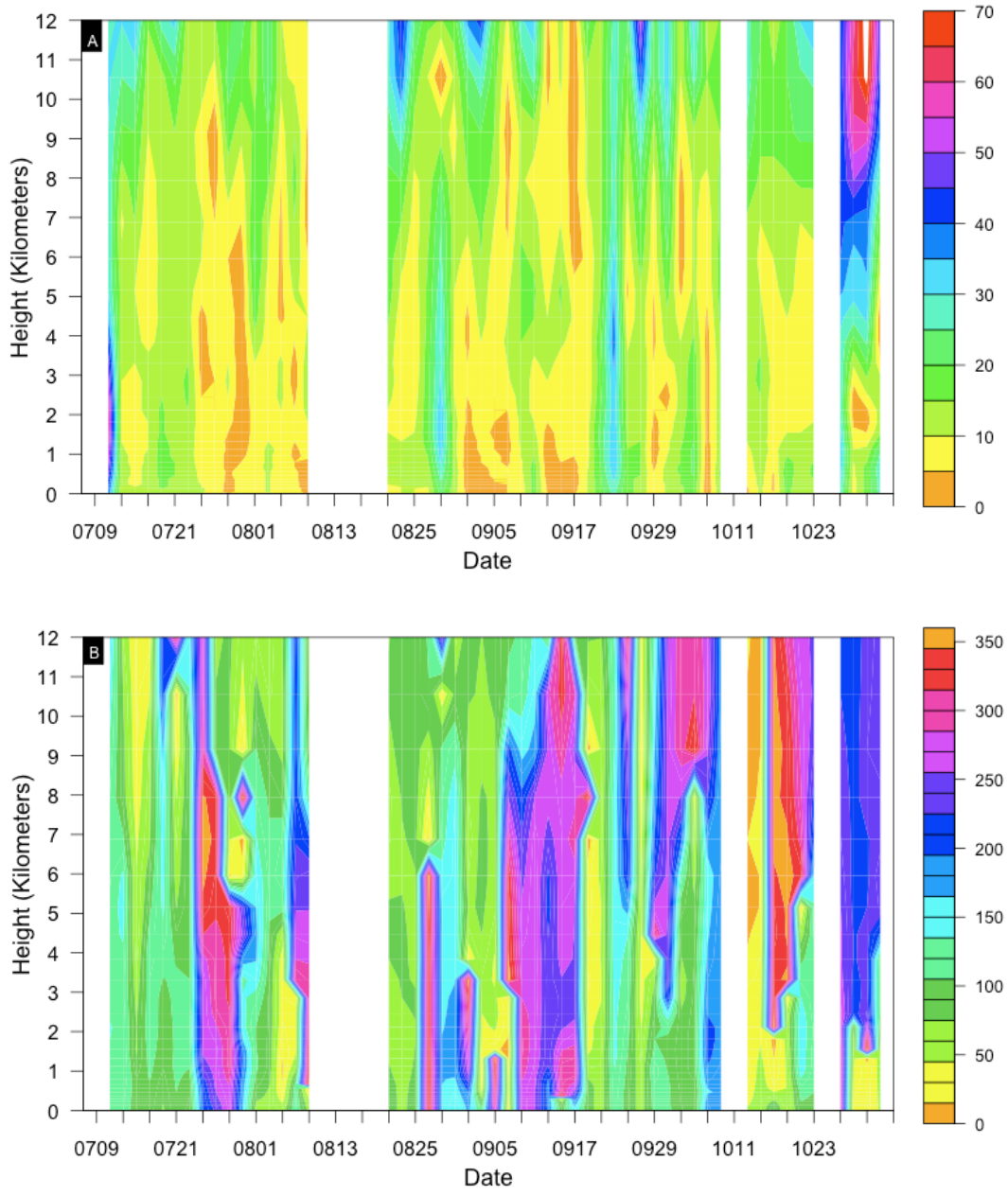

Figure 69: Time Series: Speed and Directional Shear at Point 8 in 2005: Same as Figure 54 except at Point 8 from Figure 5.

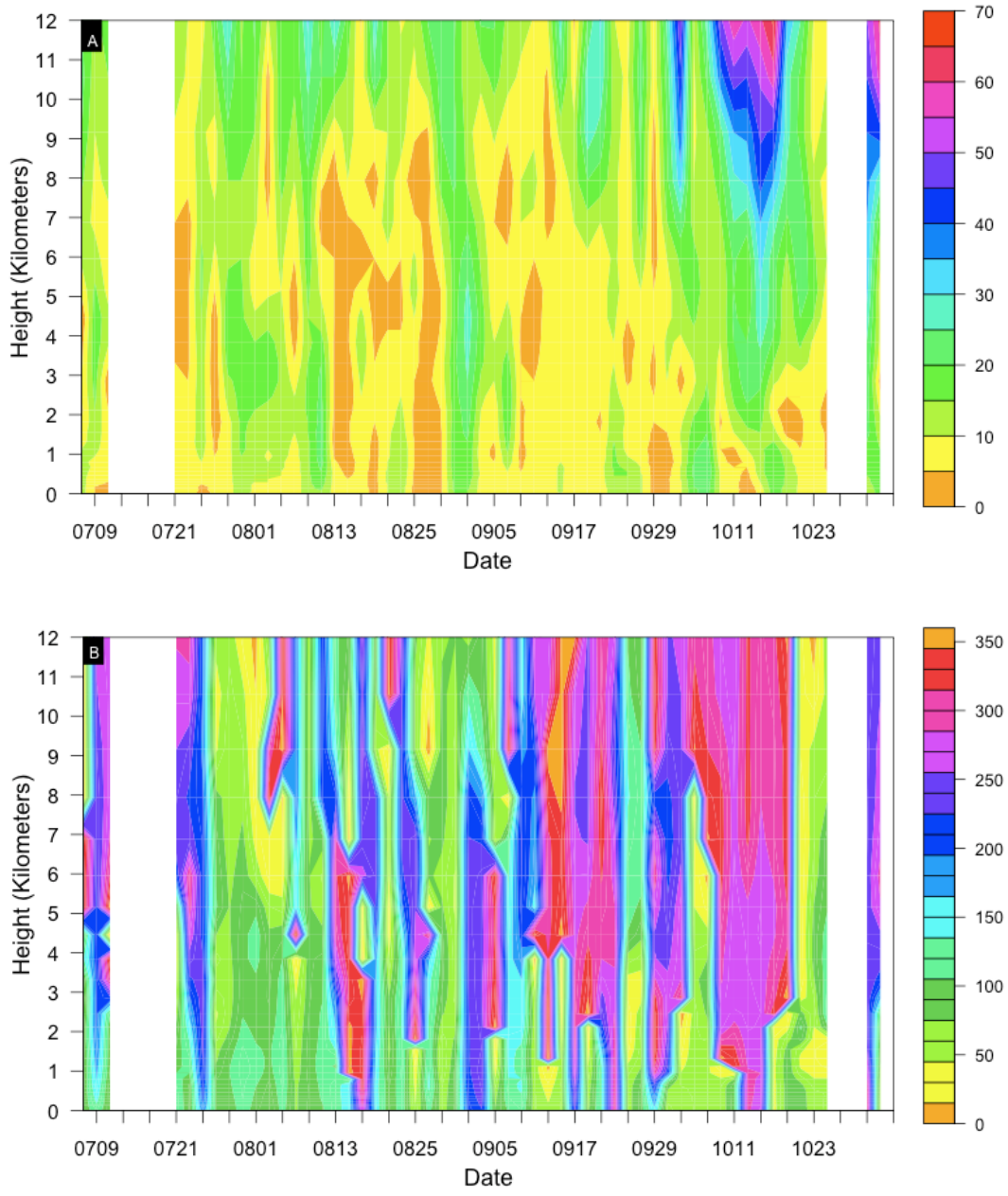

Figure 70: Time Series: Speed and Directional Shear at Point 8 in 2006: Same as Figure 54 except at Point 8 from Figure 5.

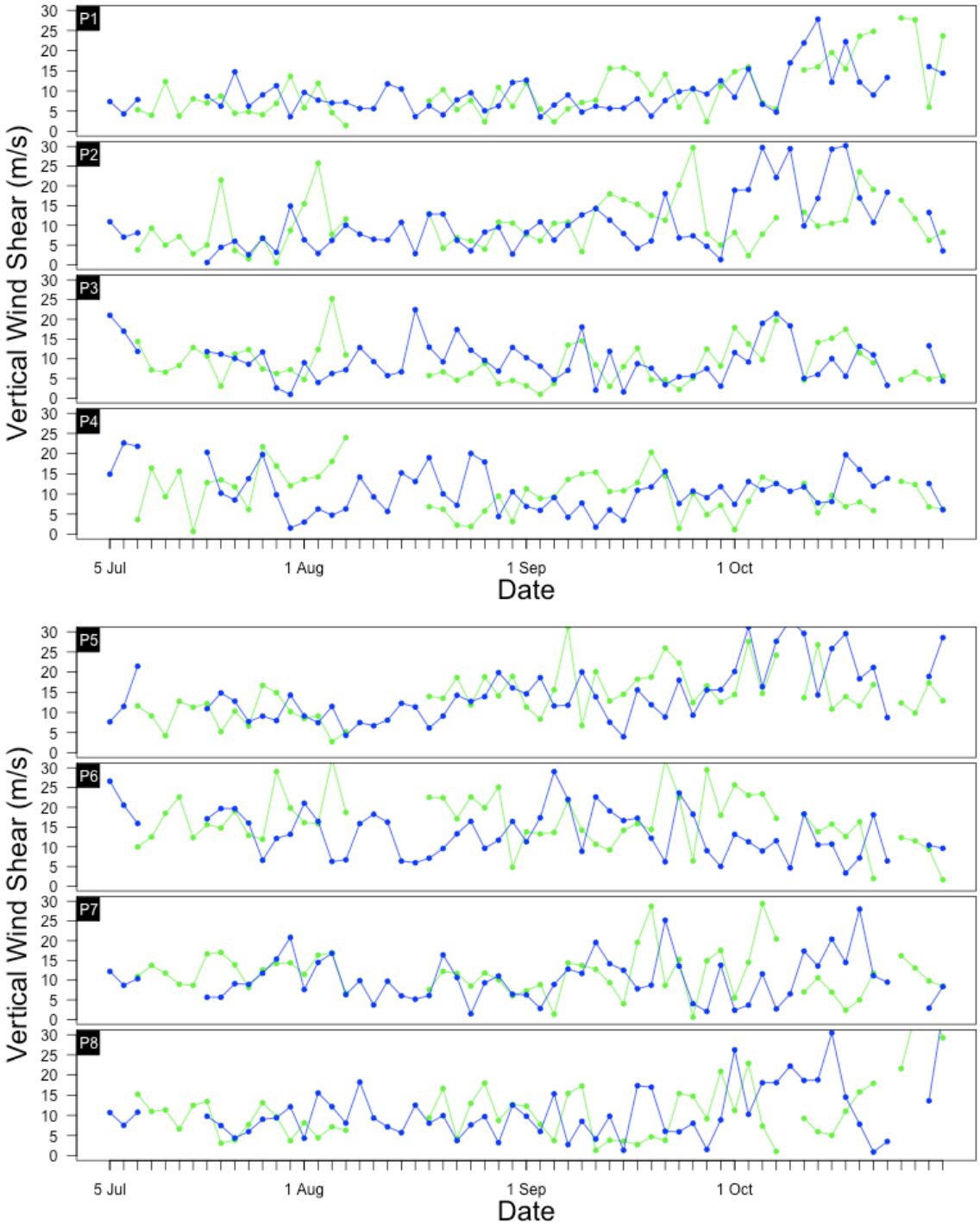

Figure 71: Tropospheric Vertical Wind Shear: Wind shear between 850 hPa and 250 hPa. Wind speeds are in meters per second.

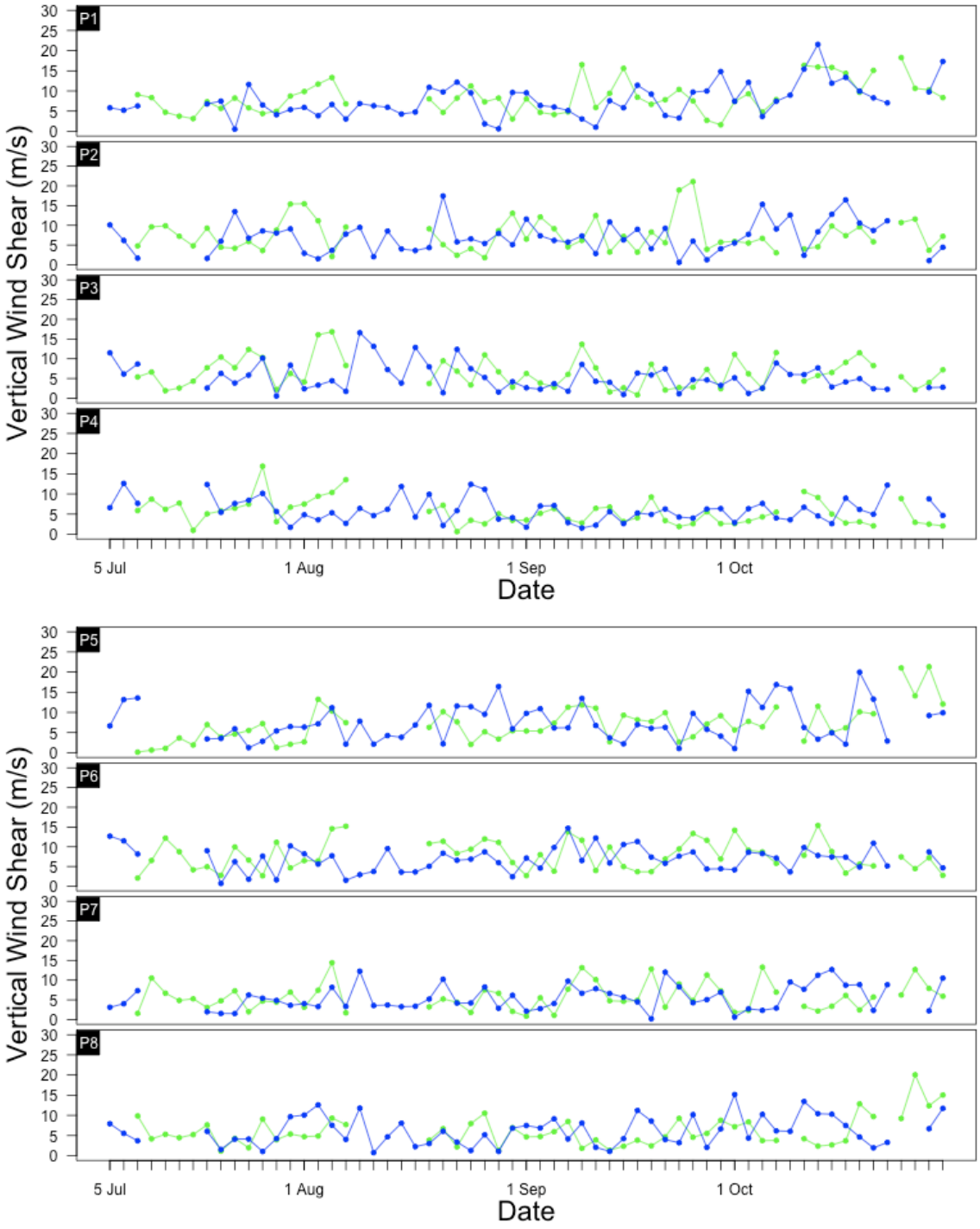

Figure 72: Mid-Troposphere Vertical Wind Shear: Wind shear between 700 hPa and 400 hPa. Wind speed is in meters per second.

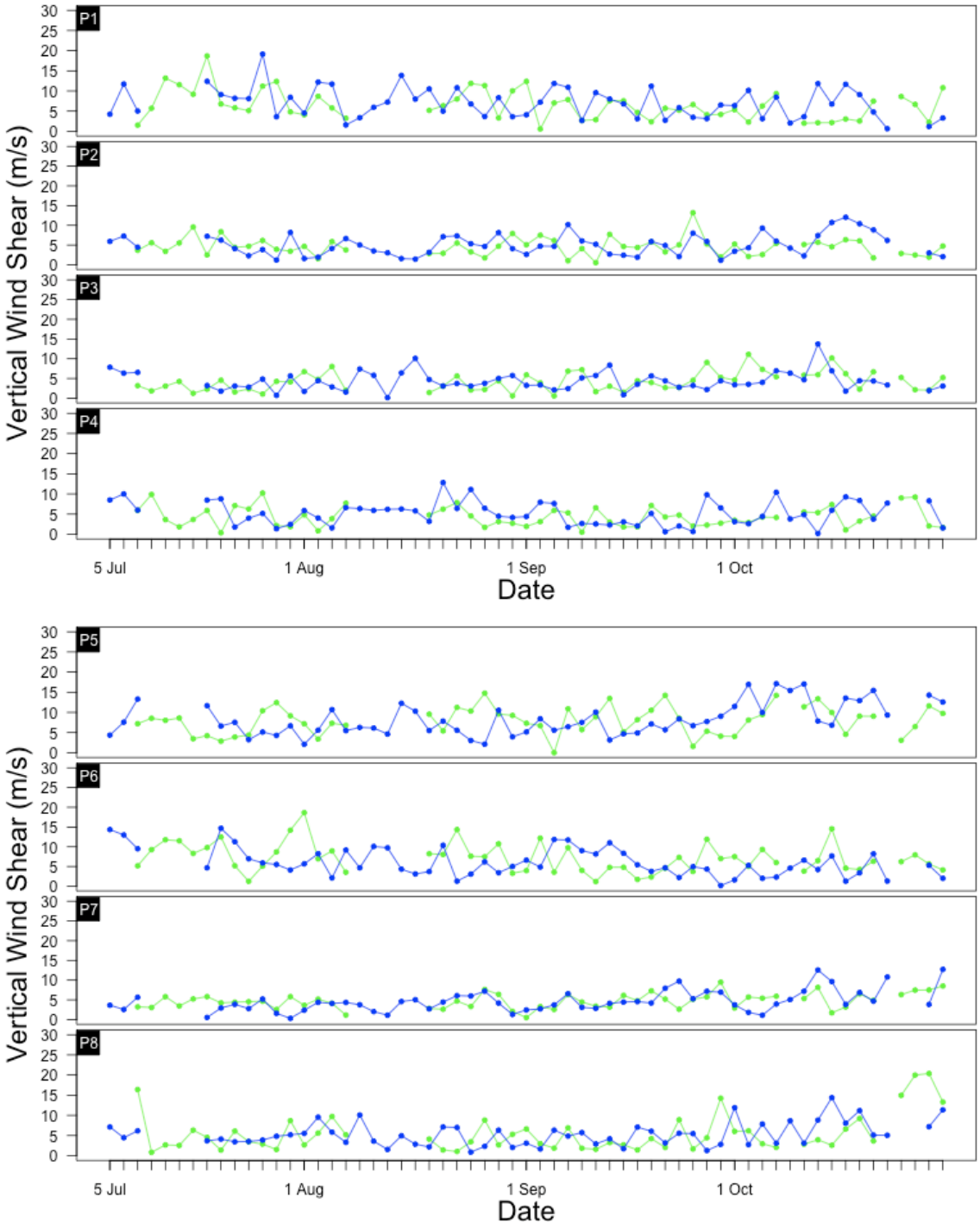

Figure 73: Lower Troposphere Vertical Wind Shear: Wind shear between 850 hPa and 500 hPa. Wind speed is in meters per second.

5.6 Individual Storm Cases

Several storms passed within two degrees of some of the Points in Figure 5. In 2005, Irene passed by Points 2 and 5, Wilma and Emily by Point 4, and Ophelia, Katrina, and Rita by Point 8. In 2006, Florence and Helene passed by Point 2, Chris by Point 3, Debby by Point 6, Gordon by Point 7, and Ernesto next to Point 8. The storm name, strength when passing the point, HURDAT recorded latitude/longitude, and date/time of passage are all given in Table 3 for 2005 storms and Table 4 for 2006 storms.

In the time series analyses when these storms occur, both the moisture and wind shear generally exhibit favorable conditions. Environmental conditions surrounding Katrina in 2005 at Point 8 were very moist with weak (near zero) southwesterly winds. When Ernesto passed Point 8 moist conditions were present up to 6 km with weak (less than 15 kts) southeasterly and easterly winds. Debby, which was studied in the NAMMA experiment and known to be influenced by Saharan dust, passed within the vicinity of Point 6 as it was transitioning from a tropical storm to a tropical depression. When looking at 25 August in Figure 41, there a sliver of moist air present at the time the storm was in the vicinity. Wilma exhibited the best surrounding environmental conditions with very moist air the day of as well as days before and after the storms passage along with light winds. When Wilma passed Point 4 it was transitioning from a tropical storm to a Category 1 hurricane.

The purpose is simply to point out several storms passing near these points and the time frame they passed by for reference with the above figures for each of the environmental conditions. When storms pass in the vicinity of points, the previously mentioned data can be put together. These environmental conditions impact the development of TCs so when the SAL affects these conditions, as seen in the comparison of between the four easternmost points (Points 1, 2, 5, and 6) and four westernmost points (Points 3, 4, 7, and 8), one can see the SAL influences the environmental conditions.

Table 3: Distance Between TCs in 2005 and Time Series Points: Displays the storm, the nearest point it passes, strength of the storm when it passes, and the date/time of passage for the 2005 season. These numbers were taken directly from the HURDAT database.

Storm name	Nearest Point	Storm latitude	Storm Longitude	Category when passed	Date/Time passed
Irene	2	17.2	-39.8	TD	6 Aug/00Z
Irene	5	23.9	-60.4	TS	11 Aug/06Z
Wilma	4	17.4	-79.6	TS to Cat 1	17 Oct/00Z
Emily	4	17.1	-79.5	TS	17 Oct/00Z
Ophelia	8	25.8	-78.6	TD	6 Sep/06Z
Katrina	8	25.9	-80.3	TS to Cat 1	26 Aug/00Z
Rita	8	24.1	-82.7	TS to Cat 1	21 Sep/00Z

Table 4: Distance Between TCs in 2006 and Time Series Points: Displays the storm, the nearest point it passes, strength of the storm when it passes, and the date/time of passage for the 2006 season. The asterisk indicates a storm within 3 km for either the latitude or longitude. These numbers were taken directly from the HURDAT database.

Storm name	Nearest Point	Storm latitude	Storm Longitude	Category when passed	Date/Time passed
Debby*	6	22.6	-41.5	TS to TD	25 Aug/06Z
Florence	2	14.7	-40	TD	4 Sep/00Z
Helene	2	15.5	-40.8	TS	15 Sep/12Z
Ernesto	8	24.7	-80.4	TS	30 Aug/00Z
Chris	3	16.8	-58.9	TD	1 Aug/00Z
Gordon	7	24.7	-58	Cat 1	13 Sep/06Z

Chapter 6: Conclusions and Future Work

It is important to summarize the goals, findings and implications of this research as well as point out areas in which further research would be beneficial. This thesis addresses two primary goals. The first analyzes the tropical system as a whole with regards to the 2005 and 2006 Atlantic hurricane seasons and works towards understanding why these seasons were so drastically different. One of the motivations for this work was the *Annual Summary: Atlantic Hurricane Season of 2005* which specifically states that further research is required to understand all the implications of the 2005 season (Beven et al., 2008). The second goal sought to determine if Saharan dust played a role in the difference between seasons. Several studies have focused on the potential solar dimming effect of Saharan dust which affects tropical cyclones (TCs) by decreasing sea surface temperatures (SSTs). According to Lau & Kim (2007) this is more of a climatic impact. The long-term effects of this proposed climate effect, induced by the dust, is yet unknown. This research addresses the dynamic effects of the Saharan Air Layer (SAL) on TC development. This work studied the environmental conditions and discussed the relationship between Saharan dust and its impact on environmental conditions known to be associated with dust.

SSTs appear to be the driving force between the seasons that causes 2005 to be stronger than 2006. Warm SSTs help fuel forming and developing TCs. The added benefit of a favorable easterly jet in 2005 also plays a role by moving convective systems into the Main Development Region (MDR) and providing more formation opportunities off the higher amplitude waves present. Additionally, more moisture is present in the mid-

troposphere in 2005. Overall, the moist stability index showed consistently more stable conditions in 2006. Vertical wind shear values in the mid and lower levels of the troposphere – below the threshold that tends to impact TCs – were low and quite comparable between both years.

The findings from this research indicate that Saharan dust does appear to impact TC development. A comparison of Saharan dust between seasons showed a greater presence of dust in 2006 than in 2005. The increased presence of Saharan dust in 2006 appears to play a suppressant role in both the number and strength of storms developing in the 2006 season. September, the month in which the greatest number of storms and strongest storms evolved, was the same time period in which dust Probability of Exceedance (POE) contours decreased in strength for 2006, covering similar extents to contours in 2005. Time series points within the Aerosol Index (AI) POE contours showed less available moisture and higher wind shear values. Outside the AI contours, more moisture and lower shear values are observed. Most importantly, no storms, in either season, develop or reach tropical storm strength until they are outside the regions where the AI thresholds of 1.5 occur less than 30% of the time or AI thresholds of 2.0 occur less than 20% of the time. This indicates that the dust plays a suppressant role and confirms research previously published by Dunion and Velden (2004), Evan et al (2006), and Zipser et al (2009).

This study also considers the effect of El Nino, which did play a role in the latter part of the 2006 season. However, the dominant factor is the presence of the dust. Therefore, at this point, it appears that the 2005 season was enhanced by record high SSTs and the

2006 season was suppressed by the increased presence of Saharan dust. Further research will enhance the understanding of these interactions.

This research adds to the growing body of data pertaining to the interaction of TCs and the SAL. As mentioned, these findings support the hypotheses of Dunion and Velden (2004) and a long-term study performed by Evan et al (2007). It also helps paint a different view of the 2005 and 2006 seasons by looking at all environmental conditions, below the climatic scale, as an integrated system. This lays the base for future qualitative and quantitative efforts.

The goal was not to answer all questions, but look at the system associated with TCs as a whole. The motivating question is how the well above average 2005 season is followed by a season, predicted to be above average, but instead experiencing an average number of storms. This effort is a step towards understanding these two seasons and a potential missing link – Saharan dust. Future work could include following the same method used in this paper to create POE maps for the moisture and vertical wind shear fields. Extending the study to include more years – for example, the 2004, 2007, and 2008 Atlantic hurricane seasons – would expand the knowledge base from a statistical point of view.

Previously, connections have been made between precipitation and Saharan dust outbreaks. More research on this connection could be useful for seasonal forecasts that are used by government planning agencies and insurance companies. The interaction of any one of these environmental factors can be the subject of a study in and of itself. Further research is particularly needed on the subject of Saharan dust. The timescale of

the dust storms in relation to the occurrence of African Easterly Waves (AEWs) or areas of intense convection and instability may play a crucial role. Accurate forecasting of TCs is continually an issue. Forecast improvements can save lives and property. Understanding the impact of the SAL may help computational models forecast periods of rapid development or the general strength of a storm better. The use of computational models would be ideal for quantitatively studying the dynamics associated with the interaction of the TCs and Saharan dust. Numerical sensitivity cases of TCs genesis and development should be run both with and without the presence of the dust. A numerical study of the microphysical processes associated with the dust would be beneficial. This could take a step towards addressing the impact of increased CCN in the storm and the influence of this on storm formation. Tropical Storm Debby of 2006 would be an ideal case to model with and without the inclusion of the SAL because a large amount of data is available for use in the models or for verification of results since Debby was studied during the NAMMA experiment.

In conclusion, record high SSTs in 2005 aided by a favorable African easterly waves and less Saharan dust storms appear to be the main factors causing such a strong 2005 season. The 2006 season, despite high expectations, resulted in an average number of storms. The primary influence for that appears to be the enhanced presence of Saharan dust and its impact upon the midlevel jet and moisture in the atmosphere. In the Climate Prediction Centers annual report for 2006, they noted that differences in local atmospheric environmental conditions as opposed to local SST anomalies tent to cause variations in Atlantic hurricane seasons. Further research, as mentioned, is critical in

increasing our understanding of TCs. These findings lay the groundwork to support computational modeling of the interaction between TCs and the SAL as an important research topic.

LIST OF REFERENCES

LIST OF REFERENCES

Aberson, S. D., 1998: Five-Day Tropical Cyclone Track Forecasts in the North Atlantic Basin. *Wea. Forecasting*, **13**, 1005-1015.

Bell, G. D., and co-authors 2006: The 2005 North Atlantic Hurricane Season: A Climate Perspective. *State of the Climate in 2005*. A. M. Waple and J. H. Lawrimore, Eds. *Bull. Amer. Meteor. Soc*., **86**, S1-S68.

Bell, G. D., and co-authors 2007: The 2006 North Atlantic Hurricane Season: A Climate Perspective. *State of the Climate in 2006*. A. M. Waple and J. H. Lawrimore, Eds. *Bull. Amer. Meteor. Soc*., **87**, S1-S68.

Beven, J.L., L.A. Avila, E.S. Blake, D.P. Brown, J.L. Franklin, R.D. Knabb, R.J. Pasch, J.R. Rhome, and S.R. Stewart, 2008: Atlantic Hurricane Season of 2005. *Mon. Wea. Rev.*, **136**, 1109–1173.

Bohren, Craig F. and Bruce A. Albrecht., 1998: Atmospheric Thermodynamics. New York. Oxford University Press, 402.

Bove, M.C., J.B. Elsner, C.W. Landsea, X.Niu, J.J. O'Brien., 1998: Effect of El Nino on U.S. Landfalling Hurricanes, Revisited. *Bull. Amer. Meteor. Soc.*, **79**, 2477-2482.

Braun, Scott A. and Chung-Lin Shie., 2008: Examination of the influence of the Saharan Air Layer on hurricanes using data from TRMM, MODIS, and AIRS. *28th Conference on Hurricanes and Tropical Meteorology.* Orlando, Fl. American Meteorological Society.

Burpee, R. W., 1972: The origin and structure of easterly waves in the lower troposphere of North Africa. *J. Atmos. Sci.*, **29**, 77-90.

Camp, J.P., and M.T. Montgomery, 2001: Hurricane Maximum Intensity: Past and Present. *Mon. Wea. Rev.*, **129**, 1704–1717.

Carlson, T.N., and J.M. Prospero, 1972: The Large-Scale Movement of Saharan Air Outbreaks over the Northern Equatorial Atlantic. *J. Appl. Meteor.*, **11**, 283–297.

Changwoo Ahn, Omar Torres, and Pawan K. Bhartia, 2008: Comparison of Ozone Monitoring Instruement UV Aerosol Products with Aqua/Moderate Resolution Imaging Spectroradiometer and Multiangle Imaging Spectroradiometer observations in 2006. *Journal of Geophys. Res*., **113**, D16S27.

Chiapello, I., J. M. Prospero, J. R. Herman, and N. C. Hsu, 1999: Detection of mineral dust over the North Atlantic Ocean and Africa with the Nimbus 7 TOMS. *J. Geophys. Res.,* **104,** 9277–9291.

Dunion, J. P., and C. S. Velden, 2004: The impact of the Saharan air layer on Atlantic tropical cyclone activity. *Bull. Am. Meteorol. Soc*., **85**(3), 353-365.

Dunion, J.P., and C.S. Marron, 2008: A Reexamination of the Jordan Mean Tropical Sounding Based on Awareness of the Saharan Air Layer: Results from 2002. *J. Climate*, **21**, 5242–5253.

Elsner, J.B., T.H. Jagger, and A.A. Tsonis, 2006: Estimated return periods for Hurricane Katrina. *Geophys. Res. Lett*., **33**, L08704.

Emanuel, K.A., 1989: The finite-amplitude nature of tropical cyclogenesis. *J. Atmos. Sci.*, **46**, 3431–3456.

Emanuel, K. A., 2005: Increasing destructiveness of tropical cyclones over the past 30 years. *Nature,* **436,** 686–688, doi:10.1038/nature03906.

Emanuel, K. A., 2007: Environmental factors affecting tropical cyclone power dissipation. *J. Climate,* **20,** 5497–5509.

Evan, A. T., J. Dunion, J. A. Foley, A. K. Heidinger, and C. S. Velden, 2006: New evidence for a relationship between Atlantic tropical cyclone activity and African dust outbreaks. *Geophys. Res. Lett*., **33**, L19813, doi:10.1029/2006GL026408.

Evan, A. T., 2007: Comment on "How nature foiled the 2006 hurricane forecasts." *EOS, Trans. Amer. Geophys. Union,* **88,** 271.

Evans, J.L., 1993: Sensitivity of Tropical Cyclone Intensity to Sea Surface Temperature. *J. Climate*, **6**, 1133–1140.

Evans, J.L. and Jaskiewicz, F.A., 2001: Satellite-Based Monitoring of Intraseasonal Variations in Tropical Pacific and Atlantic Convection. *Geophys. Res. Lett.*, **28**(8), 1511-1514.

Fraedrich, K., and L. M. Leslie, 1989: Estimates of cyclone track predictability. I: Tropical cyclones in the Australian region. *Quart. J. Roy. Meteor. Soc.*, **115**, 79-92.

Frank, W.M., and E.A. Ritchie, 2001: Effects of vertical wind shear on the intensity and structure of numerically simulated hurricanes. *Mon. Wea. Rev.*, **129**, 2249-2269.

Franklin, J.L., and D.P. Brown, 2008: Atlantic Hurricane Season of 2006. *Mon. Wea. Rev.*, **136**, 1174–1200.

Foltz, G.R., and M.J. McPhaden, 2008: Impact of Saharan Dust on Tropical North Atlantic SST http://ams.allenpress.com/perlserv/?request=cite builder&doi=10.1175%2F2008JCLI2232.1 - n101. *J. Climate*, **21**, 5048–5060.

Gray, W.M., 1984: Atlantic Seasonal Hurricane Frequency. Part I: El Niño and 30 mb Quasi-Biennial Oscillation Influences. *Mon. Wea. Rev.*, **112**, 1649–1668.

Goldenberg, S. B., C. Landsea, A. M. Mestas-Nunez, and W. M. Gray, 2001: The recent increase in Atlantic hurricane activity. *Science,* **293,** 474–479.

Goldenberg, S. B., and L. J. Shapiro, 1996: Physical mechanisms for the association of El

Niño and West African rainfall with major hurricane activity. *J. Climate,* **9,** 1169-1187.

Goudie, A. S. and Middleton, N. J., 2006: Desert Dust in the Global System. Germany. Springer.

Holton, James R., 2004: An Introduction to Dynamic Meteorology: Fourth Edition. Boston. Elsevier Academic Press, 535.

Hopsch, S.B., C.D. Thorncroft, K. Hodges, and A. Aiyyer, 2007: West African Storm Tracks and Their Relationship to Atlantic Tropical Cyclones. *J. Climate*, **20**, 2468-2483.

Hurricane Research Division: Re-Analysis Project. NOAA Revisits Historic Hurricanes. <http://www.aoml.noaa.gov/hrd/hurdat/>. Atlantic Oceanographic and Meteorological Laboratory.

Joiner, J., A. Vasilkov, K. Yang, and P.K. Bhartia. (2006) Observations over hurricanes from the ozone monitoring instrument. *Geophys. Res. Lett*., **33**, L06807. Doi: 10.1029/2005GL025592.

Karyampudi, V.M., and T.N. Carlson, 1988: Analysis and Numerical Simulations of the Saharan Air Layer and Its Effect on Easterly Wave Disturbances. *J. Atmos. Sci.*, **45**, 3102–3136.

Karyampudi, V. M., and H. F. Pierce, 2002: Synoptic-scale influence of the Saharan air layer on tropical cyclogenesis over the eastern Atlantic. *Mon. Wea. Rev.,* **130,** 3100-3128.

Kaufman, Y.J., I. Koren, L.A. Remer, D. Tanre, P. Ginoux, and S. Fan., 2005: Dust transport and deposition observed from the Terra-Moderate Resolution Imaging Spectroradiometer (MODIS) spacecraft over the Atlantic Ocean. *J. Geophys. Res.*, **110**, D10S12.

Klotzbach, Philip J., 2006: Trends in global tropical cyclone activity over the past twenty

years (1986-2005). *Geophys. Res. Lett.*, **33**, L10805, doi: 10.1029/2006GL025881.

Landsea, C. W., and W. M. Gray, 1992: The strong association between Western Sahelian monsoon rainfall and intense Atlantic hurricanes. *J. Climate*, **5**, 435-453.

Landsea, C. W., R. A. Pielke Jr., A. M. Mestas-Nuñez, and J. A. Knaff, 1999: Atlantic basin hurricanes: Indices of climatic changes. *Climatic Change,* **42,** 89–129.

Landsea, C. W., C. Anderson, N. Charles, G. Clark, J. Dunion, J. Fernandez-Partagas, P. Hungerford, C. Neumann, and M. Zimmer, 2004: The Atlantic hurricane database reanalysis project: Documentation for the 1851-1910 alterations and additions to the HURDAT database. In *Hurricanes and Typhoons: Past, Present and Future*, R. J. Murname and K.-B. Liu, Eds., Columbia University Press, 177-221.

Lau, K. M., and J. M. Kim, 2007a: How nature foiled the 2006 hurricane forecasts. *EOS, Trans. Amer. Geophys. Union,* **88,** 105–107.

Lau, K. M., and J. M. Kim, 2007b: Reply to comment on "How nature foiled the 2006 hurricane forecasts." *Eos, Trans. Amer. Geopys. Union,* **88,** 271.

Leslie, L. M., and R. F. Abbey Jr., 2000: Hurricane Predictability: are there simple linear invariants within these complex nonlinear dynamical systems? *Meteorol. Atmos. Phys.*, **74**, 57-62.

Merrill, R.T., 1988: Environmental influences on hurricane intensification. *J. Atmos. Sci.*, **45**, 1678-1687.

National Hurricane Center. National Weather Service. < http://www.nhc.noaa.gov/>.

Omar T, et al. 2007. Aerosols and surface UV products from Ozone Monitoring Instrument observations: An overview. *Journal of Geophysical Res*., **112**, D24S47.

Ortt, D., and S.-S. Chen, 2008: Effect of environmental moisture on rainbands in

Hurricanes Katrina and Rita (2005). *Preprints, 27th AMS Conference on Hurricanes and Tropical Meteorology*, Orlando, Florida, American Meteorological Society.

Pielke, R.A., C. Landsea, M. Mayfield, J. Laver, and R. Pasch, 2005: Hurricanes and Global Warming. *Bull. Amer. Meteor. Soc.*, **86**, 1571–1575.

Pielke, R.A., Jr., and R.A. Pielke Sr., 1997: *Hurricanes: Their Nature and Impact on Society*. John Wiley, 279.

Pratt, A.S., and J.L. Evans, 2009: Potential Impacts of the Saharan Air Layer on Numerical Model Forecasts of North Atlantic Tropical Cyclogenesis. *Wea. Forecasting*, **24**, 420–435.

Prospero, J.M., and T.N. Carlson, 1970: Radon-222 in the north Atlantic trade winds: Its relationship to dust transport from Africa. *Science*, **167**, 974-977.

Prospero, J.M., and T.N. Carlson, 1972: Vertical areal distributions of Saharan dust over the western equatorial North Atlantic Ocean. *J. Geophys. Res.*, **77**, 5255-5265.

Prospero, J. M., and T. N. Carlson, and P. J. Lamb, 2003: African droughts and dust transport to the Caribbean: Climate change implications. *Science,* **302,** 1024–1027.

R Project for Statistical Computing, The. WU Wien: Department of Statistics and Mathematics. <http://www.r-project.org/>.

Shapiro, L. J., and S. B. Goldenberg, 1998: Atlantic sea surface temperatures and tropical cyclone formation. *J. Climate,* **11,** 578–590

Sun, D. L., et al., 2008: Contrasting the 2007 and 2005 hurricane seasons: Evidence of possible impacts of Saharan dry air and dust on tropical cyclone activity in the Atlantic basin, *Geophys. Res. Lett.*, **35**(15), L15405.

Vecchi, G. A., and B. J. Soden, 2007a: Effect of remote sea surface temperature change on tropical cyclone potential intensity. *Nature,* **450,** 1066–1070,

doi:10.1038/nature06423.

Vecchi, G. A., and B. J. Soden, 2007c: Increased tropical Atlantic wind shear in model projections of global warming. *Geophys. Res. Lett.,* **34,** L08702, doi:10.1029/2006GL028905.

Wallace, John M. and Hobbs, Peter V., 1977: Atmospheric Science: An Introductory Survey. New York. Academic Press, 467.

Webster, P. J., G. J. Holland, J. A. Curry, and H.-R. Chang, 2005: Changes in tropical cyclone number, duration and intensity in a warming environment. *Science,* **309,** 1844–1846.

Wilkes, Daniel S., 1995: *Statistical Methods in Atmospheric Sciences*, Academic Press, 467.

Wong, S., and A. E. Dessler, 2005: Suppression of deep convection over the tropical North Atlantic by the Saharan Air Layer. *Geophys. Res. Lett.,* **32,** L09808, doi:10.1029/2004GL022295.

Wu, Liguang, Scott A. Braun, John J. Qu, and Xianjun Hao., 2006: Simulating the formation of Hurricane Isabel (2003) with AIRS data. *Geophys. Res. Lett.,* **33**, L04804. doi: 10.1029/2005GL024665.

Zhang, R., and T. L. Delworth, 2006: Impact of Atlantic multidecadal oscillations on India/Sahel rainfall and Atlantic hurricanes. *Geophys. Res. Lett.,* **33,** L17712, doi:10.1029/2006GL026267.

Zhao Bin, Duan Yihong, Yu Hui, and Du Bingyu., 2005: A Statistical Analysis on the Effect of Vertical Wind Shear on Tropical Cyclone Development. ACTA *Meteorologica Sinica*. **20**, 383-388.

Zipser EJ, Twohy CH, Tsay SC, Thornhill KL, Tanelli S, et al. (2009) The Saharan Air Layer and the Fate of African Easterly Waves NASA's AMMA 2006 Field Program to Study Tropical Cyclogenesis: NAMMA. Bulletin of the American Meteorological Society: In Press

CURRICULUM VITAE

Laura Clemente graduated from Shenendehowa High School in Clifton Park, NY, in 2003. She went on to receive her Bachelors of Science in Meteorology with a minor in Environmental Inquiries, Biodiversity focus, from The Pennsylvania State University in 2007.